Dietmar Klonner, BSc.

Purification of liquid digestate from biogas plants - technology check

Masterarbeit

zur Erlangung des akademischen Grades

Diplom-Ingenieur

Masterstudium Verfahrenstechnik

Eingereicht an der

Technischen Universität Graz

BetreuerIn:

Ass. Prof. Dipl.-Ing. Dr. techn. Marlene Kienberger

Institut für Chemische Verfahrenstechnik und Umwelttechnik

Graz, Dezember 2016

Deutsche Fassung:

Beschluss der Curricula-Kommission für Bachelor-, Master- und Diplomstudien vom 10.11.2008

Genehmigung des Senates am 1.12.2008

EIDESSTATTLICHE ERKLÄRUNG

Ich erkläre an Eides statt, dass ich die vorliegende Arbeit selbstständig verfasst, andere als die angegebenen Quellen/Hilfsmittel nicht benutzt, und die den benutzten Quellen wörtlich und inhaltlich entnommenen Stellen als solche kenntlich gemacht habe.

Graz, am ..... 19.12.2016 .....

(Unterschrift)

Englische Fassung:

STATUTORY DECLARATION

I declare that I have authored this thesis independently, that I have not used other than the declared sources / resources, and that I have explicitly marked all material, which has been quoted either literally or by content from the used sources.

Graz, ... 19.12.2016 ... .

date

(signature)

Danksagung

An dieser Stelle möchte ich mich bei meiner Betreuerin Ass. Prof. Dipl.-Ing. Dr. techn. Marlene Kienberger vom Institut für Chemische Verfahrenstechnik und Umwelttechnik für die hervorragende Betreuung und die konstruktiven Diskussionen während meiner Zeit als Diplomand bedanken. Mein Dank gilt auch besonders den Angestellten des Instituts für Chemische Verfahrenstechnik und Umwelttechnik, die mir bei Problemen im Labor stets zur Seite standen und durch die die Zeit am Institut stets unterhaltsam war.

Weiters wäre es ohne Dipl.-Ing. Dr. techn. Martin Ernst von der Firma BDI - BioEnergy International AG nicht möglich gewesen, diese Diplomarbeit zu machen, da dieser das Budget für meine Diplomarbeit bereitgestellt und mich stets mit Tipps und Hilfestellungen unterstützt hat.

Neben den fachlichen Ansprechpartnern gebührt mein Dank auch meiner Freundin Magdalena, meinem Bruder Günther und meinen Freunden in Graz, die mir in Zeiten von steigender Verzweiflung immer Mut gemacht und für die nötige Ablenkung gesorgt haben.

Zu guter Letzt möchte ich noch meinen Eltern danken, da sie mich stets auf meinem Lebensweg unterstützt und mir immer den nötigen Rückhalt gegeben haben.

Kurzfassung

Die vorliegende Masterarbeit befasst sich mit der Aufbereitung von flüssigen Gärresten, welche im Prozess der Biogaserzeugung anfallen. Verwendet man Lebensmittelabfälle zur Biogaserzeugung, ist der anfallende flüssige Gärrest mit gelösten Salzen wie zum Beispiel Chloriden oder Sulfaten beladen. Üblicherweise wird Gärrest auf Feldern und Äckern ausgebracht. Durch die Kontaminierung der flüssigen Fraktion mit Salzen ist die Möglichkeit der Ausbringung limitiert und eine Direkteinleitung in Gewässer nicht mehr möglich. Um Herausforderungen wie Einleiterqualität, Aufkonzentrierung und Entsorgungskosten erfolgreich zu bewältigen, benötigt man Verfahren, durch welche die Salzfracht abgetrennt werden kann und eine Volumenreduktion erfolgt. Das aufbereitete Wasser kann entweder im Prozess als Brauchwasser verwendet werden oder mittels selektiver Abtrennung von Nährstoffen (z.B. Phosphate, Sulfate) als Düngemittel Einsatz finden.

Die vorliegende Arbeit ist in drei Teile gegliedert. Zunächst wurde eine Literaturrecherche zum Stand der Technik der Salzabtrennung aus Abwasser und flüssigen Gärresten durchgeführt. Mittels einer Entscheidungsmatrix konnte die Literaturstudie objektiviert und im zweiten Teil der Arbeit die sich ergebenden Prozesse auf die Anwendbarkeit für die Gärrestbehandlung getestet werden. Der dritte Teil der Arbeit umfasst einen Vorschlag für eine effektive Salzabtrennung mit und ohne Düngemittelgewinnung sowie mit und ohne Recycling des Prozesswassers.

Die Literaturrecherche und die Laborergebnisse der Arbeit zeigen, dass membranbasierte Filtrationsverfahren wie Umkehrosmose, Nanofiltration und Elektrodialyse vielversprechende Technologien zur Behandlung des salzbeladenen flüssigen Gärrestes darstellen. Elektrodialyse und Nanofiltration weisen ähnliche Abscheideraten für einwertige Ionen auf – für mehrwertige Ionen ist Nanofiltration jedoch geeigneter. Unter Berücksichtigung der erreichbaren Volumenverringerung des Feed und dem vorherrschenden Stand der Technik wurden zwei Gesamtprozesse, basierend auf Nanofiltration, untersucht. Durch mathematische Modellierung konnte gezeigt werden, dass die Verwendung der gereinigten Gärrest-Flüssigfraktion als Brauchwasser eine effektive Möglichkeit ist, um den Frischwasserbedarf zu vermindern, und dass die Nährstoffgewinnung im ersten Reinigungsschritt die weiteren Aufbereitungsschritte vereinfacht.

Abstract

The present master thesis focuses on the purification of liquid digestate, which arises during biogas production. If food leftovers are used as substrate, the liquid digestate fraction contains certain amounts of dissolved salts (e.g. chloride, sulphates). The common method to process liquid digestate is the spreading on agricultural areas or grassland. In the case of salt containing digestate, the spreading of the digestate is limited and it is most likely that the concentration limits for the discharge of the liquid fraction into waters are exceeded. Therefore, methods have to be found, where the dissolved salts are separated from the liquid digestate and enable its release into the environment and furthermore to keep storage respectively disposal costs of the salt contaminated low. The purified water could be recycled as process water or used as a fertilizer after selective nutrient recovery (e.g. phosphates, sulphates).

To solve this issues, at first a literature research combined with a systematic approach to identify applicable purification processes was conducted. In the second part, the processes found due to the literature research, were investigated at laboratory experiments regarding their suitability for liquid digestate purification. The third part of the thesis addresses a suggestion for an overall purification process for effective salt removal with and without a nutrient recovery step and the recycling of the purified water as process water within the biogas facility.

The literature research and the experiments show that membrane based filtration operations like reverse osmosis, nanofiltration and electro dialysis are promising technologies for the processing of salt contaminated liquid digestate. Electro dialysis and nanofiltration have similar rejection rates for monovalent ions, whereby nanofiltration has an increased rejection efficiency regarding multivalent ions. Based on the experimental results two overall purification processes were developed and modeled. Modelling was performed in terms of the usage of the purified water fraction as process water and the production of a fertilizer in the first purification step. The modelling proves that the recycling step for process water is possible and helps to decrease the fresh water consumption. Furthermore, through the nutrient recovery following purification steps are supported.

Table of contents

1 Introduction....1
1.1 Motivation....1
1.2 Objective....1
2 Theory....3
2.1 Overview of the biogas production process....3
2.2 Feedstock for biogas utilization....5
2.3 Feedstock composition in Austria....7
2.4 Utilization of biogas....8
2.4.1 Influencing process parameters....10
2.5 Fermentation residue - Digestate....12
2.5.1 Chemical composition of the digestate....12
2.5.2 Digestate treatment....14
2.5.3 Processing of the solid digestate....15
2.5.4 Processing of the liquid digestate....17
2.6 Resulting challenges within digestate processing....25
3 Literature research on digestate purification....30
3.1 Salt removal from water/wastewater....30
3.1.1 Membrane processes....30
3.1.2 Mass transfer processes....32
3.2 Salt removal from liquid digestate....34
3.3 Development of a decision matrix....34
3.4 Process suggestion....38
4 Experimental part....39
4.1 Chemicals & Materials....39
4.2 Filtration device....41
4.2.1 Experimental setup....41
4.2.2 Test procedure....42
4.3 Electro dialysis device....43
4.3.1 Experimental setup....44
4.3.2 Test procedure....44
4.4 Analytics....45
4.4.1 Conductivity, pH and temperature....45
4.4.2 Determination of the ion concentration....45
5 Results and Discussion....46
5.1 Experimental matrix....46

5.2 Composition of the liquid digestate and the model feed 48
5.3 First purification stage 49
5.3.1 Nanofiltration at 5 - 40 bar 50
5.4 Second purification stage 53
5.4.1 Nanofiltration at 40 bar 53
5.4.2 Nanofiltration rejection behavior at 40 bar 55
5.4.3 Reverse osmosis at 30 - 50 bar 57
5.4.4 Electro dialyses 60
5.5 Comparison of nanofiltration and electro dialysis 67
5.6 Suggestion for an overall purification process 68
6 Conclusions 75
7 Literature 77
8 Appendix i

List of Figures

Figure 1: Process chain of the biogas production 3
Figure 2: Use of different feedstock substrates in Austria. Source [16] 7
Figure 3: The four stages of the anaerobic digestion. Source [7] 8
Figure 4: Digestate processing methods. Source [25] 14
Figure 5: Screw press schematics. Source [25] 15
Figure 6: Decanter centrifuge schematics. Source [25] 16
Figure 7: Ammonia volatility. Source [6] 18
Figure 8: Air stripping process. Source [25] 19
Figure 9: 3-step evaporation process. Source [25] 20
Figure 10: Struvite precipitation process. Source [25] 21
Figure 11: Process of ion exchange. Source [6] 22
Figure 12: Filtration types. Source [6] 23
Figure 13: Membrane process principle. Source [8] 24
Figure 14: Transport costs depending on the application method. Source [25] 26
Figure 15: Working principle of an ED stack. Source [36] 31
Figure 16: Configurations for membrane distillation. Source [43] 33
Figure 17: Overview of the suggested process combinations 38
Figure 18: Lab scale filtration device 41
Figure 19: Electro dialysis cell 43
Figure 20: Experimental set up for electro dialysis 44
Figure 21: NF Stage 1 – Concentrate and Permeate flows in [l/min] at 5-40 bar 50
Figure 22: NF Stage 1 - Conductivity of Permeate, Concentrate, Feed at 40 bar 51
Figure 23: NF Stage 1 - Ion rejection rates in [%] at 40 bar 52
Figure 24: NF Stage 2 - Conductivity of Permeate, Concentrate, Feed at 40 bar 54
Figure 25: NF Stage 2 – Ion rejection rates in [%] at 40 bar 55
Figure 26: NF model experiment - Ion rejection rates in [%] at 40 bar 57
Figure 27: RO Stage 2 - Concentrate and Permeate flow in [l/min] at 30-50 bar 58
Figure 28: RO Stage 2 - Conductivity of Permeate, Concentrate and Feed at 40 bar 59
Figure 29: RO Stage 2 - Ion rejections rates in [%] at 40 bar 60
Figure 30: ED Stage 2 - Cell current [mA] over cell voltage [V] 61
Figure 31: ED Stage 2 – Conductivity in the MC, AC, and CC over 8 hours 62

Figure 32: ED Stage 2 - Ion rejection rates in [%] after 8 hours 63
Figure 33: ED: Conductivity decrease with different electrolytes over 8 hours 64
Figure 34: ED: Cathode and anode after 8-hour electro dialysis 66
Figure 35: Comparison of the rejection rates for mono and divalent species at 67
Figure 36: NF1 - Process scheme digestate purification with “i” stages 69
Figure 37: NF2 - Process scheme nutrient recovery and digestate purification 70
Figure 38: Permeate salt concentration in [m%] over recycle iterations, for one step nanofiltration 72
Figure 39: Permeate salt concentration in [m%] over recycle iterations for two step nanofiltration with fertilizer recovery 73
Figure 40: NF1.1 - Process flow sheet of overall purification of Feed 1 vi
Figure 41: NF1.2 - Process flow sheet of overall purification of digestate D vii
Figure 42: NF 2.1 / NF 2.2 - Process flow sheet of nutrient recovery and purification of Feed 1 ix
Figure 43: NF 2.3 / NF 2.4 - Process flow sheet of nutrient recovery and purification of the digestate D x
Figure 44: Recycle - Mixing of the recycled permeate and initial process feed before the NF system xi

List of Tables

Table 1: Chemical composition of biogas 4
Table 2: Feed substrates 5
Table 3: Average nitrogen disposal area based on facility output and digestate amount 28
Table 4: Decision matrix mechanical unit operations 35
Table 5: Decision matrix for thermal unit operations 36
Table 6: Decision matrix reactive unit operations 37
Table 7: Chemical substances 39
Table 8: Experimental materials 40
Table 9: Experimental matrix 46
Table 10: Analysis of the digestate and experimental feed 49
Table 11: Composition of the model feeds for the additional nanofiltration experiments 56
Table 12: Electro dialysis process parameters 62
Table 13: Properties of the feed and electrolytes at the ED experiments 64
Table 14: ED: pH values in the MC, AC and CC for samples taken at 3, 5 and 8 hours 65
Table 15: Standard electrode potential in [V] for selected ions. Source [64] 66

Table 16: Results of the NF purification approaches without recycle option....70

Table 17: Complete decision matrix mechanical unit operations....i

Table 18: Complete decision matrix mass transfer unit operations....ii

Table 19: NF Stage 1: Ion concentration and SD in the permeate, concentrate and feed at 40 bar....ii

Table 20: NF Stage 2: Ion concentration and SD in the permeate, concentrate and feed at 40 bar....iii

Table 21: RO Stage 2: Ion concentration and SD in the permeate, concentrate and feed at 40 bar....iii

Table 22: NF model experiments: Ion concentration in the permeate, concentrate and feed at 40 bar....iv

Table 23: ED Stage 2: Ion concentration and SD in the membrane compartment at the 8 hour experiment....v

Table 25: Rejection rates of the NF systems....v

Table 24: Mass flows of the different overall purification processes....v

Table 26: NF1.1 - Ion concentration in the different streams of the NF system....vii

Table 27: NF1.2 - Ion concentration in the different streams of the NF system....viii

Table 28: NF 2.1 / NF 2.2 - Ion concentration in the different streams of the NF system for nutrient recovery....ix

Table 29: NF 2.3 / NF2.4 - Ion concentration in the different streams of the NF system....x

Table 30: NF 1 - Process streams for the recycle investigations with the different feeds....xii

Table 31: NF 2 - Process streams for the recycle investigations with the different feeds....xiii

Abbreviations

DM	Dry matter content
oDM	Organic dry matter
MAP	Magnesium-ammonium-phosphate
NF	Nanofiltration
RO	Reverse osmosis
FO	Forward osmosis
ED	Electro dialysis
MD	Membrane distillation
DCMD	Direct contact membrane distillation
AGMD	Air gap membrane distillation
MC	Membrane compartment
AC	Anode compartment
CC	Cathode compartment
PES	Poly ether sulfone
PA	Polyamide
MF	Model feed
Conc	Concentrate
Perm	Permeate
DC	Direct current
AAS	Atomic absorption spectroscopy
ICP	Inductively coupled plasma
D	Digestate
SD	Standard deviation

Nomenclature

p_{H2}	Hydrogen partial pressure [bar]
p_{Vapor}	Vapor partial pressure [bar]
$w_{Permeate}$	Mass fraction permeate [kg/kg]
w_{Feed}	Mass fraction feed [kg/kg]
c_i	Concentration of substance “i
m%	Mass percent
R	Rejection rate [%]
σ_i	Conductivity of substance “i” [mS/cm]
σ_Perm	Conductivity permeate [mS/cm]
σ_Conc	Conductivity concentrate[mS/cm]
σ_Feed	Conductivity feed [mS/cm]
V_Perm	Volume flow permeate [l/min]
V_Conc	Volume flow concentrate [l/min]
$\dot{M}_{Feed}$	Mass flow feed [t/h]

Chemical Symbols and Formulas

C	Elementary carbon
N	Elementary nitrogen
Na	Sodium
K	Potassium
S	Sulphur
Mg	Magnesium

Ca	Calcium
Cl	Chloride
N_2	Nitrogen
O_2	Oxygen
H_2	Hydrogen
H_2O	Water
CO_2	Carbon dioxide
CH_4	Methane
H_2S	Hydrogen sulphide
HCl	Hydrochloric acid
OH^-	Hydroxide
PO_4	Phosphate
SO_4	Sulphate
NH_3	Ammonia
NH_4	Ammonium
NH_4-N	Ammonium nitrogen
NH_4OH	Ammonium hydroxide
H_2SO_4	Sulphuric acid
NaCl	Sodium chloride
KCl	Potassium chloride
HPO_4	Hydrogen phosphate

$NaOH$	Sodium hydroxide
$MgNH_4PO_4$	Struvite
$MgCl_2$	Magnesium chloride
K_2HPO	Dipotassium hydrogenphosphate
$CaSO_4 * 2H_2O$	Calcium sulphate dihydrate
$MgCl_2 * 6H_2O$	Magnesium chloride heptahydrate
CH_3COOH	Acetic acid
$CH_3CH_2CH_2COOH$	Butyrate
CH_3CH_2COOH	Propionate
$HCOOH$	Formic acid

1 Introduction

The first chapter of the present work provides a short overview of biogas utilization in Austria, governmental restrictions and the resulting challenges on digestate processing nowadays. Based on this information, the goal of the thesis is developed.

1.1 Motivation

To limit global warming to well below 2°C, as stated at COP 2015 (Convention on Climate Change), CO_2 emissions have to be reduced drastically. A major sector to reach this goal is the energy production, whereas the goal is to increase the amount of energy produced from renewable energy resources from 16% in 2014 to 20% until 2020 and to 27% until 2030 [1] [2]. Therefore, the energy utilization with biogas became more important as well. Approximately 400 biogas facilities are presently operated in Austria, around 300 of them produce 560 GWh of 'green' energy for the grid. Such plants use feedstocks like energy crops, animal manure or organic waste (e.g. slaughterhouse waste or food leftovers) [3]. The remains of the biogas utilization, the so-called digestate, is used as a fertilizer for agricultural areas. Since the disposal of the digestate is regulated by the *Austrian Fertilizer Ordinance* and the *Drinking Water Ordinance* it has become an important economical factor for the plant operators [4] [5]. A first improvement of digestate processing is the separation of the digestate into a solid and a liquid fraction to reduce disposal costs and to gain a fertilizer from the solid fraction [6]. Food left overs as feedstock lead to high salt concentration particularly sodium chloride, in the liquid digestate fraction. The salts have a negative effect on the soil and waters and therefore the disposal is limited in respect to the available spreading area [7]. To reduce disposal costs and probably enable disposal, the liquid fraction needs further purification.

1.2 Objective

Since possibilities for the purification of salt containing liquid digestate (e.g. evaporation, ion exchange) are very energy and/or cost intensive, the goal of this study is to find alternative processes respectively process combination for liquid digestate purification. Boundary conditions for water purity is the usage as process water within the biogas facility or direct discharge. The fraction with high salt content should be reduced in its volume as much as possible to keep the disposal costs low.

The present work focuses on the described problems in three parts. First, a literature research on digestate treatment technologies is performed. Based on the literature research a decision matrix according to TIPS methodology is developed. Outcome of this part of the thesis is an objective view on the problem and a suggestion of useful technologies. The second part covers an experimental investigation of promising methods and the evaluation of their efficiency. Based on the results of the laboratory experiments, a proposal for reasonable purification processes is developed in the third part. The processes are modeled and investigated on the influence of recycling of the purified process water within the biogas utilization process. Furthermore, the effectivity of a nutrient recovery step is modeled.

2 Theory

This chapter gives an overview about the biogas production process, the used substrates in biogas plants and the principle processes, which are taking place during the fermentation of the feedstock. In addition, the chemical composition and the different treatment methods of the digestate are explained.

2.1 Overview of the biogas production process

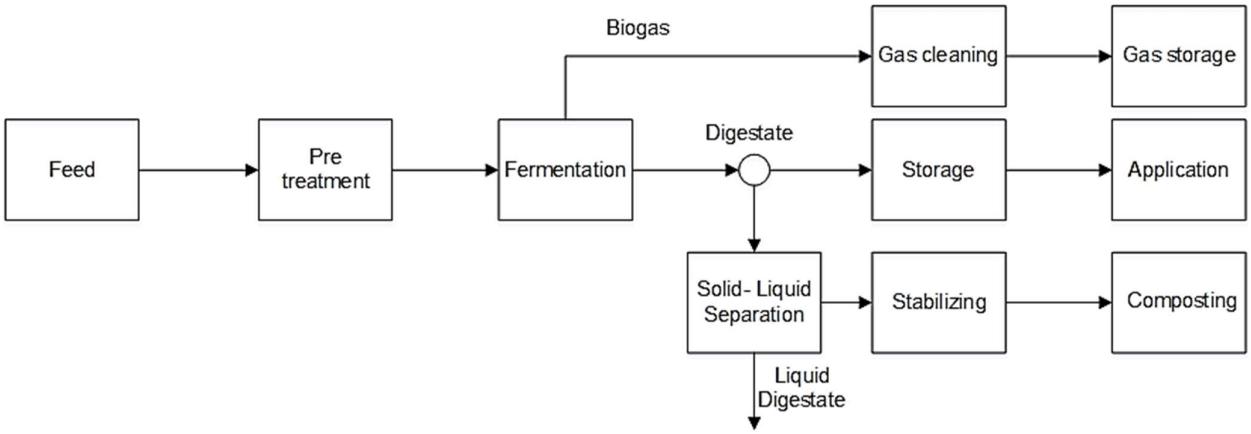

Figure 1: Process chain of the biogas production

Figure 1 shows the schematically flowchart for a biogas production. Prior to the fermentation process, feed pre-treatment ensures optimal process conditions. Due to the pre-treatment, the biogas yield increases and the feedstock is homogenized. The pre- treatment is performed physically (e.g. milling, heating), chemically (e.g. lignin disruption, hemicellulose break down) or biologically (e.g. speed up substrate degradation) [8][9]. In case of slaughterhouse residues as feedstock, sterilization is required to ensure no negative effect caused by germs on the microbiological fermentation process. By sterilization the feedstock components are thermally macerated and therefore easier to metabolize for the bacteria [10]. After the pre-treatment, the feed enters the fermenter. Typically the feed contains carbohydrates, fats, proteins, sugars, starch, cellulose, volatile fatty acids and pollutants [11]. Anaerobic bacteria convert the feedstock components into methane (50-75 vol%), carbon dioxide (25-50 vol%) and others (1-7 vol%) [12]. Table 1 summarizes the approximate chemical composition of biogas [13].

Table 1: Chemical composition of biogas

Compound	Chemical formula	Concentration [vol%]
Methane	CH_4	50-75
Carbon dioxide	CO_2	25-45
Water	H_2O	2-7
Hydrogen sulphide	H_2S	< 2
Nitrogen	N_2	< 2
Oxygen	O_2	< 2
Hydrogen	H_2	< 1

The fermentation process is performed either wet or dry. The main difference between wet and dry processes is the dry substance content. For wet fermentation the dry substance content is < 15 %, for dry fermentation > 25 % [10] [14]. Further, the fermentation process depends on the feedstock properties, the effort in substrate pre-treatment and technical facilities like pumping systems. The produced biogas undergoes cleaning before it is stored for further use like the electricity production [10]. The cleaning is necessary because the biogas contains impurities like water, hydrogen sulphide, ammonia, oxygen or nitrogen. These substances can lead to corrosion or mechanical abrasion. In addition, the impurities could lead to undesirable combustion emissions [15]. The residue in the fermentation is called digestate. It has a high content of plant nutrients, like nitrogen or phosphorus. Direct disposal on agricultural areas is possible. The disposal of digestate however is subject to restrictions like the nutrient ordinance that regulates the amount of nutrients that are allowed to be applied on fields (see Section 2.6). To meet the nutrient regulations of the government the digestate has to be stored before spreading. Another possibility is the separation of the digestate into a solid- and a liquid fraction. The solid fraction is stabilized and composted, the liquid fraction undergoes further purification steps (see Section 2.5.4) for nutrient recovery or is used for mashing of the feedstock if the substrates have a high proportion of solid content [6].

2.2 Feedstock for biogas utilization

The feedstocks used for biogas production are the following:

- Agricultural residues (slurry, animal droppings, energy crops)
- Industrial residues (organic waste, by-products from food industry)
- Municipal residues (household waste, food leftovers)
- Others (slaughterhouse residues, spent grain from breweries or residues from the biodiesel industry)

Due to the anaerobe bacteria content, low price, good availability and the ability to act as a solvent for co- substrates (e.g. energy crops, sewage sludge) agricultural residues are most often used as feedstock for the biogas production. To compensate the low yield of methane organic waste or biogenic residues are added [11]. To determine the ideal substrate combination different parameters need to be taken into account:

- Potential biogas yield
- Dry matter content (DM)
- Organic content
- Carbon to nitrogen ratio (C:N)
- Organic dry matter (oDM)

Table 2 sums up the properties of selected feedstocks [11] [13].

Table 2: Feed substrates

Feedstock	C:N	DM [%]	oDM [% of DM]	Biogas yield [m³/kgoDM]
Animal wastes & by-products				
Pig slurry	3 - 10	7	75	0.2 – 0.36
Cattle slurry	6 - 20	8.5	80	0.2 -0.26
Pig manure	3 - 8	35	85	0.2 – 0.3

Feedstock	C:N	DM [%]	oDM [% of DM]	Biogas yield [m³/kgoDM]
Cattle manure	5 - 15	25	80	0.2 – 0.3
Chicken manure	3 - 10	70	77	0.2 – 0.43
Energy crops				
Corn silage	-	29 - 34	85 - 95	0.68 – 0.86
Barley	-	33	93	0.73
Triticale	-	41	95	0.74
Weed silage	20	35	91	0.54
Organic residues				
Leftovers	-	87	87	0.5 - 0.6
Gardening residues	-	60 - 70	90	0.2 – 0.5
Apple pomace	-	8	98	0.68
Rape cake	-	90	82	0.63

Table 2 show, that the slurry or the manure from animals is a suitable feedstock because of their high C:N (carbon to nitrogen) ratio and the nutrient concentration, which support the growth of anaerobic bacteria during the fermentation process. Furthermore, animal waste has a high pH buffer capacity. The negative aspect of these substrates is that either low dry matter content of the slurry or the straw content in animal manure negatively affect the biogas yield. Straw contains a lignocellulose fraction, which anaerobic bacteria are not able to metabolize. To achieve a high methane yield it is useful to co-digest agricultural residues with energy crops or organic residues because of the high amount of organic dry matter (oDM) [11].

2.3 Feedstock composition in Austria

Feedstock for biogas plants in Austria differ due to geographical reasons. In southern and eastern Austria, typically renewable resources for example corn or grass silage are preferred. In western Austria, the content of agricultural residues in the feedstock is higher. Moreover, the amount of organic residues used has increased over the last years. Figure 2 summarizes data from 2014 of substrates used in biogas facilities in Austria [16].

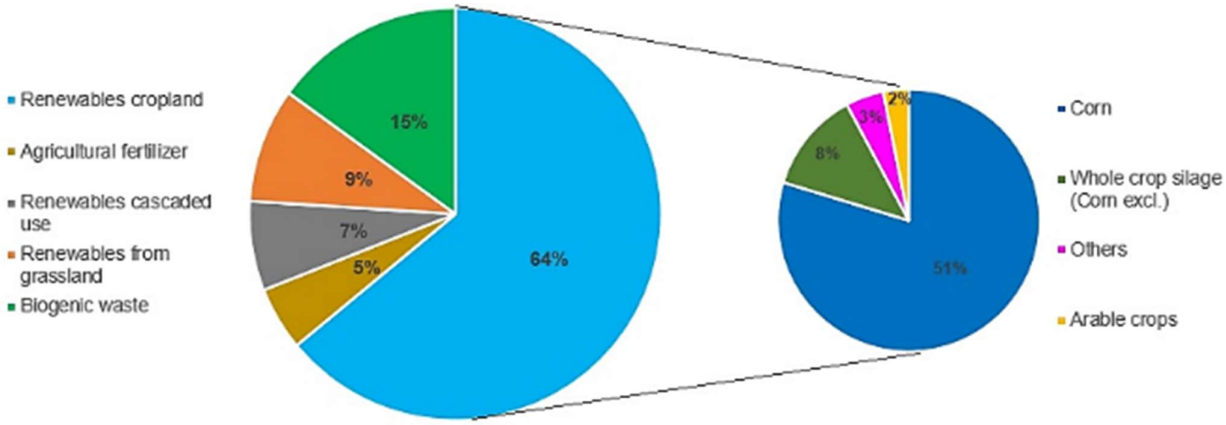

Figure 2: Use of different feedstock substrates in Austria. Source [16]

The data given in Figure 2 are from the "*ARGE Kompost and Biogas"* in Austria in the year 2014 and represent 147 biogas production facilities in Austria. Percentage shares refer to the produced energy. Concerning the renewables related to crops, corn accounts for the main amount of energy generated [16]. Approximately 300 biogas plants in Austria supply 560 GWh electricity for the power grid. This is one-tenth of the electricity consumption in Vienna in the year 2014 [17].

2.4 Utilization of biogas

The organic substance in the feedstock is converted to biogas through anaerobic fermentation. The main fermentation product is methane (CH_4). The by-products are carbon dioxide (CO_2), water (H_2O), oxygen (O_2), hydrogen sulphide (H_2S), hydrogen (H_2) and nitrogen (N_2) (see Table 1).

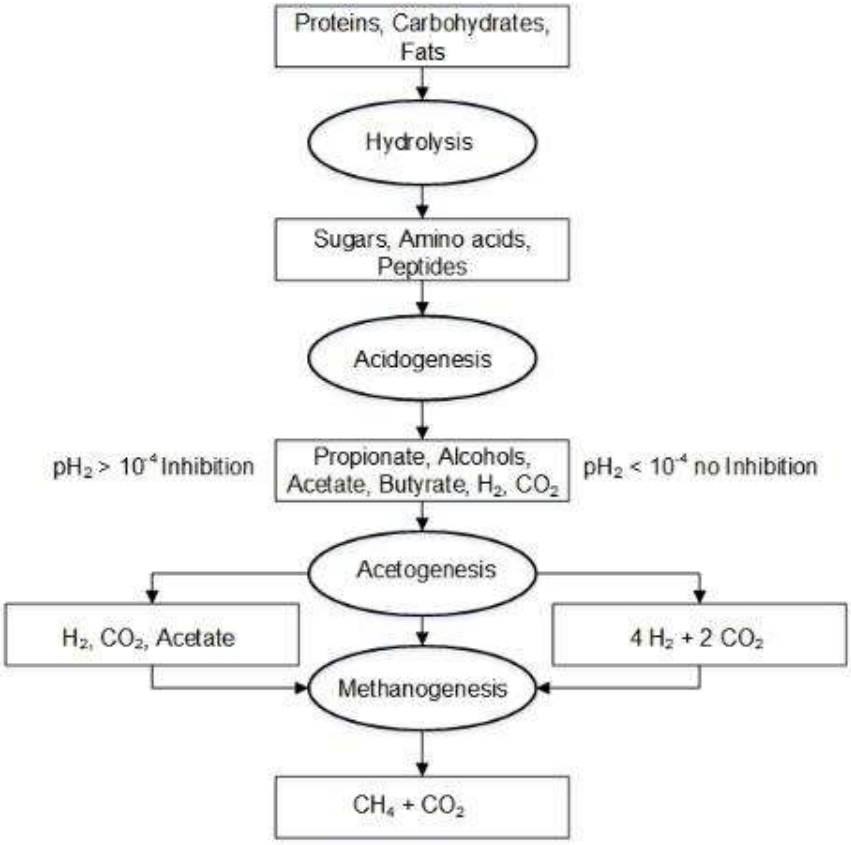

Figure 3: The four stages of the anaerobic digestion. Source [7]

Figure 3 shows the transformation of the feedstock into methane. Anaerobic digestion consists of four stages and different types of bacteria dominate each stage. The stages of anaerobic digestion are [14]: Hydrolysis, Acidogenesis, Acetogenesis and Methanogenesis.

As in Figure 3 shown, the first stage of the anaerobic digestion is hydrolysis, where hydrolytic bacteria convert complex polymers, like proteins or carbohydrates, into soluble monomers or oligomers (sugars, amino acids, peptides). In the second stage, the acidogenesis, fermentative bacteria metabolize the monomers and oligomers from hydrolysis into fatty acids (propionate, butyrate) and other products like alcohols,

hydrogen and acetate. An important factor regarding the produced substances at the acidogenesis is the process inhibition through the influence of the hydrogen partial pressure (p_{H2}). An excess of substrates ($p_{H2} > 10^{-4}$ bar) lead to the formation of butyrate and propionate. A limitation of substrates ($p_{H2} < 10^{-4}$ bar) lead to the formation of hydrogen (H_2), carbon dioxide (CO_2) and acetate. The hydrogen partial pressure should be $p_{H2} > 10^{-4}$ bar for optimal methane production. In the next step, the acetogenesis, organic acids and alcohols are converted by the influence of acetogenic bacteria to acetate, acetic acid, hydrogen and carbon dioxide. The reaction equations below show the chemical transformation of butyrate (1) and propionate (2) to acetate in the stage of acetogenesis [14].

$$CH_3 - CH_2 - CH_2 - COOH + 2\,H_2O \rightarrow 2\,CH_3 - COOH + 2\,H_2 \quad (1)$$

$$CH_3 - CH_2 - COOH + 2\,H_2O \rightarrow CH_3 - COOH + CO_2 + H_2 \quad (2)$$

The reaction products H_2 and acetate always have to be used up to ensure an effective biogas utilization. Therefore, the proximity of the acetogenic and methanogenic bacteria plays an important role, which is provided by soft mixing of the fermentation broth [18]. The final step of the utilization of methane through anaerobic digestion is the methanogenesis. Thereby methanogenic bacteria convert products of the acetogenic step. The bacteria metabolize hydrogen and carbon dioxide (Equation (3)), formic acid (Equation (4)) and acetate (Equation (5)) mainly to methane, water and carbon dioxide [14].

$$4\,H_2 + CO_2 \rightarrow CH_4 + 2\,H_2O \quad (3)$$

$$4\,HCOOH \rightarrow CH_4 + 3\,CO_2 + 2\,H_2O \quad (4)$$

$$CH_3 - COOH \rightarrow CH_4 + CO_2 \quad (5)$$

2.4.1 Influencing process parameters

To achieve optimal methane yield through anaerobic digestion the parameters for the ideal bacteria environment need to be addressed. As mentioned before the different steps of biogas production need different types of bacteria. Each bacteria have a certain region of pH-value, temperature, oxygen content and redox potential where they work best. Moreover, factors like mixing, residence time, solids- and water content influence the reaction and hence the overall biogas yield. Besides pH value and oxygen content the temperature is very important for the biogas production, because bacteria growth is limited or even may stop by an increase of the process temperature [14].

2.4.1.1 Feedstock preparation

Homogenization of the feedstock before entering the fermenter positively affects the mass transfer in the reactor, but the resulting sheer forces through mixing could negatively affect the proximity of the acetogenic and methanogenic bacteria, which is necessary for untroubled methanogenesis (see Section 2.4). Therefore, mixing is performed considering the sheer resistance of the substrate aggregates. The shorter the proximity of the acetogenic to the methanogenic bacteria, the more effective is the transport of the hydrogen to the methanogenic bacteria, which produce methane (see reaction equations (1) and (5)). As a result, one has to take into account that the positive effects of mixing is reliant to the sheer stability of the bacteria [14].

2.4.1.2 Residence time

The residence time of the biomass in the reactor is of importance because if it is lower as the doubling time of the bacteria culture, the bacteria leave the reactor with the removed biomass and lead to an incomplete conversion. Additionally, the residence time regulates the degradation grade of the substrates. The longer the residence time of the substrates in the fermenter the more efficient is the process. In conventional biogas utilization from solid waste like crops or food leftovers, the risk of bacteria wash-out is negligible because the residence time is sufficient. That way even slower growing bacteria have enough time for optimal growing [14] [18].

2.4.1.3 Process pH- value

The pH level in the biogas reactor depends on the feed composition, the mineral acids (e.g. HCl, H_2SO_4) and the bases (e.g. NH_4). In the stage of acidogenesis, the pH level

decreases because of the formation of organic acids. Through acetogenesis and methanogenesis, the organic acids are metabolized and the pH level increases. The pH range at hydrolysis and acidogenesis should be 5.2 to 6.3 while the pH should range around 6.7 to 7.5 in the stages of acetogenesis and methanogenesis. These ranges show that the optimal pH level during the digestion process should not descend below 6.7 because the acetogenic and methanogenic bacteria are very sensible to low pH values [14]. Furthermore, the concentration of nitrogen influences the process. The digestion is inhibited, if the nitrogen concentration is too high. This depends on the NH_4-NH_3 equilibrium, whereas ammonia is known to be more toxic for methanogenic bacteria than ammonium ions are. The equilibrium is a function of pH value and temperature. Starting at a pH value of 7 the concentration of ammonia increases. Therefore, the pH values should stay below 7 to prohibit the arising of ammonia [19] [20] [21].

2.4.1.4 Process temperature

Regarding the temperature range for the digestion process empirical measurements show that the growth of micro bacteria can take place from freezing level up to 100 °C [14]. Methane reactors could work in a psychrophilic (<10 to 20 °C), mesophilic (20 to 40 °C) or thermophilic (45 to 65 °C) range. Usually the reactors are operated mesophilic at 35 to 38 °C because of ideal yield rates and low energy expense. Higher temperature levels up to 60 °C would lead to a slightly higher yield and sterilizes the digestate, however process stability would be negatively affected. Sterilization of the digestate could be relevant if animal wastes are digested [11] [14].

2.4.1.5 Oxygen content and redox-potential

The bacteria, which enable the methane formation, only survive in an anaerobic environment. Hence, the presence of oxygen during the fermentation process has to be prevented. In addition, the methanogenic bacteria need a negative redox potential from -200 to -400 mV for their growth [14]. Research has shown that up to an oxygen concentration of 10% oxygen bacteria are not harmed [21]. An alteration of the redox potential during the fermentation process is regulated by methanogenic bacteria [14]. Another aspect regarding the oxygen concentration within biomass digestion is the risk of explosion. Therefore, the oxygen content has to be monitored to decrease the possibility of explosions or fire cases due to the oxygen content [22]. A positive aspect

of the oxygen presence is given, if H_2S is present within the fermenter. Due to the oxygen, microorganisms oxidize H_2S to sulphur and sulphates. H_2S is known to be toxic for humans and animals and furthermore could lead to corrosion [23].

2.5 Fermentation residue - Digestate

As mentioned before digestate accrue in the biogas production facility. The quantity of the digestate depends on the mass loss of the used substrates and the inserted water from cleaning procedures or mashing. Mass loss of the used substrates depends on the content of organic dry matter, residence time, biological degradability and the process temperature. Typical values for mass loss are 3 % for slurry, 20 – 30 % for silages and 70 – 80 % for grain [6]. To estimate the mass of the digestate, one can assume 32 % average content of organic dry matter and 79 % organics degradation lead to roughly 25 % of the feedstock mass that leaves the fermenter as biogas [6]. Taking the amount of the inserted water into account, one can point out that 850 kg digestate arise per 1000 kg feedstock. For the calculation of the digestate amount and the mass loss equations (6) and (7) are applied [6].

Mass balance:

$$m_{digestate} = m_{feedstock} - m_{loss} + m_{water} \tag{6}$$

$$m_{loss} = \frac{V_{biogas} * (x_{methane} * \rho_{methane} + x_{CO2} * \rho_{CO2})}{m_{feestock}} \tag{7}$$

2.5.1 Chemical composition of the digestate

The digestate from biogas facilities has a high potential for the fertilization of agricultural areas. Three groups of digestate constituents need to be mentioned [6]:

- Nutrients
- Organic components which improve the soil quality
- Pollutants which could impede the agricultural processing

For use of digestate as fertilizer, the most important nutrients are nitrogen, phosphorus and potassium. Furthermore, calcium, magnesium, sulphur, sodium and chloride are worth mentioning. The digestate mainly consists of nutrients but also the concentration

of organic components, which act as a humus layer and therefore improves the soil quality, is of interest. During the digestate treatment, where it is separated into a solid and a liquid fraction, the essential nutrients are differently enriched in the two phases. The nitrogen occur as ammonium-nitrogen (NH_4-N) mostly in the liquid phase and as a component bound in the solid fraction of the digestate. While the ammonium-nitrogen as a nutrient is directly available to plants, the bound nitrogen in the organic fraction is enriched in the soil and has a long-term fertilizing effect. The water- soluble phosphate ion PO_4^{3-} is released from organic compounds and is primarily constituted in the solid digestate fraction after the separation step. As a nutrient, it is instantly available to plants because of its weak digestate bonding. Potassium in the digestate occurs mainly dissolved in the liquid fraction. The second important group of digestate constituents are the organic components. The degradable organic fraction forms a humus layer and therefore supports the ability to keep water and nutrients in the soil. This relation shows that the solid digestate fraction has a high benefit when it is applied on agricultural areas, and is instantly used as a soil conditioner. As mentioned before digestate can contain a pollutant fraction too. The pollutants are heavy metals like cadmium, chromium, mercury, lead, copper, nickel and zinc or also organic pollutants like antibiotics, pesticides, aromatics or halogenated hydrocarbons. The heavy metal fraction stays within the solid fraction of the digestate. In general, if the substrates from food for humans or animals are used the concentration of heavy metals is negligible. It is worth mentioning that pig slurry, municipal or industrial waste have an increased concentration of heavy metals [6]. The agricultural use is generally regulated based on concentration limits of heavy metals given in the Austrian fertilizer ordinance [4]. In the case of harmful organic substances in the digestate, research has shown that their concentration is negligibly small [6].

As mentioned above the used feedstock defines the type of pollutant in the digestate. If municipal or industrial waste like food leftovers or by-products from food production are components of the feedstock, it is most likely that the digestate contains a certain amount of salts like sodium chloride or alike. These salts remain dissolved in the liquid fraction of the digestate after separation operations. The negative aspect of salts in the digestate is that they downgrade the fertilizer effect and furthermore pollute soil and waters [7] [24]. If the concentration of salts like sodium chloride is too high, the spreading on agricultural areas is forbidden respectively limited in respect to the

spreading area and therefore the salt containing digestate may has to be disposed separately. These facts emphasize the necessity of an effective digestate treatment process that is investigated in this work. Analysis of the used digestate for the experiments, which contains high salt loads are summarized in Section 5.2.

2.5.2 Digestate treatment

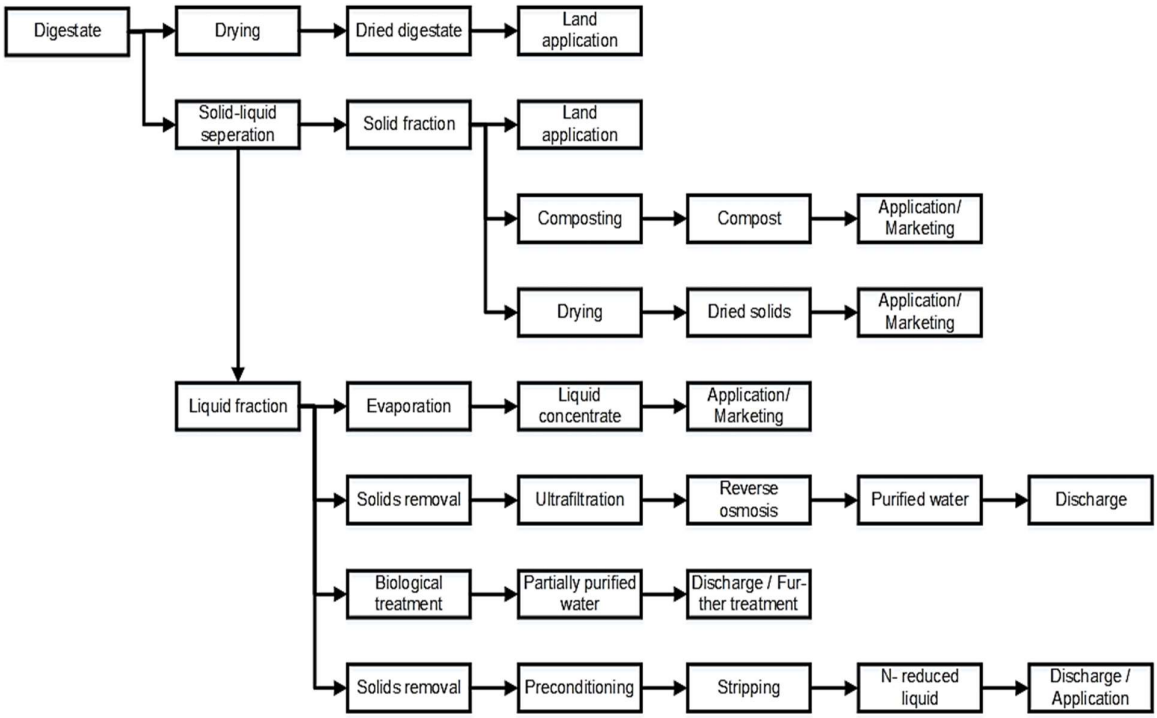

Figure 4: Digestate processing methods. Source [25]

This section deals with basic treatment methods, which are applied in digestate processing. At first, an overview of the possible processes is given. Based on that the approaches for solid and liquid digestate processing are explained in detail. Furthermore, the resulting challenges within digestate processing are highlighted.

As the process chain in Figure 4 shows, the first possibility for digestate processing is the direct application of the digestate on agricultural areas or for sale and trade as a nutrient source. The process step drying is performed rarely. If the digestate is separated into a solid and a liquid fraction, latter can be purified and disposed. Another possibility is to integrate the liquid digestate into a value chain for nutrient recovery through stripping, evaporation or other techniques which are discussed later [25].

2.5.3 Processing of the solid digestate

The two main reasons for the solid–liquid separation of digestate is the dewatering of the digestate and the reduction the solid content in the liquid fraction. Purification steps of the liquid fraction require a low solid content. Screw press or decanter centrifuge are the most common techniques applied for solid-liquid separation [6].

2.5.3.1 Screw press separation

Figure 5 shows the principle of a screw press separator, which consists of a screw rotating in a cylindrical sieve. The digestate is pumped into the aggregate and transported through the screw press. The liquid fraction leaves the press through the cylindrical sieve and is drained by a sieve basket in the middle of the separator. To influence the solids concentration resistor flaps are installed at the end of the aggregate. In combination with an increasing auger diameter, the solid fraction is compressed at the separator end and separation effectiveness increases. Solids separation efficiency can be regulated through the width of the sieve holes, but solid particles that are smaller than one millimeter are most likely in the liquid fraction [25].

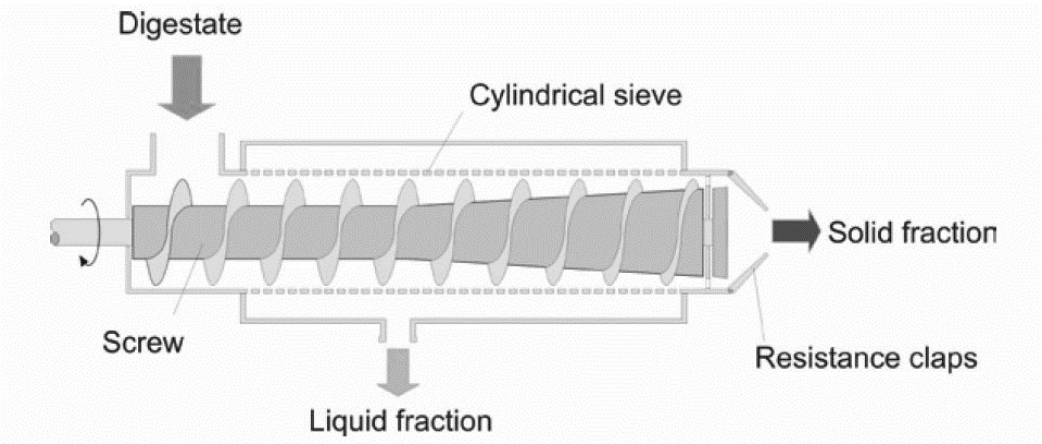

Figure 5: Screw press schematics. Source [25]

The separation efficiency mainly depends on the digestate properties, dry substance, fiber content and the screw press settings. Typical concentrations after the separation are 48 % dry substance content in the solid fraction [6].

2.5.3.2 Decanter centrifuge

The decanter centrifuge (see Figure 6) uses centrifugal forces and the sedimentation effect to separate small particles and colloids from the digestate. It consists of a rotating sheath drum and a transport auger, which is inside the drum. The screw has a higher rotating velocity as the sheath drum. Through an inlet pipe and the hollow auger, the digestate continuously enters the centrifuge in the middle. Based on centrifugal forces the solid fraction deposits on the drum wall and is transported out of the centrifuge by the screw. The liquid fraction flows towards the end of the cylindrical section of the sheath drum where fine particles sediment and then leave the aggregate through a level plate. The separation efficiency is influenced by drum speed, screw speed, height of the level plate and the digestate volume flow. Often flocculation additives are added to support the separation process [25].

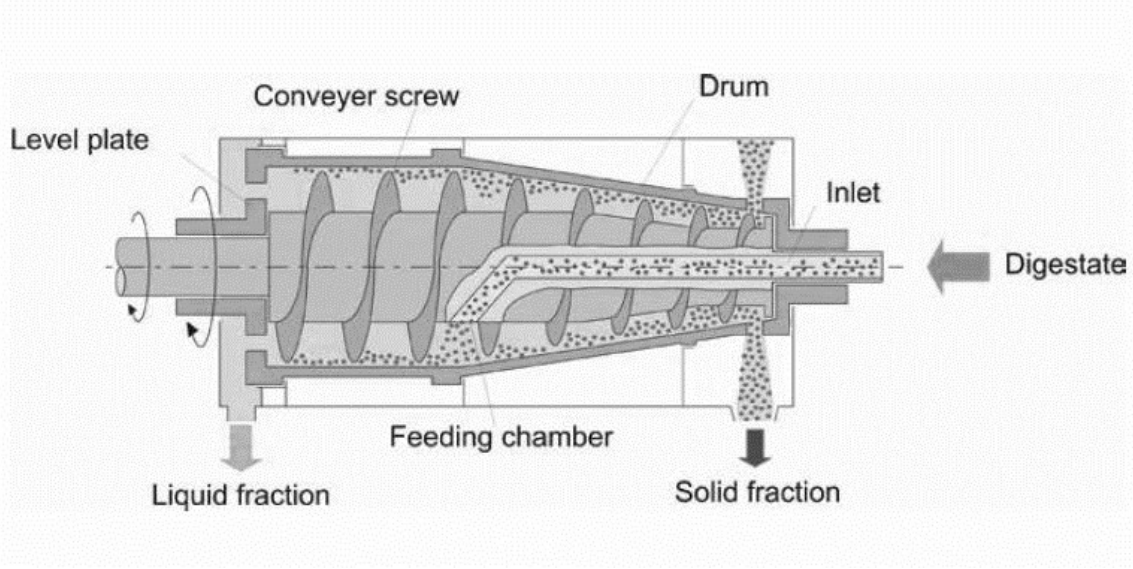

Figure 6: Decanter centrifuge schematics. Source [25]

The main advantage of a decanter centrifuge compared to a screw press is the better separation grade and thereby less solid particles in the liquid digestate fraction. However, on the contrary it comes along with higher investment costs and energy consumption. Theoretically, 59 % dry substance content in the solid fraction is possible [6].

There are two other techniques, which are applied to separate the digestate: a belt filter and discontinuously working centrifuges. Their application is rare and not

discussed in detail, it is referred to the relevant literature [6] [25]. If there is a necessity for further solids removal after the major purification step other techniques like precipitation, flocculation, flotation and vibrating screens are applied. They are indispensable if further liquid fraction purification through membrane processes follows. After the separation of the solid fraction, the digestate has about 20 - 30 % of dry matter concentration and can be applied on agricultural areas as a fertilizer or soil improver. If the solid fraction is desired for marketing it has to be stabilized through composting or drying [25].

2.5.3.3 Composting

Compost is formed under influence of microbes, which metabolize the organic material in the solid digestate under aerobic conditions. Compost releases nutrients over a long time span and contains humic substances, which improve the soil. For the composting process of solid digestate, bulking material (e.g. woodchips) has to be added because of the digestate's level of moisture and partial degradation. Further, such material provides a stable aerobic degradation process [6].

2.5.3.4 Drying

The application of drying stabilizes and reduces the mass of the solid digestate. Another advantage is the high nutrient concentration due to the mass loss of the fraction. The heat demand can be provided by solar power or excess heat from a combined heat and power biogas facility. Generally belt dryers are used for the drying process [25].

2.5.4 Processing of the liquid digestate

After the solid-liquid separation, the remaining liquid fraction contains nutrients like ammonium nitrogen (NH_4), potassium (K), sulphur (S) and about 5 % dry substance content too. If the feedstock has a high solid content, the liquid fraction can be recycled for mashing purpose at the stage of anaerobic digestion. The used amount of mashing liquid depends on the degree of dryness of the feedstock and on the effect of concentration of key substances for the anaerobic digestion like NH_4-N or salts (see Section 2.4). The benefit of liquid digestate recycling is the reduced volume of the liquid fraction, which has to be treated further on. Recycling of the liquid fraction leads to lower expenses for the treatment of the remaining liquid digestate fraction. The

following purification processes aim to achieve water qualities that allow one side releasing the water into the environment and on the other side get a nutrient enriched liquid phase [6] [25].

2.5.4.1 Mass transfer purification methods

Common purification methods of digestate are stripping or evaporation. The different types and processes are described in the following sections.

Stripping

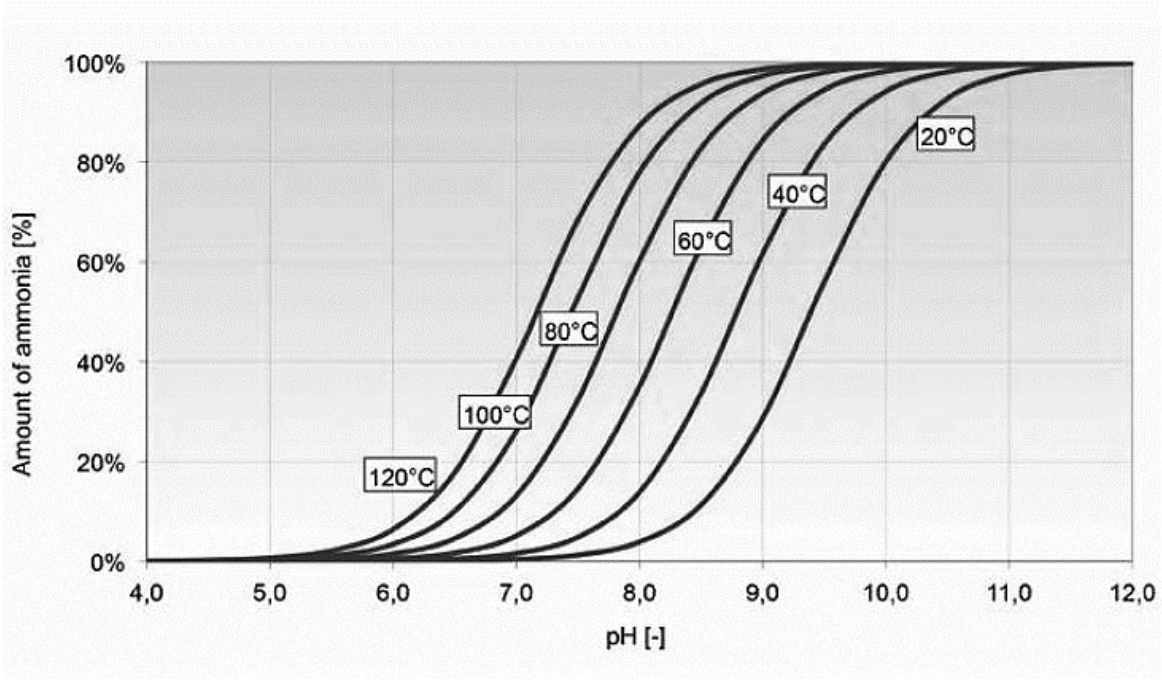

Figure 7: Ammonia volatility. Source [6]

The main goal of stripping in digestate processing is to recover ammonia from the liquid phase to get a nitrogen rich liquid fertilizer. Mass transfer of the volatile ammonia from the liquid into gas phase achieves the nitrogen enrichment. The gaseous phase is therefore conducted through the liquid fraction of the digestate. The volatility of ammonia in the liquid digestate depends on the pH value and the temperature (see Figure 7). Higher temperature levels may be achieved by the usage of excess heat from the biogas facility whereas an increasing pH value is realized through alkali addition or carbon dioxide (CO_2) drive out.

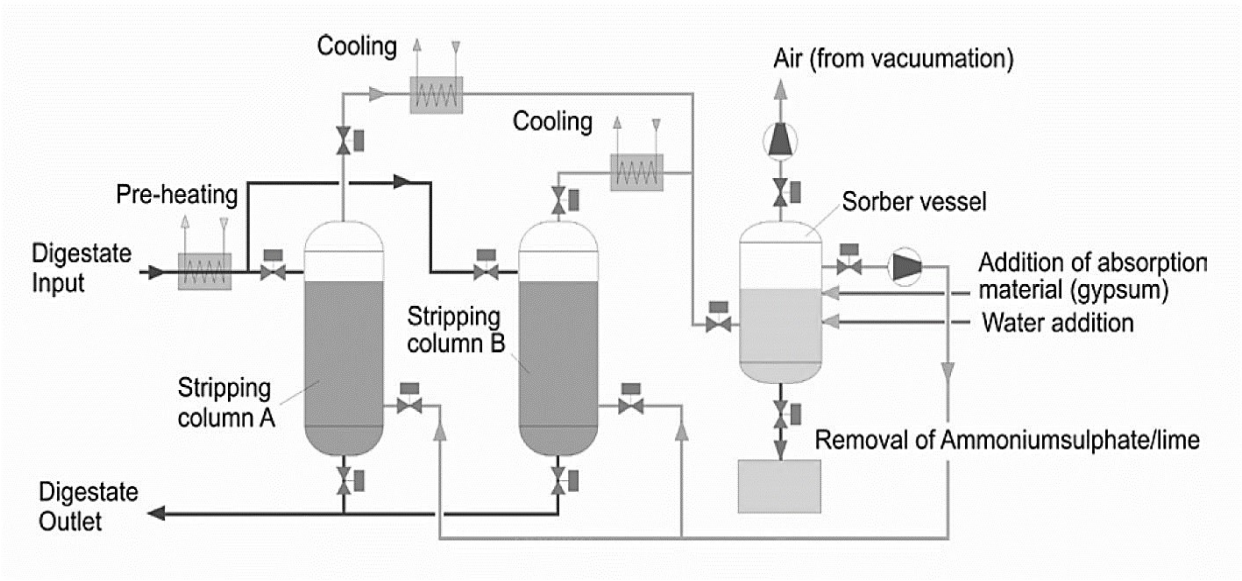

Figure 8: Air stripping process. Source [25]

Two ammonia-stripping methods are commonly used: air or vapor stripping. Both stripping processes are conducted in packed columns for an efficient mass transfer. Using air stripping first driving out of the CO_2 is performed from the pre-heated digestate. Then, the liquid enters the column and the ammonia is transferred to the stripping air. After the stripping process, ammonia is scrubbed with sulphuric acid in a column. The scrubbing has the advantage that the cleaned gas can be sent back into the stripping column and an ammonium sulphate fertilizer is produced [25]. An overview of a stripping process combined with scrubbing is shown in Figure 8. Here, ammonia is adsorbed on gypsum; lime is formed, which again is used as fertilizer.

The second method used is stripping with hot steam where the ammonia is transferred to the vapor phase. Due to steam production, higher temperatures are required. This method lead to ammonia present in the liquid phase after condensation, the last scrubbing stage is not needed. The ammonia water mixture has an ammonia concentration from 25-35 % and suits well as a fertilizer. A problem arising regarding stripping is that remaining solids in the liquid fraction may plug the packing of the column, hence a solid-liquid separation before the stripping process is required. Other disadvantages are the maintenance and regular cleaning of the column [25]. The main advantage of stripping is the generation of a fertilizer for sales and marketing [24].

Evaporation

The purpose of evaporation is to reduce the volume of the digestate fraction significantly and to get a liquid concentrate with ammonia and volatile acids [26]. Due to its high energy demand the evaporation heat has to be provided from excess heat of power plants or other sources around the facility. Figure 9 shows a common evaporation process. In the first step the solid digestate fraction is removed by solid-liquid separation. To ensure that the ammonia remains in the concentrate the pH value is lowered through the addition of sulphuric acid. Before a multistep evaporation process, the CO_2 is driven out in the degassing step. The advantage of the multistage evaporation is, that it works under low pressure and hence low temperature levels of about 90°C. The vapor fraction is condensed afterwards and contains ammonia and volatile acids. The use of the condensate as process water is possible as well as further purification to e.g. purified water [25].

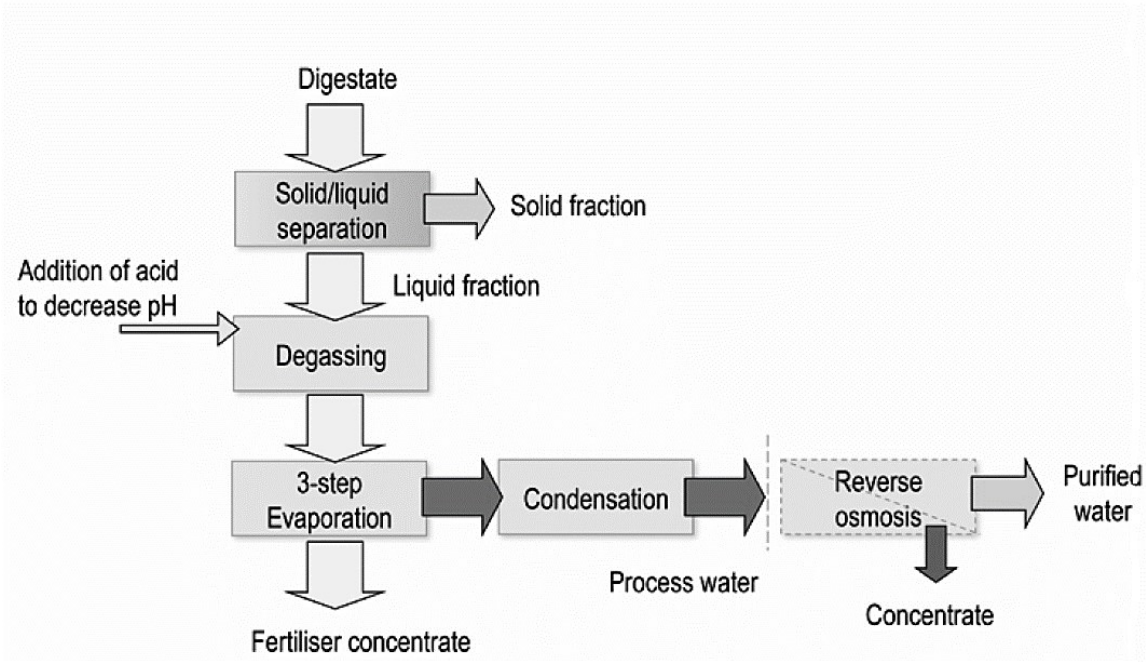

Figure 9: 3-step evaporation process. Source [25]

2.5.4.2 Reactive purification methods

Besides mass transfer purification methods, reactive techniques for digestate processing are applied. Techniques used are the precipitation of phosphorus or ion

exchange. Which technique is applied depends on the strategy of digestate processing [27].

Precipitation

For the precipitation of phosphorus, also called struvite or MAP precipitation, magnesium ions are added into the liquid digestate to form phosphate salts. The ammonia is precipitated too according to reaction equation given in equation (8) [26]:

$$Mg^{2+} + NH_4^+ + HPO_4^{2-} + OH^- + 5\,H_2O \rightarrow MgNH_4PO_4 * 6\,H_2O \quad (8)$$

To achieve the best precipitation yield, the ratio of magnesium: ammonium: phosphate (MAP) should range around 1.3:1:0.9. As ammonia is most likely the main component in the digestate the addition of magnesium oxide and phosphoric acid is necessary. This step increases the pH value to 8.5 - 9.0. The outcome of the precipitation reaction is struvite, which again has good fertilizer abilities based on its key components nitrogen, phosphate and magnesium. A negative aspect of the struvite precipitation is the required amount of chemicals, which lead to high costs [25].

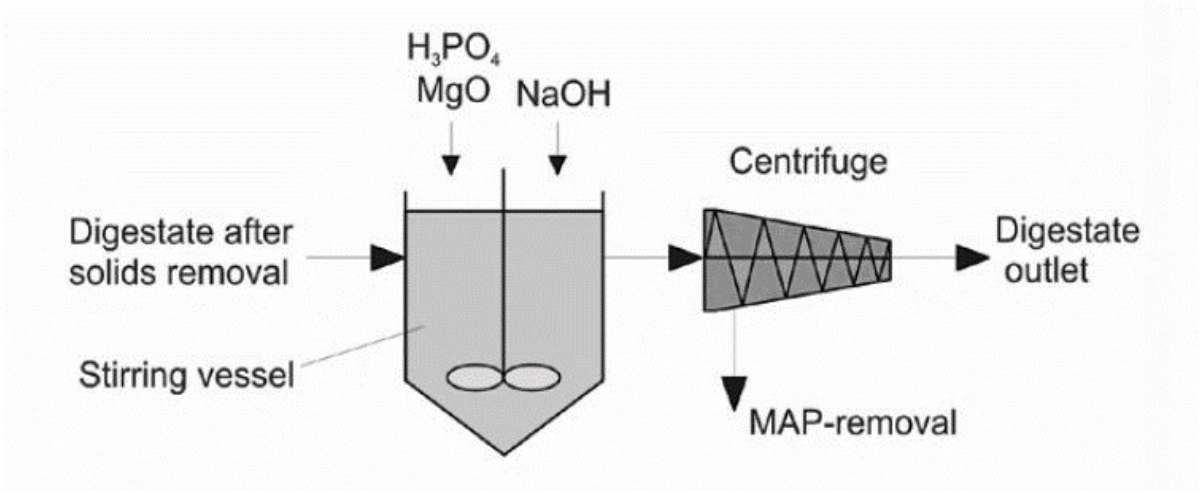

Figure 10: Struvite precipitation process. Source [25]

Figure 10 shows a possible struvite precipitation process where the chemicals are added in a stirring vessel and the precipitated struvite is separated by a centrifuge after the vessel.

Ion exchange

The principle of this process is the transfer of ions from the digestate (e.g. ammonia) into the ion exchange material by the replacement of ions located in the used exchange material. Typically, synthetic resins or zeolites are used.

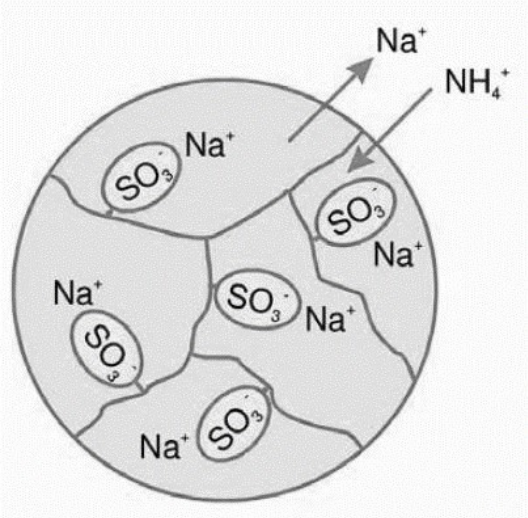

Figure 11: Process of ion exchange. Source [6]

The advantage of resins is the higher ion acceptance capacity compared to zeolites but resins are more cost intensive than zeolites [6]. The basic process of the ion exchange is shown in Figure 11.

The use of ion exchange materials requires a regeneration step. Regeneration reagents are sodium chloride, acids or bases. The porous structure of the resin lead to blocking by solids present in the digestate. If the pores are blocked the ion exchange effectivity is lowered. Hence the application of ion exchange is only reasonable when it is used as a post treatment stage after membrane operations for the recovery of ammonia [25].

2.5.4.3 Filtration operations

Additionally to mass transfer or reactive purification methods of liquid digestate, the purification by pressure driven membrane processes has gained in importance [6]. The main advantage of membrane processes is, the applied type of filtration operation can be selected in respect to the medium and its components, like solids or dissolved salt. The used membrane decides which component is rejected in respect to its pore size and the trans-membrane pressure [27].

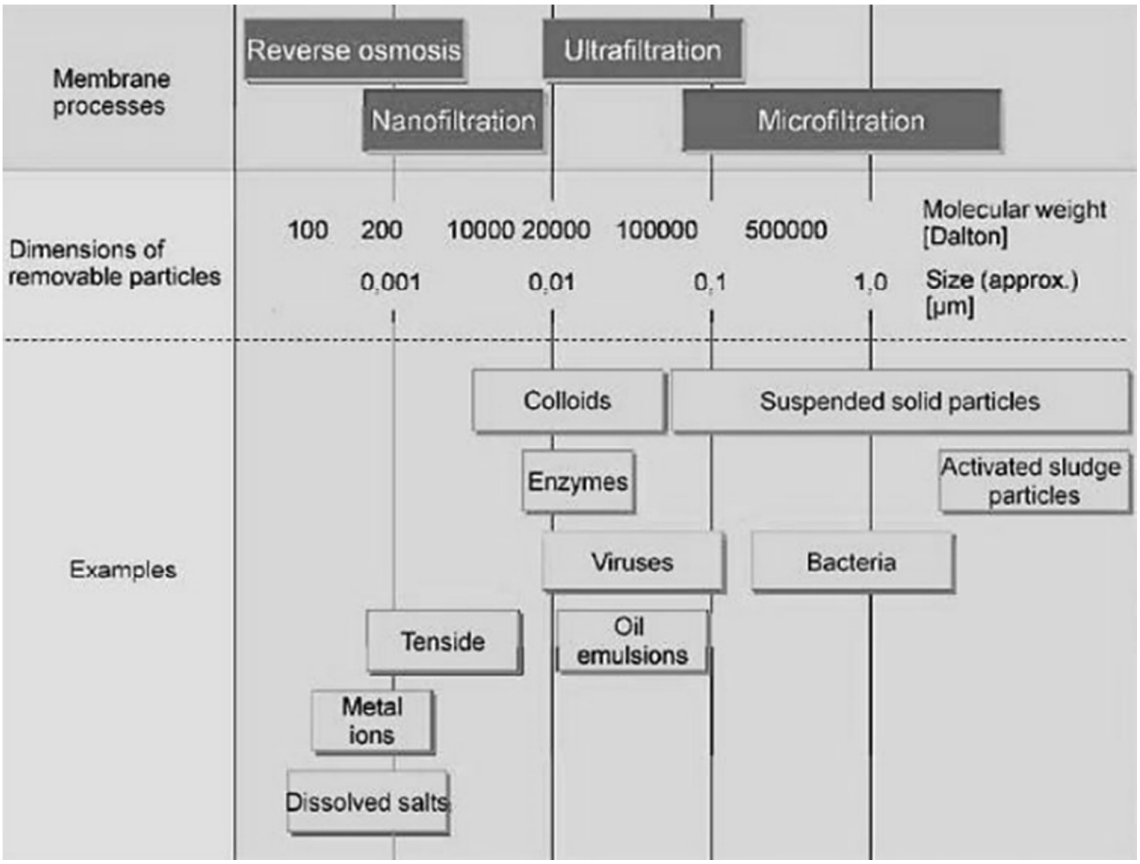

Figure 12: Filtration types. Source [6]

Membrane processes are classified by the pore size of the membranes. Figure 12 shows an overview of the common pressure driven membrane processes. If microfiltration (MF) is applied, suspended solids or bacteria down to 0.1 µm are filtrated. Ultrafiltration (UF) separates colloids, enzymes and other substances down to 0.01 µm. Through nanofiltration (NF) or reverse osmosis (RO), even dissolved salts and ions can be rejected [28]–[30]. One advantage by the use of membrane processes is the combination of different membrane processes. The components in the feed, which are not small enough to pass stay on the membrane and build a layer on the membrane that increases the hydraulic resistance. If suspended solids are adsorbed on the membrane surface, fouling occurs. Fouling leads to a decreased flow rate and separation efficiency. Fouling is prevented by effective pre-treatment of the feed. The effect of bio fouling occurs if bacteria get into the membrane pores. This process is very hard to stop and could be prevented through the sterilization of the feed [6] [28]–[30]. Figure 13 shows the principle of a membrane processes.

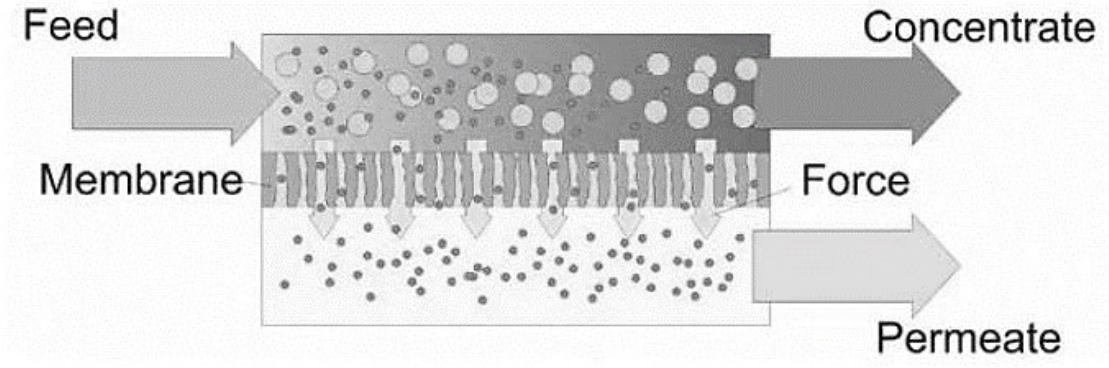

Figure 13: Membrane process principle. Source [8]

The filtration process type usually applied in digestate treatment is the surface filtration where the filtration happens on the surface of the membrane. Through the influence of the applied pressure force the permeate passes the membrane. In dependency on the membrane type and the pressure, a small amount of pollutants stays in the permeate stream. The rejected components stay in the concentrate, and on the membrane surface. Because the concentrate contains a high amount of the rejected components it has to be disposed of or further purified.

For economics of a biogas plant this has a huge impact as 5-20 % of the feed leaves the process as concentrate [6]. The process of membrane filtration can be performed by dead-end filtration or cross- flow filtration. At dead end filtration the feed is pushed through the membrane. Besides the advantages namely low energy consumption and small aggregate sizes, disadvantageous namely membrane cleaning due to accumulated particles on the membrane surface leading to increased membrane resistance have to be taken into account. When cross- flow filtration is applied, the feed flows continuously over the membrane. A fraction of the feed passes through the membrane and the rejected components stay on the membrane surface. The evolving layer on the surface is washed away through the continuous cross-flow and leaves the process within the concentrate stream. Main advantages of cross-flow filtration are the continuous process operation and a constant permeate flow. On the negative side the energy consumption is higher compared with dead end filtration [27].

At digestate treatment the filtration methods microfiltration and ultrafiltration are used to purify the liquid digestate from suspended solids and macromolecules, by this procedure it is ensured, that the membrane of the next purification step nanofiltration

or reverse osmosis won't be blocked [26]. The concentrate of micro- or ultrafiltration can be used for the mashing of the feedstock to decrease the amount of needed fresh water. Through the application of nanofiltration or reverse osmosis a highly purified permeate is produced which contains significantly less ions than the feed. This fraction is either drained or used as process water. The concentrate after nanofiltration or reverse osmosis could be used as process water as well but one have to take into account that this could lead to an increase of the salt concentration of the feedstock [27].

Additionally, at reverse osmosis or nanofiltration, salts with low solubility could precipitate on the membrane surface and block the pores. This effect is called scaling and is prevented through the addition of anti-scalants and pH regulators [6]. For the evaluation of the process effectivity, the rejection efficiency has to be calculated. Equation (9) shows the calculation of the rejection efficiency in percent with the concentrations of the targeted substance in the permeate and feed [28].

$$R = 100 * (1 - \frac{w_{Permeate}}{w_{Feed}}) \quad (9)$$

2.6 Resulting challenges within digestate processing

As emphasized before the benefit of the digestate use is the fertilizing effect when applied on agricultural areas. The separation of the digestate into a solid and a liquid fraction leads to lower storage afford and transport costs of the solid fraction. Another benefit is the marketing of the solid digestate as a bio fertilizer after composting or drying. The remaining liquid phase may directly applied in fields or purified further on to produce a nutrient concentrate and water [25]. The disposal and the fertilization with digestate has to comply with the statutory requirements of the government. Important restrictions and requirements are pointed out on the next pages. Moreover, the established governmental guidelines seem to undergo an update. The disposal of digestate will be regulated stricter and therefore, the necessity of effective digestate purification methods get more important [31]. The modifications of the guidelines are quoted at the end of this section.

There are different challenges through digestate processing which one has to take into account and justify the necessity of further treatment processes [32]:

- Excess of nutrients
- High lease costs for digestate disposal areas
- Increasing digestate amount requires longer transport
- Digestate spreading prohibition in water protection areas

Besides those challenges negative properties of the digestate have to be taken into account [10],[33]:

- Low nutrient content in respect of the digestate amount
- Fluctuation of the nutrient concentration
- Ammonia emissions during digestate application
- Possible methane emissions through open storage
- Dissolved salts in the liquid digestate
- High water content results in high storage and transport costs
- Expanses for transport and application on fields

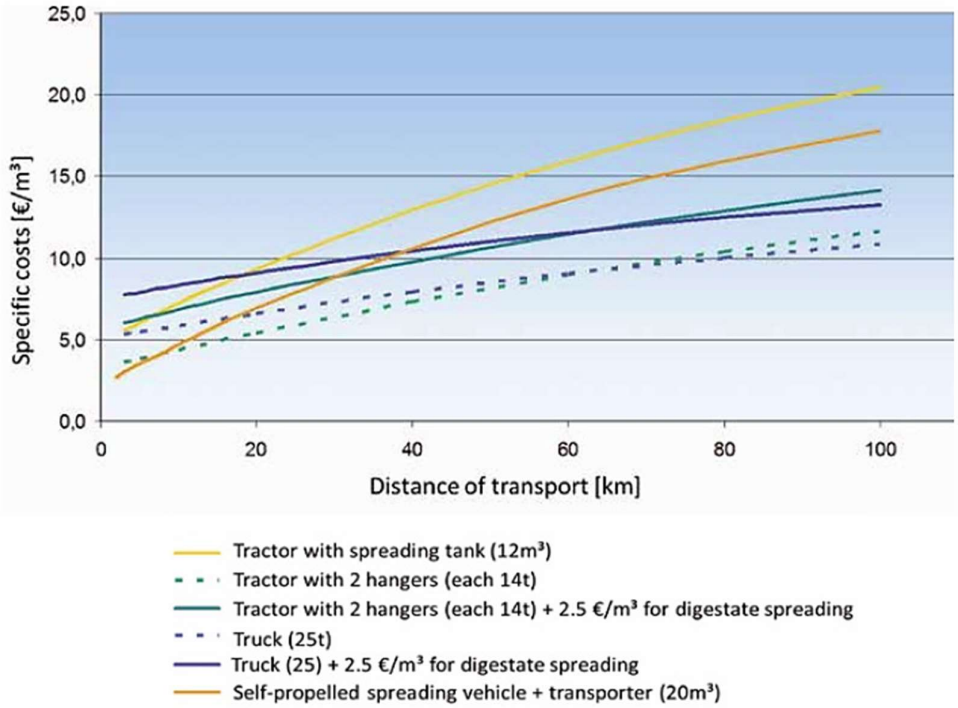

Figure 14: Transport costs depending on the application method. Source [25]
Note: The dashed lines only refer to transportation costs of the digestate

Main cost driver is the distance between digestate storage and disposal. Figure 14 gives an overview about different application types and the resulting costs. The curves in Figure 14 proves that the most economical way is the digestate spreading with a tractor and a manure trailer for shorter distances. If the distances are increasing the transport with trucks to the field, followed by spreading with agricultural vehicles are more cost effective. The data in Figure 14 show an estimation of the application respectively transport costs because the effective expenses differ due to regional conditions [25].

Another important aspect is that the nitrate directive based on the water legislation regulates the statutory amount applied. The directive regulates the maximum amount of nitrogen which can be spread on agricultural areas in one year [33]:

- 175 kg/ha on cropland
- 210 kg/ha on agricultural grassland
- 170 kg/ha of nitrogen from animal excrements

Moreover, the disposal is prohibited from the 30th of November until the 28th of February on grassland and from the 15th of November until the 15th of February on cropland or if the soil is frozen, covered with snow or saturated with water [34]. The disposal prohibition implicates that storage capacities for at least 6 month are required. The nitrogen limitations above lead to a required size of the nitrogen disposal area in respect to the biogas facility output and the average digestate amount. The data in Table 3 show required area sizes [32]:

Table 3: Average nitrogen disposal area based on facility output and digestate amount

Facility output [kWel]	Digestate amount [t/a]	Disposal area [ha]
500	11,500	300
1,000	23,000	600
2,000	46,000	1,200
4,000	92,000	2,400

Table 3 implicates that storage conditions have a direct impact on digestate processing because the required areas have high lease expanses and are usually not available next to the biogas facility. The average costs for digestate storage are approximately 60 €/m³ depending on the type of storage facility [24].

As mentioned before the listed restrictions on the previous pages will undergo an update through the European Union. The main drivers for these changes are the reduction of ammonia emissions and nutrient raise in water. In Germany, following modifications of the fertilizer ordinance regarding digestate will take effect in 2017 [31]:

- Storage capacities for 9 month
- Maximum 170 kgN/ha of any digestate
- In early spring only 60 kgN/ha
- Spreading in autumn only on fields with significant nutrient needs (rape, barley)
- Distance from water at least 1 m and spreading only with special equipment (thrower shield)

Since the European Union drives these changes, it is most likely that they will affect the digestate processing in Austria too.

Apart from these facts, there is another important point that makes digestate-processing necessary. The application of substrates from municipal or industrial waste, for example food leftovers or by-products, gained significant in recent years. As emphasized in Section 2.2 their high organic dry matter content (see Table 2) has a

positive effect on the achievable biogas yield [11], but high salt concentrations or availability of substances like flavor enhancer and alike of such feedstocks is a main drawback. The dissolved salts stay in the liquid fraction of the digestate after solid/liquid separation. Therefore, salt containing liquid digestate requires further purification or special disposal and leads to higher digestate exploitation costs. As mentioned in Section 1 the goal for the purification of salt containing liquid digestate is on one side to produce a water fraction that could be drained into the environment or used as process water and on the other side to enrich the concentrate as much as possible to keep the disposal costs low. The following section deals with the challenges mentioned on the previous pages.

3 Literature research on digestate purification

One of the major tasks of this thesis is to identify the most effective processes to purify salt containing digestate. First, a literature research on salt removal technologies from water respectively wastewater and liquid digestate was performed. Second, a process flow chart for the liquid fraction of the digestate treatment was developed. The literature research focus on state-of-the-art processes for salt removal from water or wastewater. General purification technologies, applied in modern digestate treatment and capable to remove dissolved salts from the liquid digestate fraction were identified. To put the problem from a subjective to an objective perspective, the systematic approach of a decision matrix based on the physical properties of the liquid digestate was applied. This approach leads to a decision matrix which is based on the decision support system TIPS (Theory of Inventive Problem Solving), where different unit operations and purification concepts depending on substance properties are compared [35]. The results of both, the literature research and the developed decision matrix, are explained in detail in Sections 3.1 to 3.4.

3.1 Salt removal from water/wastewater

Since liquid digestate has similar properties as water after the solid-liquid digestate separation (see Section 2.5.2), the literature research was focusing first on treatment methods whereby dissolved salts from water or waste water are removed [6]. The result of this research was the identification of different approaches that are state-of-the-art in water purification.

3.1.1 Membrane processes

Membrane processes are one of the most commonly used techniques for water desalination respectively drinking water production [30]. Regarding the capability to reject dissolved salts, reverse osmosis (RO), nanofiltration (NF) and electro dialysis (ED) are the processes usually applied [29] [36] [37]. The basic principles of nanofiltration and reverse osmosis are explained in Section 2.5.4.3. RO is used for seawater or brackish water desalination since the salt rejection rates are very high (95-99 %). The system pressure ranges between 10-80 bar, depending on the intended rejection rates and feed concentrations [38]. At nanofiltration, the pressure ranges between 5-50 bar and the achievable ion rejection depends on the size of the dissolved

ions [29]. Research showed that the rejection rates for divalent ions like Magnesium (Mg^{2+}) or Calcium (Ca^{2+}) are approximately 60 %. Monovalent ions like sodium (Na^{+}), chloride (Cl^{-}) or potassium (K^{+}) pass easier through the membrane. Typical rejection rates range around 40% [39]. Through the arrangement of the membrane modules, the system can be customized in respect to the feed volume that has to be purified. Regarding the energy consumption of both process types, RO is the more energy consuming one [29].

Another desalination technique is electro dialysis where the dissolved salts are rejected through the application of an electric potential. The physical principle bases on the transport of electric charges through ions in a solution between two electrodes [36]. The schematics and the working principle of an ED stack is shown in Figure 15.

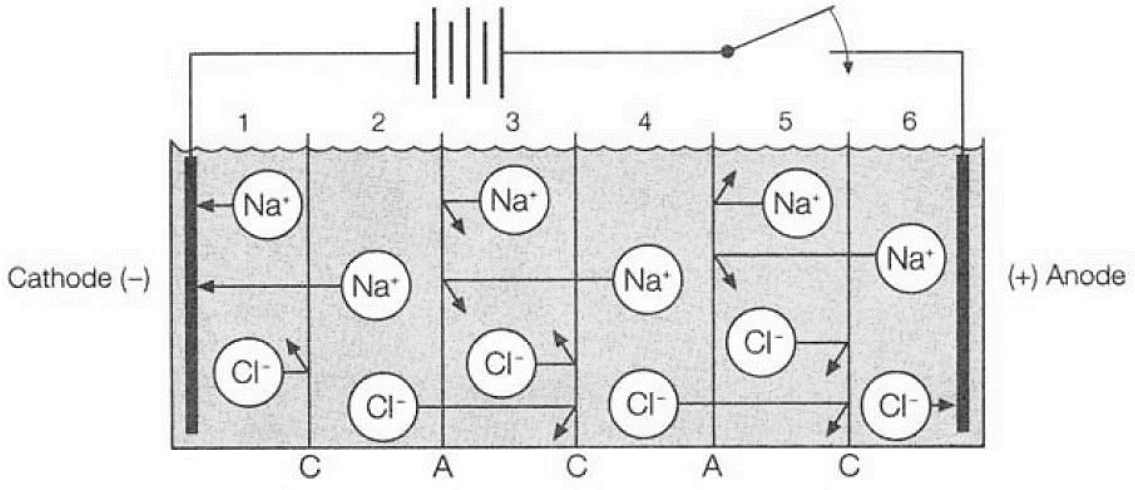

Figure 15: Working principle of an ED stack. Source [36]

An ED stack (Figure 15) consists of a positive charged anode and a negative charged cathode. The compartments are filled with a salt solution, e.g. NaCl. Moreover, it is equipped with cation- and anion exchange membranes that separate the different compartments of the stack and control the movement of the ions. Anion exchange membranes (A) are only permeable for anions and cation exchange membranes (C) for cations. Through the application of an electric potential (direct current) on the electrodes the positive charged cations move towards the cathode and the negative charged anions to the anode. As Figure 15 shows, the ions in compartment 2 and 4 pass through the membranes and the solution is desalinated. The solution in the

compartments 3 and 5 contains a higher concentration of ions whereas the electrode compartments 1 and 6 contain lower ion concentration. Through this membrane arrangement, two major and two minor concentrate streams and two deionized streams are produced. In industrial applications, several hundreds of such compartments are combined to one ED system. According to literature ED is comparable to RO regarding the rejection efficiency of ions [36]. Moreover, ED systems have a higher fouling and scaling resistance than RO. However, one has to take into account that the ED membranes provide no barrier against microorganisms whereas RO and NF do [36]. Research has shown that ED is more economical if the salt concentration is less than 5 g/l, but at salt concentrations above 6 g/l RO is preferred [40].

3.1.2 Mass transfer processes

Besides membrane techniques, mass transfer processes are used in water desalination. Industrially applied is distillation (multi-stage flash or multiple effect boiling). A promising technique is membrane distillation (MD), which needs to be further developed for industrial applications [37] [41]. Both processes use the physical principle of phase change where to lower boiling component is vaporized and separated from the contaminants with a higher boiling point [37] [41].

At multi-stage flash distillation, salt containing water enters an evacuated chamber and evaporates. The process is repeated in different stages at temperatures around 100°C. The process runs in several stages where the steam produced in the first stage heats up the salt solution in the next stage and so on. This is possible because every following stage operates at a lower pressure and temperature as the stage before. The operation temperature of the multiple effect boiling distillation is at 70°C. Multi-stage flash distillation is the most applied mass transfer unit operation (93 %) whereas RO with 88 % is the most applied membrane process [37].

When membrane distillation (MD) is performed, the salt containing feed is evaporated and the steam is transported through hydrophobic membranes. The hydrophobic membranes form a barrier for the liquid phase and let the vapor phase pass. The transport is driven by the vapor pressure gradient across the membrane [42]. In Figure

16, different possible configurations of MD are shown. Common types applied are Direct Contact MD (DCMD) and Air Gap MD (AGMD).

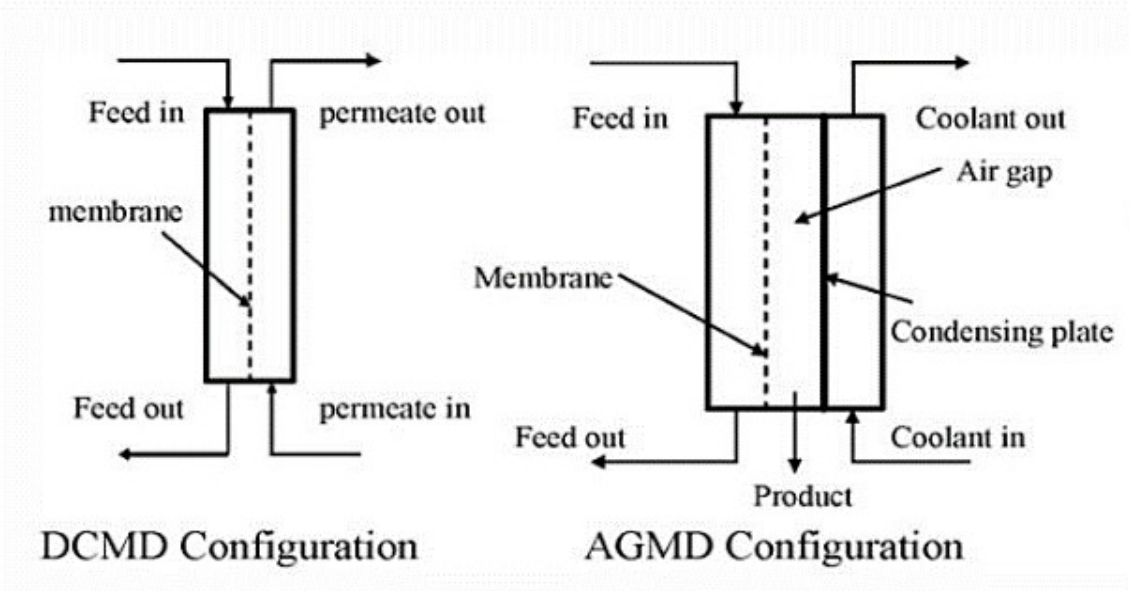

Figure 16: Configurations for membrane distillation. Source [43]

At DCMD, the permeate is in direct contact with the membrane. On the permeate side an aqueous solution, colder than the heated feed, causes a vapor pressure difference over the membrane. The volatile molecules on the feed side evaporate, cross the membrane and condense inside the membrane at the cold liquid/vapor interface of the membrane module. The AGMD has an air gap between the membrane and a condensing plate. The vapor phase of the feed flows through the membrane and condenses on the cold surface of the condensing plate [43] [41]. Membrane distillation respectively other distillation methods has a high potential because it has theoretical salt rejection rates of 100 %, low operating temperatures (60-90 °C), operating pressures lower than RO and are additionally not limited by the salt concentration in the feed [44] [41]. Recent research on MD shows that it could be an interesting option to selective remove ammonium from liquids. So MD could be applied to gain a fertilizer concentrate out of the digestate fraction [45] [46]. The bottleneck for the industrial application of membrane distillation are the membranes used. They need high anti-wetting qualities, high temperature resistance and a high flux to prevent fouling or scaling [44].

3.2 Salt removal from liquid digestate

As emphasized in Section 2.5.4, different approaches exist to purify the liquid digestate after the solid-liquid separation. A few of them are capable to remove dissolved salts from the digestate. Regarding mass transfer processes, evaporation is a process which could be applied for the purification task (e.g. concentration of the salts before the disposal). The application of ion exchange or precipitation as reactive purification methods are other purifying possibilities. In terms of filtration processes that are applied in digestate cleaning, RO and NF have been found to be the best choice (see Section 2.5.4) [6] [25]. As an alternative to RO, the principle of forward osmosis (FO) is under investigation for digestate treatment [26] [47]. The main difference of RO and FO is that in FO the feed is not forced through the membrane by means of external pressure. The permeate flow is forced due to the influence of a so-called draw solution (e.g. NaCl) that has a higher osmotic pressure than the feed. The draw solution flows on the permeate side of the membrane. The osmotic pressure difference between the draw solution and the feed forces the water to permeate through the membrane. That way the feed stream is concentrated and the draw solution diluted. Advantages of FO are the lower energy consumption since the osmotic pressure is the only driving force, less membrane fouling occurs and technical equipment costs are lower because of lower pressure generation. The need of research in effective draw solutions and appropriate membranes are the drawbacks of FO. Since FO is under development and the commercial applications are still limited, it is currently no an urgent alternative to RO [48] . As mentioned before ED is an option to purify salt containing liquids (see Section 3.1.1). According to literature about digestate treatment, it is a possible purification process, which is still under investigation. The principles and the advantages/disadvantages of ED where emphasized before in Section 3.1.1. In literature the possible application of it as a pre- treatment to RO is mentioned [6] [26].

3.3 Development of a decision matrix

Besides a theoretical research of appropriate purification processes a systematic approach was applied based on a the systematic approach of TIPS namely the decision [35]. The approach aims to develop a decision matrix where the physical properties (e.g. boiling point, enthalpy, molecular weight) of a target substance are matched with different unit operations. Thereby their suitability to purify the target

substance based on their physical properties is estimated. For the matrix development, it is assumed that a binary mixture of water and salts has to be separated. The stages of development are:

- Identifying the physical properties of the target substance (water)
- Matching the substance properties with mechanical unit operations
- Rating the substance properties with thermal unit operations
- Opposing the substance properties with reactive unit operations

If it is possible to apply the unit operation in respect to the substance property, a "**y**" is set for the possibility. "**n**" refers to the impossibility of using a process for the purification process as well as to an irrelevant parameter which doesn't influence the decision. At the end of the opposing step, the assigned **y**'s are summed up. The highest scores of the evaluation show possible processes, which may lead to a successful separation of the binary mixture. Even if a high total score is shown, the purification task can still not be suitable because for example one of the processes meets a knock out criterion. Table 4 summarizes some mechanical unit operations, missing unit operations fulfill a knock out criterion already.

Table 4: Decision matrix mechanical unit operations

Proberty	Value	Chromatography	Electrophoresis	Nanofiltration	Reverse Osmosis
MW [g/mol]	18.02	y	y	y	y
Boiling point [°C]	100	n	n	n	n
Density at 20°C [kg/dm³]	0.998	n	n	n	n
Viscosity [mPa*s]	1.001	n	n	n	n
Dieelectric constant at 20°C	80	n	y	n	n
pH value	7	n	n	n	n
p_{vapour} at 20°C [mbar]	23.4	n	n	n	n
Freezing point [°C]	0	n	n	n	n
Enthalpy [J/mol]	2257	n	n	n	n
Molecular Size [nm]	0.28	y	y	y	y
Acidity (pKa)	15.7	n	y	n	n
∑		2	4	2	2

Electrophoresisis is not mentioned further, because of its conventional use as an analytical method and the complexity of the experimental setup. The seperation principle of chromatography is suitable for the removal of dissolved ions too, but as well as electrophoresis it is applied as an analytical method and not designed for the purification of the liquid fraction of the digestate. Additionaly, electrophoresis and chromatography would be not economical in processing big volume streams [49]. NF and RO as the other two purification operations have been found in literature as suitable processes (see Section 3.1) and the matrix confirms this results [6] [25] [39]. The complete matrix for the mechanical unit operations can be seen in the Appendix in Table 17.

Table 5: Decision matrix for thermal unit operations

Properties of target substance		Thermal unit operations				
Proberty	**Value**	**Distillation**	**Electro dialysis**	**Stripping**	**Extraction**	**Membrandestillation**
MW [g/mol]	18.02	y	n	n	n	y
Boiling point [°C]	100	n	n	n	y	n
Density at 20°C [kg/dm³]	0.998	n	n	y	y	n
Viscosity [mPa*s]	1,001	n	y	n	n	n
Dieelectric constant at 20°C	80	n	n	n	n	n
pH value	7	y	n	n	n	y
p_{vapour} at 20°C [mbar]	23.4	n	n	n	n	n
Freezing point [°C]	0	y	n	n	n	y
Enthalpy [J/mol]	2257	n	y	n	n	n
Molecular Size [nm]	0.28	n	y	y	y	n
Acidity (pKa)	15.7	n	n	n	y	n
∑		3	3	2	4	3

Regarding the mass transfer unit operations opposed to the substance properties, several appropiate processes can be distinguished when evaluating the decision matrix in Table 5. The complete matrix can be seen in the Appendix in Table 18. Extraction shows the highest rate but it is not suitable for the purification task because of economical reasons and the lack of knowledge of a solvent which is able to separate all salt from the feed. Due to economical reasons the unit operations adsorption, desorption, molecular sieve, drying and crystallization are excluded. Distillation, flash vaporization and evaporation base on the same physical principle and are applied in

digestate cleaning already. Nevertheless, they are not investigated further because of their energy consumption, economical reasons and their development progress [51]. Stripping is applied too in digestate purification processes, however, due to limited utilizability only partial purifcation or the extraction of a special substance in the digestate, e.g. ammonium, it is not investigated further here [6] [25]. Pervaporation and membrane distillation use the boiling point difference for the separation and are capable to separate the water phase from the salts in the liquid digestate [37] [52]. Because of the progress of development as digestate purification methods and the extend of the time frame for the experiments they where not investigated further in the lab experiments. The process of ED got three positive ratings and because of its potential in digestate treatment and the simple fabrication of a lab scale device (see Section 4.3) research on its performance in digestate cleaning has already been conducted [26] [36].

Table 6: Decision matrix reactive unit operations

Properties of target substance		Reactive unit operations	
Proberty	**Value**	**Precipitation**	**Ion exchange**
MW [g/mol]	18.02	n	y
Boiling point [°C]	100	n	n
Density at 20°C [kg/dm³]	0.998	y	n
Viscosity [mPa*s]	1.001	n	n
Dieelectric constant at 20°C	80	y	y
pH value	7	y	y
p_{vapour} at 20°C [mbar]	23.4	n	n
Freezing point [°C]	0	n	n
Enthalpy [J/mol]	2257	n	n
Molecular Size [nm]	0.28	y	y
Acidity (pKa)	15.7	y	n
∑		5	4

Table 6 shows the decision matrix of the reactive unit operations. Precipitation and ion exchange are evaluated as possible processes. Due to disproportionate expanses for chemicals respectively ion exchangers they are not investigated further. To fortify the obtained results through the literature research and the evaluation of the decision

matrix three purification processes and their combination with each other have been picked for further lab scale research:

- Nanofiltration
- Reverse osmosis
- Electro dialysis

3.4 Process suggestion

Both, the literature research and the decision matrix lead to a process suggestion for the lab scale experiments. The three processes nanofiltration, reverse osmosis and electro dialysis are investigated as stand-alone processes and as combined purification process. Figure 17 shows schematically the performed process combinations. The first stage of the proposed process combination is nanofiltration. Nanofiltration as the first step fractionally remove dissolved ions and a high volume reduction of the digestate stream is desired. The concentrate stream after the nanofiltration is the feed for the second stage, where three different processes are compared: RO, NF and ED. The permeate streams of the different processes can be used as process water within the biogas facility (e.g. mashing) or drained if the salt concentration is at permissible limits [6]. The concentrate stream of the second process stage has to be disposed, stored or could be used for further purification and nutrient recovery [6] [24]. Chapter 5 discusses the performed experiments and their results.

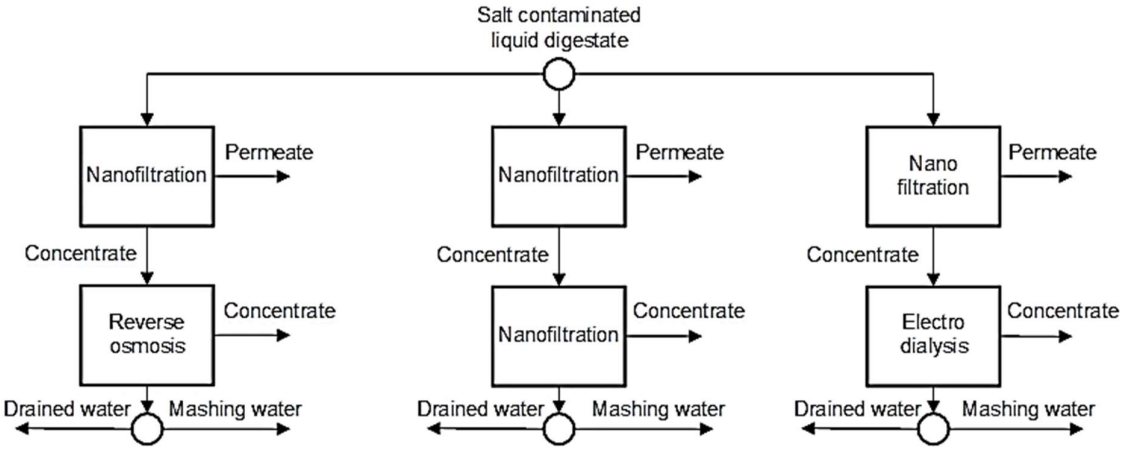

Figure 17: Overview of the suggested process combinations

4 Experimental part

This section summarizes the chemicals and materials used in the laboratory experiments as well as the laboratory devices, test procedures and analytical devices are explained in detail.

4.1 Chemicals & Materials

The substances listed in Table 7 were used for the preparation of the experimental feed and the electrolytes used for ED experiments.

Table 7: Chemical substances

Substance	CAS Number	Fabricant	Purity [%]	Concentration [%]
NaCl (s)	7647-14-5	Sigma-Aldrich	≥ 99.50	
$MgCl_2$ * 6 H_2O (s)	7791-18-6	Merck	≥ 99.00	
KCl (s)	7447-40-7	Merck	≥ 99.99	
K_2HPO_4 (s)	7758-11-4	Carl Roth	≥ 99.00	
$CaSO_4$ * $2H_2O$ (s)	10101-41-4	Merck	≥ 99.00	
$(NH4)_2SO_4$ (s)	1336-21-6	Carl Roth	≥ 99.50	
NH_4OH (l)	7783-20-2	Merck		32 %
HCl (l)	7647-01-0	Sigma-Aldrich		37 %
NaOH (l)	1310-73-2	Carl Roth		32 %

The materials used for the filtration operations and ED experiments are summarized in Table 8.

Table 8: Experimental materials

Application	Designation	Fabricant	Application
Nanofiltration	NP 030	Microdyn Nadir	Flat sheet PES membrane
Reverse osmosis	SW30HR-380	DOW Filmtec™	Flat sheet PA membrane
Electro dialysis	St 1.4571 2 mm	Zultner GmbH	Steel cathode
	Pt. - Ti. mesh 2mm		Pt. – Ti. anode
	Hydrophilic PE Membrane 1,5 mm	Porex	Ion exchange Membrane ED
	Senodur PVC	Senova	Cell material
	Hylotyte Red 100	Hylomar	Salt resistant sealant
	EA-PS-3032-10B	EA	0-32 V DC power supply
	Fluke 177	Fluke	Digital multimeter
	M 3900	Eumig	Digital multimeter
	R = 0.3 Ω		Resistor
	Lauda B	Lauda	Thermostat

4.2 Filtration device

The company *OSMO Membrane Systems GmbH* provided the device for the filtration experiments. The filtration device has a membrane test cell, which is similar to a spiral wound membrane module in its hydraulic properties, which means that a transfer to pilot scale is possible [53]. The test cell can be equipped with different flat sheet membranes for UF, NF or RO and has an effective membrane area of 80 cm². The maximum working pressure is at 64 bar in dependency of the temperature resistance of the membrane. For the NF experiments, the test cell was equipped with a flat sheet membrane (NP030) from *Microdyn Nadir* with theoretical rejection rates of 30 % for sodium chloride. The membrane used at RO was a flat sheet membrane manufactured by *DOW Filmtec*^{TM} with NaCl rejection of 99.65 %.

4.2.1 Experimental setup

Figure 18 shows the lab scale device used for the NF and RO experiments. The main components are a feed tank with a maximum volume of two litres combined with a temperature indicator, a high-pressure plunger pump and the membrane test cell for flat sheet membranes. A water cooling system provides constant operating temperature during the test runs.

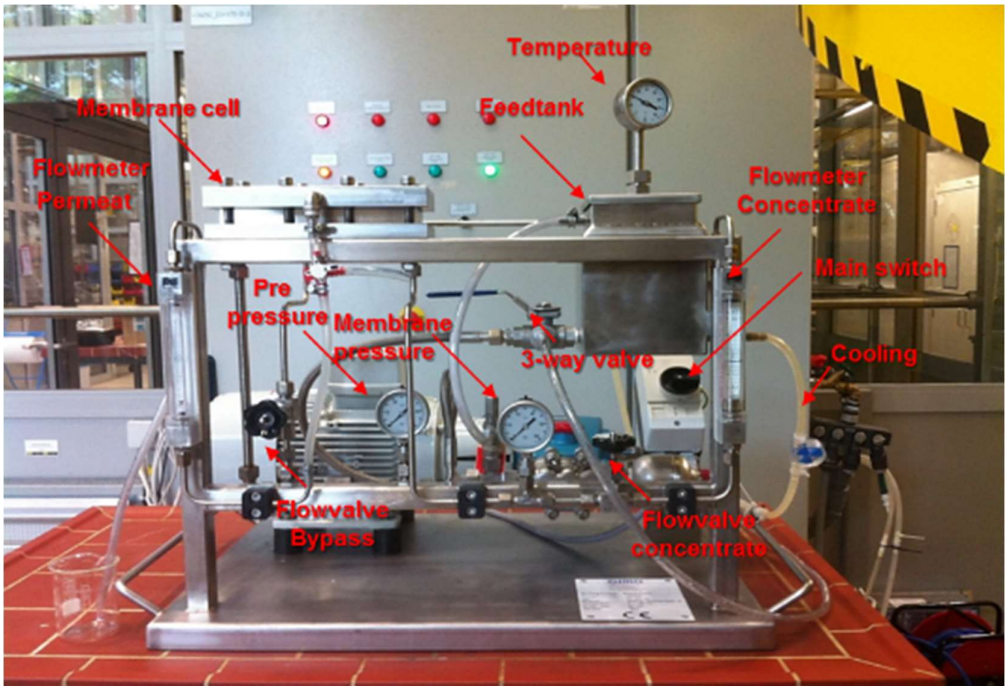

Figure 18: Lab scale filtration device

By the flow valves indicated with “flow valve bypass” and “flow valve concentrate”, the pre-pressure of the test cell respectively the membrane pressure is adjusted. Furthermore, both valves control the volume flows of the permeate and concentrate. The permeate leaves the process into a beaker through a flow meter on the left hand side of the facility and the concentrate stream flows through a flow meter back into the feed tank.

4.2.2 Test procedure

Before the filtration experiments, the test cell was equipped with a flat sheet membrane for NF or RO and the cooling system was turned on. Than the feed tank was filled with 2 litres of the experimental feed. The detailed feed composition is presented in section 5.2. A minimum liquid level of 0.5 litres is required to prevent pump damage. The filtration system was flushed twice with 0.5 l of the experimental feed before the test runs to reduce the influence of the remaining cleaning water on the salt concentration respectively conductivity of the feed. After the starting procedure, the pump was activated and the operation pressure adjusted. The investigation of different pressures was performed from low pressure to high pressure, whereas each experiment was performed at least two times. To ensure constant feed concentration the permeate and the concentrate are returned back into the feed tank. At each pressure set points, the first samples of the feed, concentrate and permeate where taken after 15 minutes along with conductivity, pH- value and temperature measurements. This procedure was repeated every 10 minutes until the conductivity of the permeate remains constant. The samples of every set point were subsequently analyzed on their salt concentration with atomic absorption spectroscopy (AAS) and inductively coupled plasma spectrometry (ICP, see Section 4.4). The detailed results on the experiments performed are summarized and discussed in section 5.1 and Table 9.

4.3 Electro dialysis device

The electro dialysis device was designed and built at the Institute of Chemical Engineering and Environmental Technology at the Technical University Graz [54]. The ED cell (see Figure 19) is made of poly- vinyl- chloride with 120 mm height and 90 mm width. For an effective sealing a salt and chemical resistant sealant was applied (see Table 8). Previous ED experiments at the showed that porous polyethylene membranes can be applied instead of anion- and cation exchange membranes that are usually used at ED applications [54]. The ED cell consists of three compartments, further on called membrane compartment (MC), anode compartment (AC) and cathode compartment (CC) with a volume of 65 ml each. Two membranes with an effective area of 40 cm² and 1.5 mm thickness separated the MC from the electrode compartments. The pore sizes of the membranes were 20 – 60 µm. Based on previous research on appropriate electrodes for ED experiments a cathode made of 1.4571 stainless steel and a platinized titanium mesh anode where applied [54]. The used materials can be seen in detail in Section 4.1.

Figure 19: Electro dialysis cell

4.3.1 Experimental setup

The basic experimental ED setup can be seen in Figure 20. It consists of the ED cell as explained in the previous section 4.3, a laboratory power supply, a 0.3 Ω resistor for the determination of the cell current, two digital multimeters for the voltage measurements. The cell current was calculated through the value of the measured voltage drop over the resistor and its electrical resistance. For a constant temperature of 25°C during the experiments, the ED cell was placed in a water bath with a thermostat. The detailed information of the components used are described in section 4.1.

4.3.2 Test procedure

Figure 20: Experimental set up for electro dialysis

The experiments were performed in a batch operation. Before the experiment, the MC was filled with 65 ml of the experimental feed. CC and AC where filled with 65 ml electrolyte. The electrolyte used in the AC was a 0.1 molar HCl and in the CC a 0.1 molar NaOH solution. To avoid air inclusions in the porous membrane, the filled ED cell was placed in an ultrasonic bath for 20 minutes. Afterwards the ED cell was placed in the water bath and the power supply connected to the anode and cathode. The cell voltage was set to a level where the measured voltage over the resistor reached 0.4 volts. This value was derived through previous experiments to determine the limiting current density of the experimental feed (see Section 5.4.4). During the experiment,

the current was held constant by 1.33 mA. After a defined time, the experiment was stopped, samples were taken for further analytics. The experiments performed and their parameters can be seen section 5.1.

4.4 Analytics

The measurement of the process parameters conductivity, pH value and temperature where performed during the experiments with the devices explained in section 4.2 and 4.3. The taken samples of the representative feed, both at the filtration and electro dialysis experiments, were analyzed on their salt concentration through the application of various devices that are mentioned in the following sections.

4.4.1 Conductivity, pH and temperature

For the investigation and recording of the conductivity, pH value and process temperature the measurement device *WTW multi 340i* was used. The measurement device was equipped with a conductivity cell (*WTW Tetra con 325*) with an integrated temperature sensor and a pH electrode from *Hamilton.* The conductivity cell consists of four graphite electrodes and has a measurement range from 1 µS/cm to 2000 mS/cm. Through the cumulative parameter of conductivity, the progress of the laboratory experiments was monitored since the conductivity is depending on the ion concentration in the feed [55].

4.4.2 Determination of the ion concentration

The concentration of sodium (Na^+), potassium (K^+), calcium (Ca^{2+}) and magnesium (Mg^{2+}) was determined through atomic absorption spectroscopy (AAS) at the institute. Therefore, the AAS spectrometer *AAnalyst 400 AA* from *Perkin Elmer* was used. Every sample was analyzed three times to calculate the mean value of the cation concentration.

The determination of ammonium (NH_4^+) was accomplished photometrically at the laboratory of the company *Bioenergy 2020+ GmbH* in Graz [56]. In addition, the concentration of the anion's sulphate (SO_4^{2-}), phosphate (PO_4^{3-}) and chloride (Cl^-) were measured with an inductively coupled plasma device (ICP) at the laboratory of the company *Bioenergy 2020+ GmbH*.

5 Results and Discussion

In the sections 5.1 - 5.6 the performed lab experiments along with their results are shown. First, an overview of the different experiments and their process parameters is given. In addition, the composition of the experimental feed based on digestate analysis of a food leftover biogas plant is shown. The results of the different purification processes and a comparison of their effectiveness followed by a suggestion for an overall purification process, based on the results obtained, finishes this chapter.

5.1 Experimental matrix

Table 9 gives an overview about experiments performed in the laboratory along with the experimental parameters and the purification type. Each experiment was performed at least two times to ensure reproducible results. As highlighted in Figure 17, stage one of the purification processes is NF. Basic lab research, regarding the volume flows in respect to the economic efficiency of NF, resulted in the decision for an operation pressure of 40 bar. A single test run was performed to produce the feed for the second stage. As shown in Figure 17, the feed for stage two is the concentrate from the first purification step. The composition of the experimental feeds is summarized in Table 10. The NF experiments in the second step where performed for pressures ranging from 5-40 bar and RO experiments from 20-50 bar whereby the operation pressure of 20 bar at RO was not steady and no useable data was gained. The ED experiments where performed for 1, 3, 5 and 8 hours. The cell voltage of 2 volts respectively the voltage drop of 0.4 volts and the cell current of 1.33 mA where held constant. These values for the operation of the ED cell where determined through pre-test runs on the limiting current density (see Section 5.4.4).

Table 9: Experimental matrix

ID	Process	Pressure [bar]	Voltage [V]	Current [mA]	Feed	Duration [h]	Comments
20	NF	40	-	-	Feed	0.5	
21	NF	40	-	-	Feed	0.5	
NF1	NF	40	-	-	Feed	1	Feed 2

ID	Process	Pressure [bar]	Voltage [V]	Current [mA]	Feed	Duration [h]	Comments
22	NF	5	-	-	Feed	0.5	
23	NF	10	-	-	Feed	0.5	
24	NF	20	-	-	Feed	0.5	
25	NF	30	-	-	Feed	0.5	
26	NF	40	-	-	Feed	0.5	
27	NF	5	-	-	Feed	0.5	
28	NF	10	-	-	Feed	0.5	
29	NF	20	-	-	Feed	0.5	
30	NF	30	-	-	Feed	0.5	
31	NF	40	-	-	Feed	0.5	
32	RO	20	-	-	Feed	0.5	Not steady
33	RO	30	-	-	Feed	0.5	
34	RO	40	-	-	Feed	0.5	
35	RO	50	-	-	Feed	0.5	
36	RO	20	-	-	Feed	0.5	Not steady
37	RO	30	-	-	Feed	0.5	
38	RO	40	-	-	Feed	0.5	
39	RO	50	-	-	Feed	0.5	
46	ED	-	2	1.33	Feed	3	
47	ED	-	2	1.33	Feed	3	
48	ED	-	2	1.33	Feed	1	
49	ED	-	2	1.33	Feed	1	
50	ED	-	2	1.33	Feed	8	
51	ED	-	2	1.33	Feed	8	
52	ED	-	2	1.33	Feed	5	
53	ED	-	2	1.33	Feed	5	

5.2 Composition of the liquid digestate and the model feed

For the experiments, a model feed was used. Based on analysis results of the liquid digestate from two biogas plants, operated with food leftovers, the model feed (Feed 1) was prepared. Main values were the salt concentration [g/l], the pH-value and the conductivity (σ). The company *BDI BioEnergy International AG* provided the digestate samples, which were taken after a membrane bio reactor, where the organics content in the digestate is removed and the dissolved salts stay within the liquid digestate Therefore, the salts for the composition where chosen in respect to their occurrence in food to receive the most realistic feed. Results of the feed analysis are shown in Table 10. The total salt concentration was 34.1 g/l and analysis of Feed 1 show a salt concentration of 23.4 g/l. This deviation originates from the difference of the molecular weight of the used chemicals to the pure substances. The feed was produced with deionized water.

Table 10 summarizes the data from the digestate samples. Besides the ion concentration, the pH-value and the conductivity were measured. The pH-value was 8.20 in the original feed samples and around 8.40 in the model feed. The conductivity was at 36.4 mS/cm at the original feed samples and around 49 mS/cm at the model feed. Differences between the sample and the model sample are due to molecular mass of the chosen salts as well as from pH adjustment with HCl. To reach the pH-value of the sample feed 32 ml HCl per litre feed were added. The salt concentration without the influence of HCl is further called the “corrected feed” and is summarized on the right side of Table 10 (Feed 1 corrected, Feed 2 corrected). The experiments where performed with an increased chloride content because in real biogas plants the feedstock composition and therefore the resulting salt concentration could vary as well [6]. With the increased salt concentration, a worst-case scenario was investigated. Due to the increased chloride content of Feed 1, respectively Feed 2, the conductivity is almost 14 mS/cm higher as in the original digestate sample. The concentration of magnesium and calcium in Feed 1 respectively Feed 2 is 10 times lower as in the digestate sample. During the composition salts precipitated due to their limits of solubility. For instance, magnesium phosphate, calcium phosphate and calcium sulphate are hardly soluble salts that could have precipitated [57].

Table 10: Analysis of the digestate and experimental feed

Ion	Unit	Digestate (D)	Feed 1	Feed 2	Feed 1 corrected	Feed 2 corrected
Na^+	[g/l]	1.89E+00	1.68E+00	1.69E+00	1.68E+00	1.69E+00
K^+	[g/l]	1.33E+00	1.52E+00	1.55E+00	1.52E+00	1.55E+00
Ca^{2+}	[g/l]	2.75E-02	6.31E-03	7.48E-03	6.31E-03	7.48E-03
Mg^{2+}	[g/l]	5.69E-03	5.38E-04	6.59E-04	6.59E-04	6.59E-04
NH_4^+	[g/l]	4.92E+00	5.29E+00	5.34E+00	5.29E+00	5.34E+00
Cl^-	[g/l]	3.87E+00	1.42E+01	1.47E+01	3.88E+00	3.88E+00
PO_4^{3-}	[g/l]	3.41E-01	6.46E-01	6.77E-01	6.46E-01	6.77E-01
SO_4^{2-}	[g/l]	6.62E-02	8.17E-02	8.73E-02	8.17E-02	8.73E-02
∑	[g/l]	1.24E+01	2.34E+01	2.41E+01	1.31E+01	1.32E+01
pH		8.20	8.45	8.54	8.45	8.54
σ	[mS/cm]	36.4	48.9	49.2	48.9	49.2

5.3 First purification stage

This section shows the results obtained at the first purification stage. The process investigated was nanofiltration with the NP030 membrane at 5 - 40 bar (see Figure 17). In the first stage the goal was to reduce the salt concentration in the permeate and find the optimal operation point for the NF process.

5.3.1 Nanofiltration at 5 - 40 bar

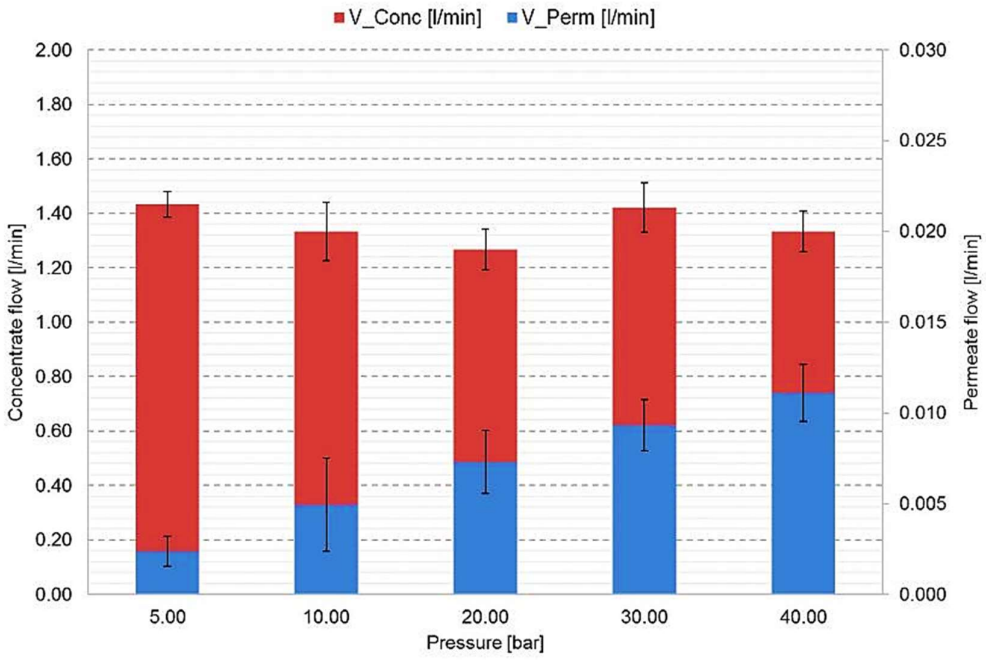

Figure 21: NF Stage 1 – Concentrate and Permeate flows in [l/min] at 5-40 bar

Experiments with pressures from 5-40 bar where performed to decide which operation pressure in respect to the volume flows is valid for the test series. Figure 21 shows the volume flows of the concentrate on the primary axes and permeate on the secondary axes and their standard deviation in respect to the different operation pressures investigated. The results show that with the increasing pressure the permeate flux increases. The concentrate flow at 40 bar is 1.40 ± 0.1 l/min and the permeate flow 0.010± 0.002 l/min (see Figure 21). The standard deviation is related to the experiments, which were performed twice. Because the valves of the filtration device (see Figure 18) are regulated manually. Since one goal is to reduce the liquid digestate fraction as much as possible at the first purification stage, the decision resulted in 40 bar operation pressure. Moreover, as literature about nanofiltration points out, the ion rejection rate increases with the transmembrane pressure because besides the water flux, the salt flux through the membrane increases [28].

Figure 22 shows the measured conductivity and standard deviation in mS/cm of the permeate (σ_Perm), the concentrate (σ_Conc) and the feed (σ_Feed) at a system pressure of 40 bar. The conductivity of the permeate decreased about 6 mS/cm during

nanofiltration. The divergence in conductivity between the feed in the nanofiltration unit and the value of Feed 1, measured before the experiment (see Table 10) originates from remaining volume of washing water in the filtration device. Through the filtration, the conductivity of the concentrate should rise above the feed conductivity. The conductivities of the concentrate and feed are almost similar. This is because the permeate fraction is 140 times lower than the concentrate fraction. In other words, the rejected salt ions of the permeate stream do not have a significant impact on the concentrate's conductivity at this lab scale device.

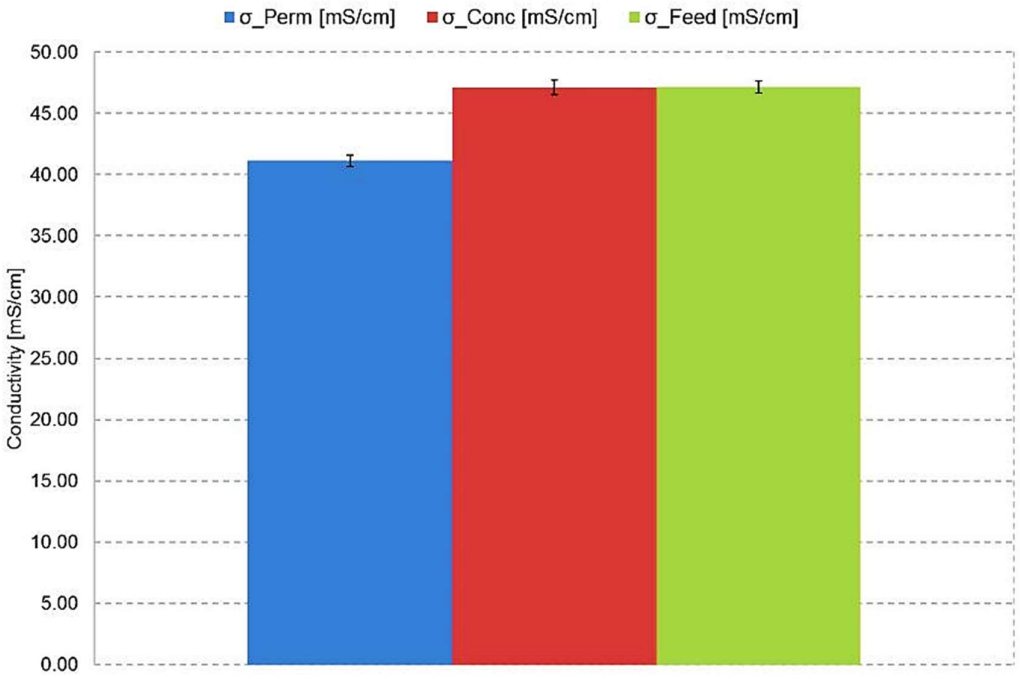

Figure 22: NF Stage 1 - Conductivity of Permeate, Concentrate, Feed at 40 bar

As mentioned above in section 2.5.4.3 the ion rejection efficiency is an important value to evaluate the process. Figure 23 shows the rejection rates of the different salt ions and the SD in respect to the operation pressure. The concentration values for the calculation are listed in the Appendix in Table 19.

In Figure 23, the ion rejection rate for the NF stage at 40 bar is depicted. The rejection of sulphate and phosphate ions ranges between 70 and 80 %. These aligns with the separation efficiency of sulphate mentioned in the datasheet of the membrane and data given in the literature [58].

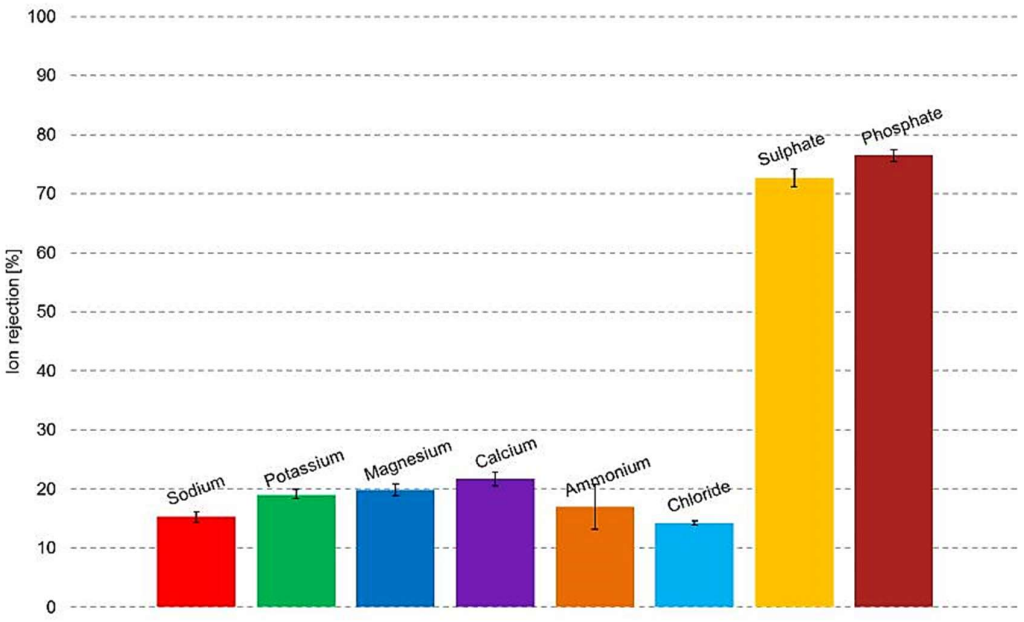

Figure 23: NF Stage 1 - Ion rejection rates in [%] at 40 bar

Since phosphate ions have almost the same molecular weight as sulphate ions it is expected that their rejection rates are similar [59]. Regarding the divalent ions magnesium and calcium, their rejection rate was remarkably small at around 20 %.Research on NF, using membranes with similar properties, lead for the divalent ions magnesium and calcium to rejection rates of approximately 55 % [39] [58]. Taken into account that the concentrations of magnesium and calcium are quite in the range of 10^{-3}-10^{-4} g/l, measurement inaccuracies have a significant impact on the calculations of the rejection rates. Regarding sodium and chloride the rejection rates given in relevant literature range in general between 30-50 % [28] [60]. The data sheet states that the NP030 membrane has 30 % rejection rate for NaCl. The rejection rate in the performed experiments is for sodium 15 % ±1 and for chloride 14 % ±0.5. Literature about NF points out that the rejection rate is influenced by the anion concentration, as mentioned above the feed has a high chloride content, which may lead to the reduced rejection rates. There are different effects, which influence the rejection rate. First, the Donnan effect has to be mentioned. If anions with different valences are in the feed, the so-called Donnan effect occurs, which implies that high anion concentrations in the feed lead to increased anion concentrations in the membrane pores and further to higher anion concentrations in the permeate [28]. Thus, the rejection rate decreases. Second, the concentration dependency of the ion rejection, is the covering of fixed ions

through movable ions. That means the movable positive charged ions are enriched on the negative charged pore walls (fixed ions) of the membrane. Through the enrichment the negative charges of the pore walls are shielded and do not affect the inner side of the pores. Because of this shielding, negative charged anions can easier penetrate into the pores and decrease the rejection rates [28] [30] [61]. The mentioned mechanisms may influence the rejection rate of potassium too. Since ammonium has the lowest molecular weight (M_{NH4} = 18.04 g/mol) the achievable rates with nanofiltration are below 20 %.The achieved rejection rates fit well to values found in literature [62].To clarify the rejection behavior of the NF membrane experiments have been conducted with different chloride concentrations in the feed (see section 5.4.2). The results of the first NF stage show that the high chloride content has a negative influence on the rejection rate respectively the purification capability of the NF system. In a next step, the concentrate of the NF stage 1 is the feed for the next purification processes shown in section 5.4, where the NF performance is investigated a second time respectively compared with the effectivity at RO and ED.

5.4 Second purification stage

At the second purification stage, three different processes were investigated. As mentioned in Section 3.4 the concentrate of the first stage (Feed 2) was used as the experimental feed for the second stage. The three processes investigated are NF at 40 bar, RO 30 – 50 bar and ED. The detailed experiments performed are summarized in Table 9.

5.4.1 Nanofiltration at 40 bar

As decided in the first purification stage, NF was operated with 40 bar system pressure because of the volume fluxes and the higher ion rejection rates the higher the pressure [28] [29].

The concentrate flow was at 1.67 ±0.04 l/min and the permeate flow 0.007 ± 0.001 l/min. The deviation of the flows is a result of pressure fluctuations.

Figure 24 shows the measured conductivity of the permeate (σ_Perm), the concentrate (σ_Conc) and the feed (σ_Feed) at 40 bar system pressure. The conductivity of the permeate decreased about 6 mS/cm of the initial feed conductivity. Compared to the results obtained in Stage 1 (see Figure 22) the reduction of the conductivity remained the same. The increase of the concentrate conductivity is visible but due to the fact that only a small volume fraction of the permeate leaves the filtration device the difference compared to the feed is 0.5 mS/cm.

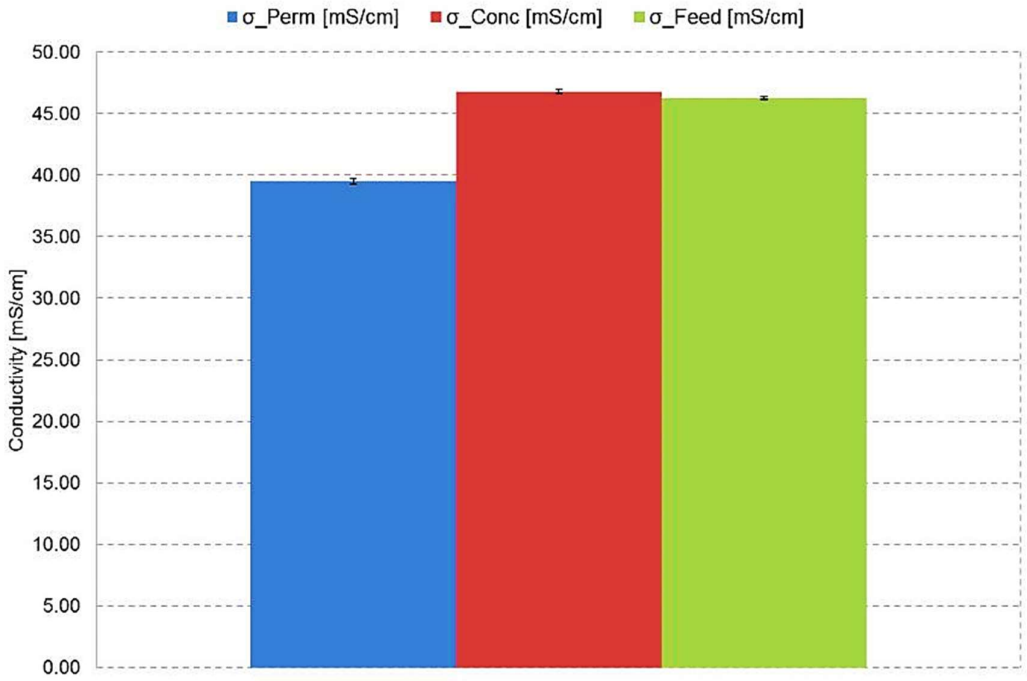

Figure 24: NF Stage 2 - Conductivity of Permeate, Concentrate, Feed at 40 bar

Figure 25 shows the rejection rate of the different salt ions in respect to the system pressure at Stage 2. The concentration values for the calculations are shown in the Appendix in Table 20. The rejection rate of sulphate and phosphate ranges between 70 % and 80 %. This rates correlate with the obtained results in Stage 1 (see Figure 23) and data found in literature [58].

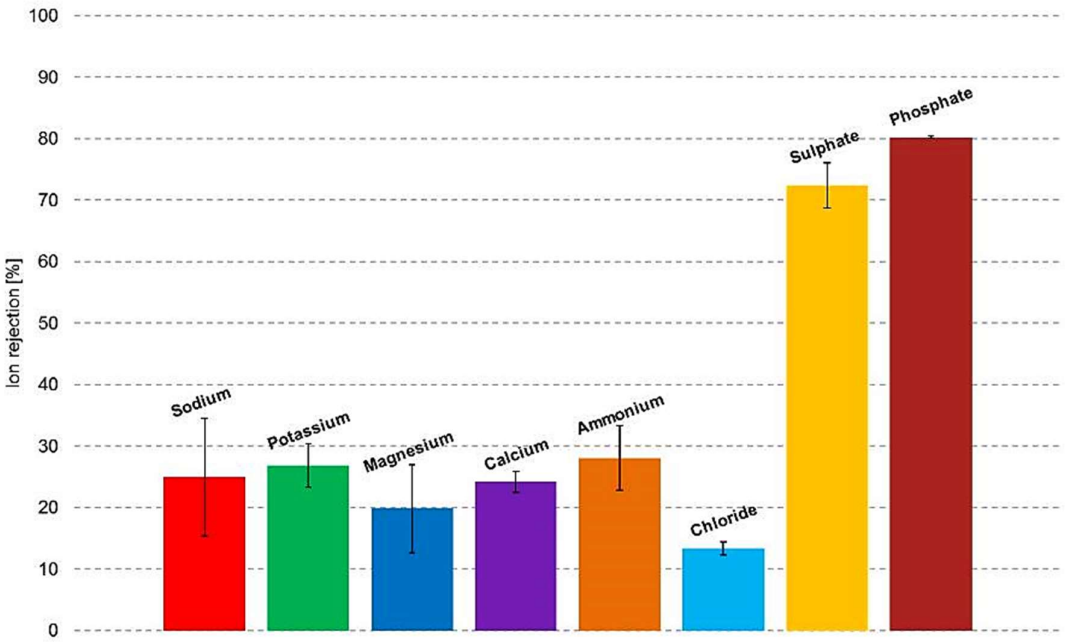

Figure 25: NF Stage 2 – Ion rejection rates in [%] at 40 bar

The rejection rate of magnesium and calcium are between 20 % and 30 % and thus below values found in literature [39] [58]. As mentioned in Section 5.3.1 this can be caused by the influence of measurement deviations connected with the low concentrations of magnesium (10^{-4} g/l) and calcium (10^{-3} g/l) in the feed (see Table 10). Another possibility of decreased rejection rates is the high concentration of chlorides in the feed which leads to reduced rejection efficiency [28]. The rejection rate of ammonium has increased compared to stage 1. Regarding sodium, the rejection is higher than in stage 1 but the standard deviation for sodium is with 10 % high. Regarding chloride ions the rejection rate is comparable to stage 1 and below values mentioned in literature [28] [60]. As explained in Section 5.3.1 the rejection rates are influenced by the Donnan equilibrium, which says that high anion concentration in the feed lead to a higher salt content in the permeate. Due to the shielding effect of the negatively charged pore walls through positive charged ions, the ion rejection efficiency is decreased as well [28] [29] [30].

5.4.2 Nanofiltration rejection behavior at 40 bar

The rejection rates of NF at 40 bar operation pressure were investigated with different concentrations of magnesium sulphate and sodium chloride dissolved in deionized

water. The goal was to show the influence of the chloride concentration on the rejection rate of monovalent sodium and divalent magnesium ions. Table 11 shows the different feed compositions investigated.

As listed in Table 11, three model feeds (MF) where composed for the experiments. The difference between those three is the increasing sodium chloride concentration. MF 0 contains no NaCl but 10 g/l $MgSO_4$, MF 1 the same concentration as in the digestate sample with 4.81 g/l NaCl and 10 g/l $MgSO_4$ and MF 2 contains 23.08 g/l NaCl as it occurred in the experimental Feed 1, with the excess of chloride (see Table 10) and 10 g/l $MgSO_4$. For the model experiments, a new NP030 NF membrane was installed to achieve representative results. Samples were taken for the analysis of sodium and magnesium concentration by AAS.

Table 11: Composition of the model feeds for the additional nanofiltration experiments

Feed ID	**c_{NaCl} [g/l]**	**c_{MgSO4} [g/l]**
MF 0	0.00	10.00
MF 1	4.81	10.00
MF 2	23.08	10.00

With the results of the analysis the rejection rates for the cations where calculated (acc. Equation (9) section 2.5.4.3). Figure 26 shows the rejection rates, achieved by purifying the three model feeds MF 0, MF 1, MF 2. The rejection rate of magnesium without the presence of chlorides in the feed MF 0 is 49 % and aligns with values given in the datasheet and in published literature [39] [58].

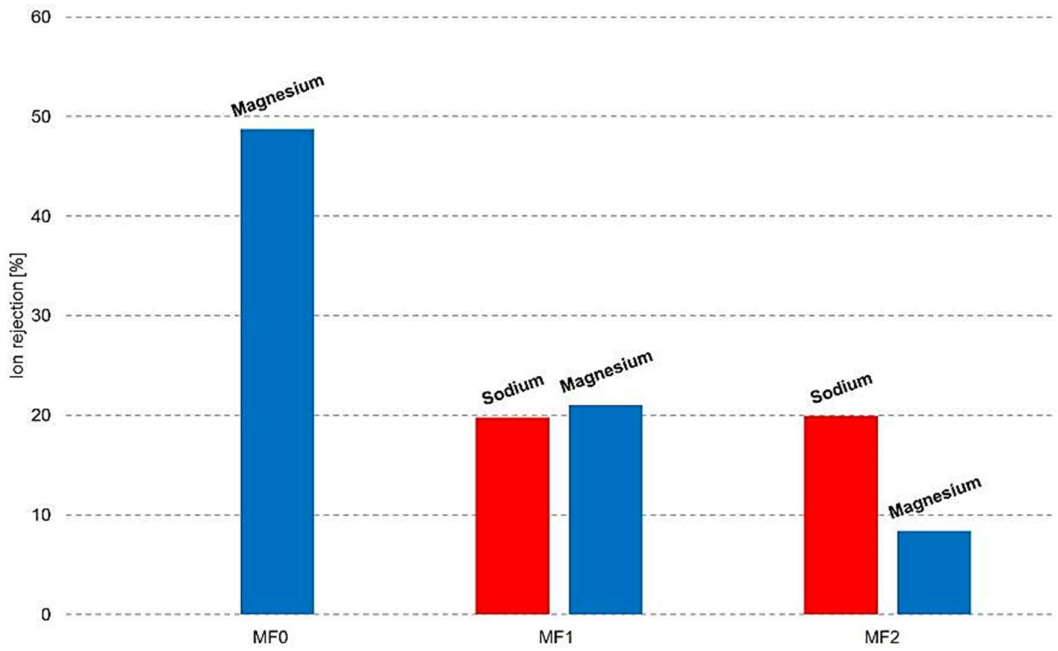

Figure 26: NF model experiment - Ion rejection rates in [%] at 40 bar

By increasing the chloride concentration from 0 to 4.81 g/l at the second experiment with MF 1 the rate decreased significantly from 49 % to 21 %, this level is below values found in literature and in the membrane datasheet [39] [58]. The same accounts for the third model feed MF3, which contained the highest concentration of chloride ions. The rejection rate of magnesium decreased further to 8.4 %, the sodium rejection rate remained the same. The experiments show, that the presence of chloride ions lead to decreased filtration effectivity of monovalent and divalent ions respectively [28] [30] [61]. The data show that the chlorides have a stronger effect on the magnesium ions than on the sodium ions. Due to the charge shielding of movable cations the negative charged anions permeate into the membrane. Because positive and negative charged ions attract each other, the magnesium diffuses into the pores and the rejection rate decreases [28] [29]. The concentration values for the calculations performed are shown in the Appendix in Table 22.

5.4.3 Reverse osmosis at 30 - 50 bar

The second investigated purification processes for the second stage of digestate processing was RO.

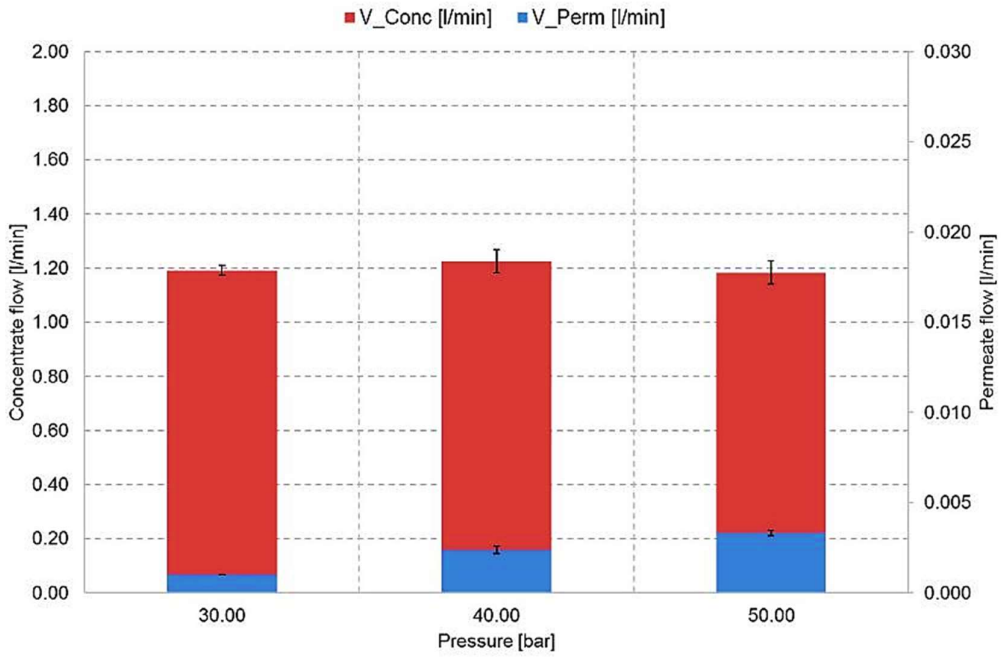

Figure 27: RO Stage 2 - Concentrate and Permeate flow in [l/min] at 30-50 bar

To define an operation point, RO was investigated in dependence on the operation pressure. Based on these experiments, an operating point for further investigations was selected. In Figure 27 the volume flows of the concentrate and the permeate are depicted in respect to the operation pressures from 30 - 50 bar.

The achieved flows show that with a rising operation pressure the permeate flow increases. As an effective volume reduction and a preferably low energy consumption is targeted, the further discussion will focus on the operation point at 40 bar. The volume flow at 40 bar of the concentrate was at 1.23 ±0.04 l/min and the resulting permeate stream was 0.0024 ±0.0002 l/min.

Figure 28 shows the conductivities of the permeate, the concentrate and the feed for the 40 bar RO experiments. The conductivity reduction of the permeate through reverse osmosis is more effective as at nanofiltration (see Figure 22 and Figure 25).

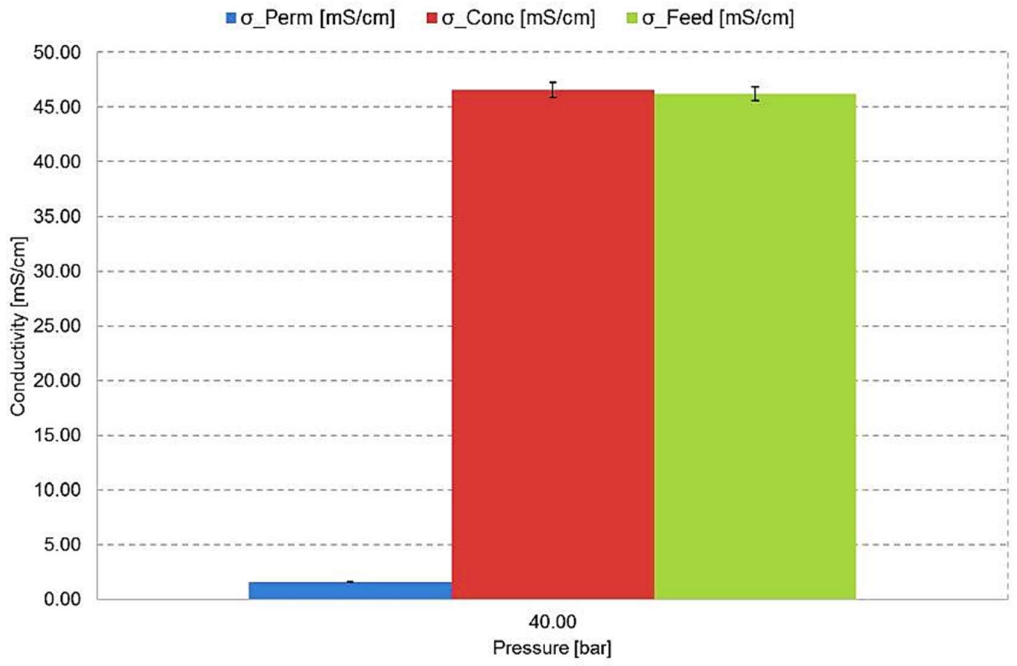

Figure 28: RO Stage 2 - Conductivity of Permeate, Concentrate and Feed at 40 bar

Compared to the initial feed conductivity of 46.2 mS/cm the permeate conductivity decreased by a factor of almost 30 to 1.61 mS/cm in the permeate. As a reference, the limiting conductivity value for water stated in the *Austrian Drinking Water Ordinance* is 2.5 mS/cm [5]. The effective reduction of the conductivity implicates that RO has high rejection rates for the different salts in the feed (see Figure 29) [27] [29] [47]. Similar to the NF experiments (Section 5.3.1 and 5.4.1) the conductivity of the concentrate is almost not affected by the permeate purification.

The rejection rates for RO, calculated with the concentration values (see Appendix Table 21) are shown in Figure 29. The rejection rate is in a range between 90 % and 98 %, which is typically for RO processes [29] [30]. The SD for sodium is at ±1.9 % and for sulphate at ± 2.5 %. This is most likely the influence of measurement inaccuracies. Compared to the influenced rejection rates through the high chloride concentration (see Table 10) at NF (see Figure 23 and Figure 25) the achieved rates at RO are not negatively affected. Due to the small pore size of RO membranes (0.1-1 nm) and their geometry the rejection behavior is not influenced through the anions in the feed like the NF membrane is [30] [38].

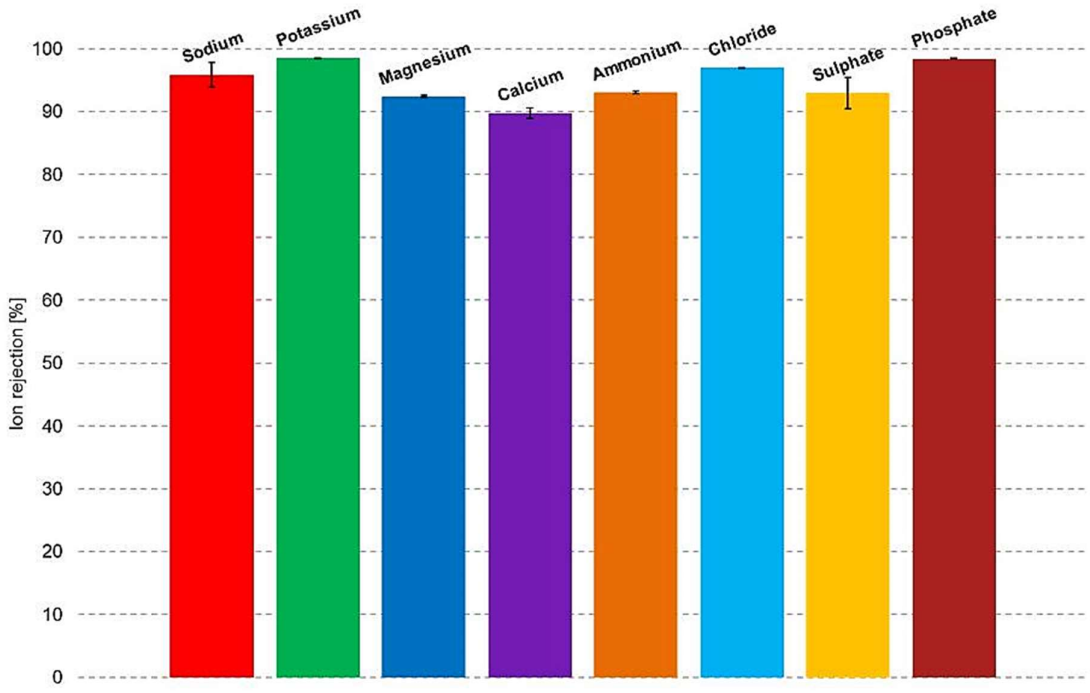

Figure 29: RO Stage 2 - Ion rejections rates in [%] at 40 bar

5.4.4 Electro dialyses

The ED process was investigated for the second stage of the purification processes shown in see Figure 17. During the ED experiments the process parameters cell current and temperature were held constant. The used equipment does not provide the possibility to take samples continuously, hence the experiments were stopped after a certain time. The experimental matrix is summarized in section 5.1, in Table 9.

First, the limiting current density was determined. The limiting current density specifies the point where water decomposition occur and where the process becomes uneconomically. Water dissociation leads to a decreased performance of the process (e.g. gas formation on the electrodes, membrane fouling). Furthermore, the occurring OH^- ions on the cathode lead to the formation of hardly soluble salts such as magnesium hydroxide [36]. The limiting current density has to be determined in respect to the used ED device and the feed solution [28]. For the experimental determination, the cell was filled with the feed and the cell voltage was increased gradually. The rise of the cell current was determined by the measurement of the increasing voltage drop over a resistor (see Section 4.3.1).

Figure 30 shows the change of the cell current in respect to the cell voltage. The determination of the limiting current was performed twice (i_1, i_2). The intersection point of the asymptotes shows that the value of the limiting current for this process is at 1.67 mA. The equations of the linear fits are shown in the Appendix (equation (10) and (11)). For the operation of the ED cell, the current should be 80 % of the limiting current [30] [54]. Which results at a cell current for this process of 1.33 mA. Considering the 40 cm² effective membrane area, the current density is at 0.33 A/m². After the determination of the operation limiting current respectively limiting current density for the ED process, the experiments where performed for different durations.

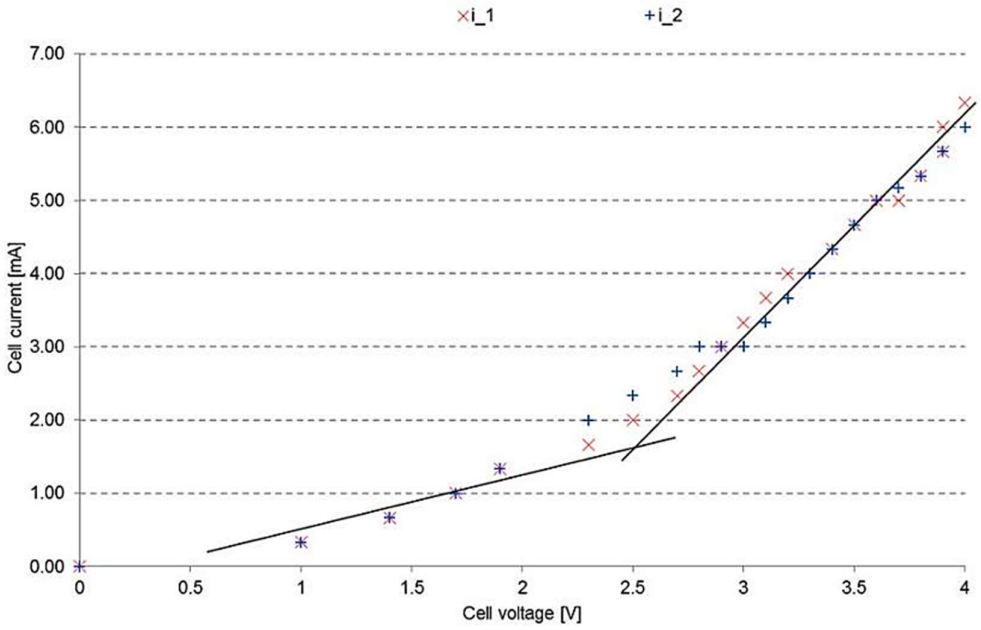

Figure 30: ED Stage 2 - Cell current [mA] over cell voltage [V]

As mentioned in Section 4.3.2, the membrane compartment of the ED cell was filled with Feed 2, the anode compartment contained a 10^{-1} mol/l HCl electrolyte and the cathode compartment a 10^{-1} mol/l NaOH electrolyte. During the experiment, the temperature was held constant at 25°C.

Figure 31 shows the measured conductivities of the solutions in the MC, AC and CC in dependence of the time. The measured conductivity of the feed in the membrane compartment (σ_MC) indicates that the solution is purified from salts. After 8 hours, the conductivity of the feed decreased by 4 mS/cm. During the ED experiment, salt

precipitation was observed on the anode and on cathode. Further investigations on this behavior can be seen at the end of this section.

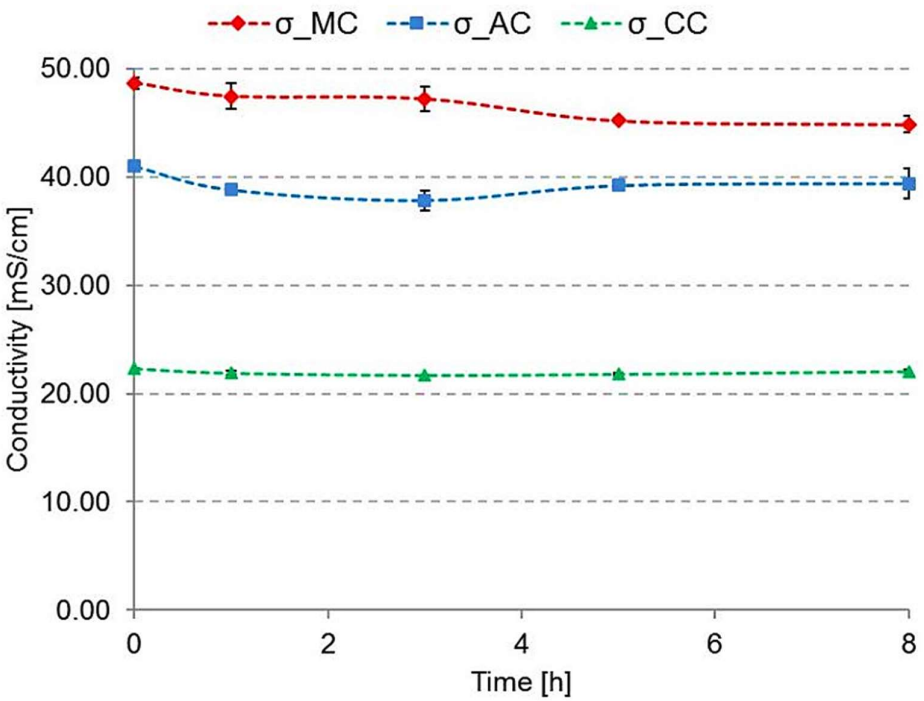

Figure 31: ED Stage 2 – Conductivity in the MC, AC, and CC over 8 hours

Table 12: Electro dialysis process parameters

t [h]	pH_{MC}	pH_{AC}	pH_{CC}	T [°C]	I [mA]
0	8.51 ±0.03	1.89 ±0.00	12.45 ±0.00	23.14 ±0.69	1.33
1	8.39 ±0.01	1.78 ±0.03	12.42 ±0.08	25.35 ±0.65	1.33
3	8.19 ±0.08	1.81 ±0.01	12.45 ±0.02	25.90 ±1.40	1.33
5	8.27 ±0.04	1.95 ±0.12	12.44 ±0.01	25.05 ±0.05	1.33
8	7.89 ±0.12	1.88 ±0.01	12.43 ±0.03	25.00 ±0.00	1.33

The process parameters and their mean values during the ED experiments are summarized in Table 12. The temperature of the solutions in the ED cell was around 23 °C and after 1 hour it stayed almost constant at 25 °C. The pH value in the MC decreased with time whereas the pH values in the electrode compartments remained stable. The operation point with the 10^{-1} mol/l electrolytes was chosen to ensure good conductivity and to see the mass transfer. But at this concentrations, the pH changes

in the AC and CC cannot be seen. Therefore, additional experiments were carried out with different pH values of the electrolytes (see Table 13). With the concentration values of the feed after the respective time (see Appendix Table 23), the ion rejection rate was calculated.

Figure 32 shows the rejection rates after 8 hours. The achieved rejection rates in ED are lower than the rejection rates when NF experiments were performed (see Figure 23 and Figure 25). Remarkable small are the rejection rates for sulphate at 11 % respectively phosphate at 6 %. This behaviour is discussed in the following section 0 were the rejection rates of NF and ED are compared.

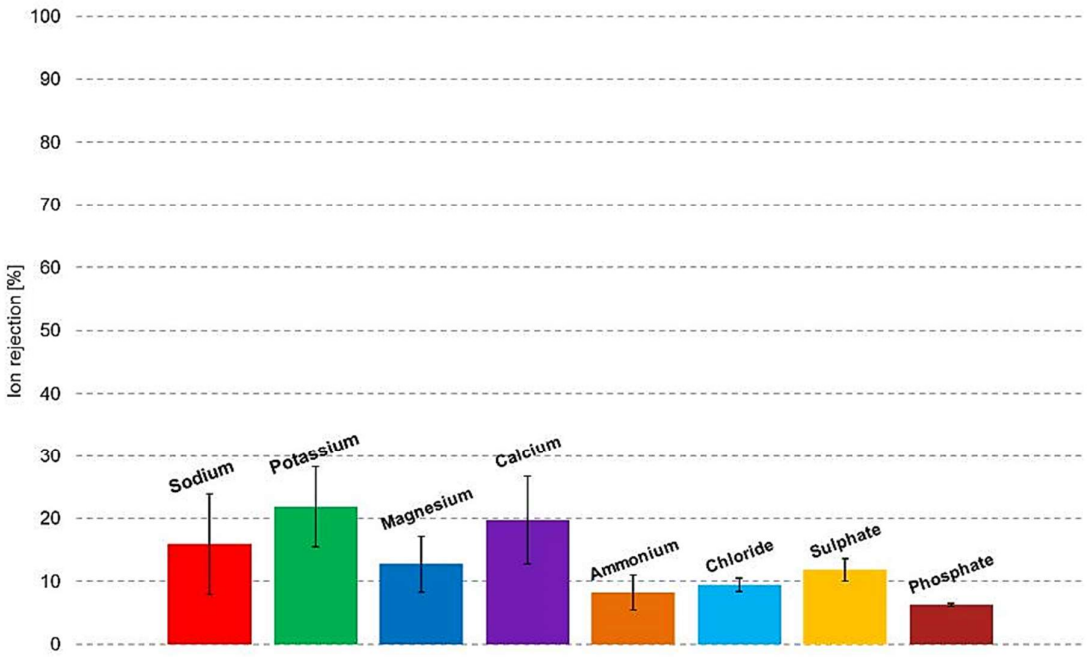

Figure 32: ED Stage 2 - Ion rejection rates in [%] after 8 hours

Goal of the following experiments was, in addition to the third separation process (ED), to investigate the influence of the salt concentration and type in the cathode and anode chamber on the rejection rate. Therefore, three experiments with different solutions as electrolytes, see Table 13, were performed. Besides the conductivity investigations, the alteration of the pH values in the different compartments where measured.

Table 13: Properties of the feed and electrolytes at the ED experiments

ID	Substance	pH	$c_{Electrolyte}$ [mol/l]	$\sigma_{i,0}$
E1_MC	Feed 2	8.54	–	48.25
E1_AC	HCl solution	1.89	$10^{-1.89}$	41.00
E1_CC	NaOH solution	12.45	$10^{-12.45}$	22.30
E2_MC	Feed 2	8.54	–	48.25
E2_AC	HCl solution	3.25	$10^{-3.25}$	5.29
E2_CC	NaOH solution	8.74	$10^{-8.74}$	0.16
E3_MC	Feed 2	8.54	–	48.25
E3_AC	Feed 2	8.54	-	48.25
E3_CC	Feed 2	8.54	–	48.25

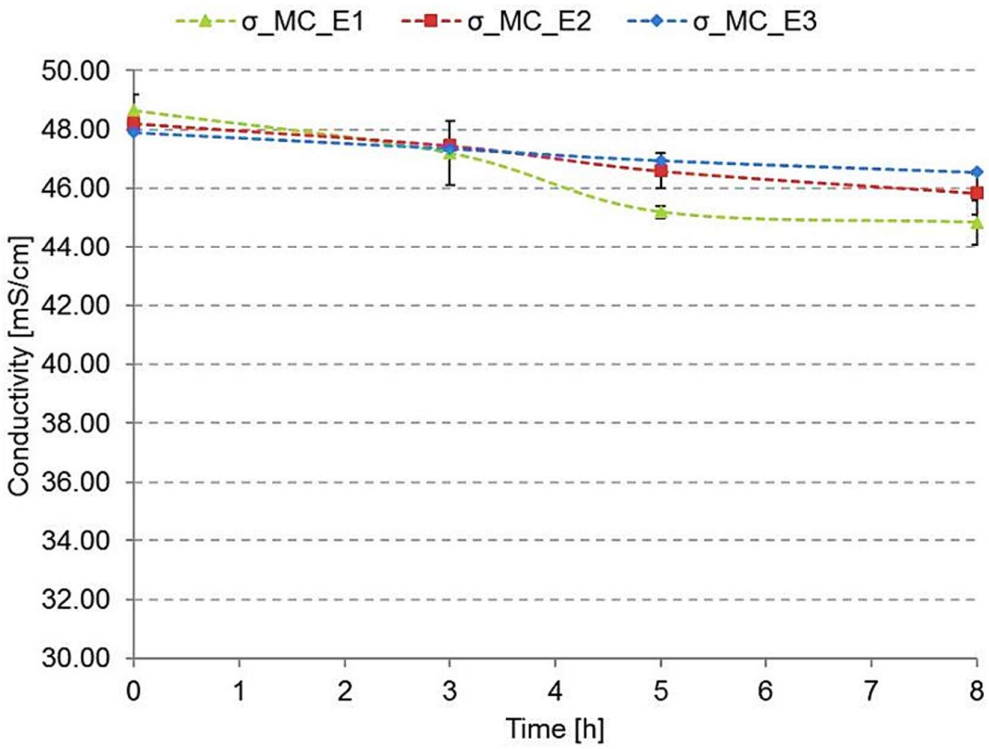

Figure 33: ED: Conductivity decrease with different electrolytes over 8 hours

Figure 33 shows the outcome of the conductivity measurements. The conductivity drop in the membrane compartment varies with the used electrolytes. The most effective conductivity decrease was achieved with the 10^{-1} mol/l NaOH respectively 10^{-1} mol/l HCl electrolytes (σ_MC_E1= 44.85 mS/cm) followed by the experiment E2 with a conductivity in the membrane compartment of 45.85 mS/cm. The third test was performed with the experimental feed in the MC and as electrolyte in the AC and CC. The conductivity decreased from 48.99 mS/cm to σ_MC_E3= 46.55 mS/cm, which represents the lowest conductivity drop. Due to the presence of anions and cations in the electrode chambers, the process is slowed down, because the ions have to diffuse through the membranes to the attracting electrode. The measured pH values during the experiments are summarized in Table 14. The pH change is more significant using the electrolytes E2_AC and E2_CC (E2 composition see Table 13) because of their lower concentration of H_3O^+ respectively OH^- ions at the beginning of the experiment. The pH values with the index E1 represent the data for the experiment with the 10^{-1} mol/l electrolytes. Because of the high concentration of OH^- respectively H_3O^+ ions in the electrolytes, the pH values was almost unaffected. Regarding the experiment E3, where the feed was used in all three chambers, no change of the pH value in the CC and MC is observed. The pH-value in the AC decreases in the first three hours and remains stable afterwards. In this experiment, electrolysis on the anode respectively precipitation on the cathode was observed. The drop of the pH-value during the different experiments was caused by the occurring H_3O^+ ions due to electrolysis on the anode [36].

Table 14: ED: pH values in the MC, AC and CC for samples taken at 3, 5 and 8 hours

ID	t = 0 [h]	t = 3 [h]	t = 5 [h]	t = 8 [h]
pH_MC_E1	8.51±0.55	8.19±1.1	8.27±0.20	7.89±0.75
pH_AC_E1	1.89±0.03	1.81±0.08	1.95±0.05	1.88±0.12
pH_CC_E1	12.45±0.00	12.45±0.90	12.44±0.50	12.43±1.4
pH_MC_E2	8.54±0.00	7.84±0.01	7.66±0.01	7.60±0.01
pH_AC_E2	3.25±0.00	2.87±0.02	2.48±0.03	2.29±0.02
pH_CC_E2	8.74±0.00	10.18±0.08	10.58±0.00	10.54±0.01

pH_MC_E3	8.54±0.01	8.50±0.00	8.46±0.01	8.44±0.00±
pH_AC_E3	8.54±0.00	6.57±0.03	6.50±0.00	6.46±0.01
pH_CC_E3	8.54±0.00	8.71±0.01	8.67±0.01	8.61±0.00

The observed water electrolysis in the AC during experiment E3 is caused by the applied cell voltage. Due to the varying electrical resistance of the ED cell during the experiment, the cell voltage was adjusted to keep the cell current constant, the voltage during the experiments ranged between 2-4 volts. Cell Voltage over the limiting value of 2 V leads to a reduction reaction in the cathode camber where salts are formed on the electrode (see Figure 34 detail 1). The standard electrode potentials given in Table 15 indicate, the lower the electrical potential of the species the easier it is oxidized respectively acts as a reducing agent [63]. The values in Table 15 show that most likely sodium, potassium, calcium or magnesium salts precipitated on the cathode.

Table 15: Standard electrode potential in [V] for selected ions. Source [64]

	Na^+	K^+	Ca^{2+}	Mg^{2+}	Cl^-	PO_4^{3-}	SO_4^{2-}
E^0 [V]	-2.71	-2.93	-2.87	-2.37	1.36	-1,05	-0,93

An evidence of the mechanisms mentioned was observed after the 8 hour experiments. On the steel cathode, salt precipitation was visible and the platinum anode was oxidized on some points, which can be caused by chlorine corrosion (see Figure 34). Since the anode was used for several experiments before, it is probable that the protecting platinum layer on the surface is missing in some areas of the mesh.

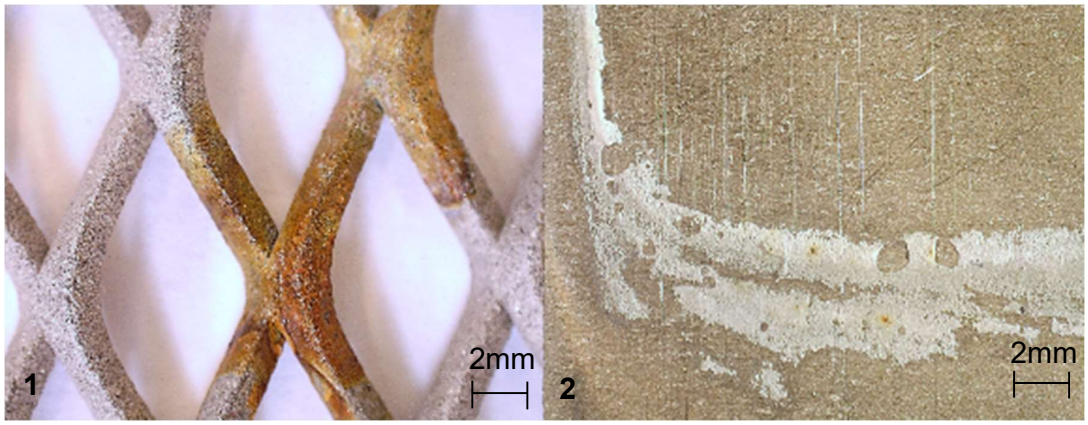

Figure 34: ED: Cathode and anode after 8-hour electro dialysis

The corroded platinum anode (Detail 1 in Figure 34) and the precipitated salt on the cathode (Detail 2 in Figure 34) are shown in the pictures below. As mentioned before, the precipitated salt can be magnesium hydroxide which has a solubility of 0.009 g/ [57].

5.5 Comparison of nanofiltration and electro dialysis

This section compares the achieved rejection rates of nanofiltration and electro dialysis. Reverse osmosis has rejection rates that are 4 times higher as at NF or ED, thus RO is not compared to the two other processes (see Section 0 Figure 29).

Figure 35 shows the ion rejection rates for the NF at 40 bar and electro dialysis after 8 hours at 1.33 mA cell current. The values for the calculations are summarized in the Appendix in Table 20 and in Table 23.

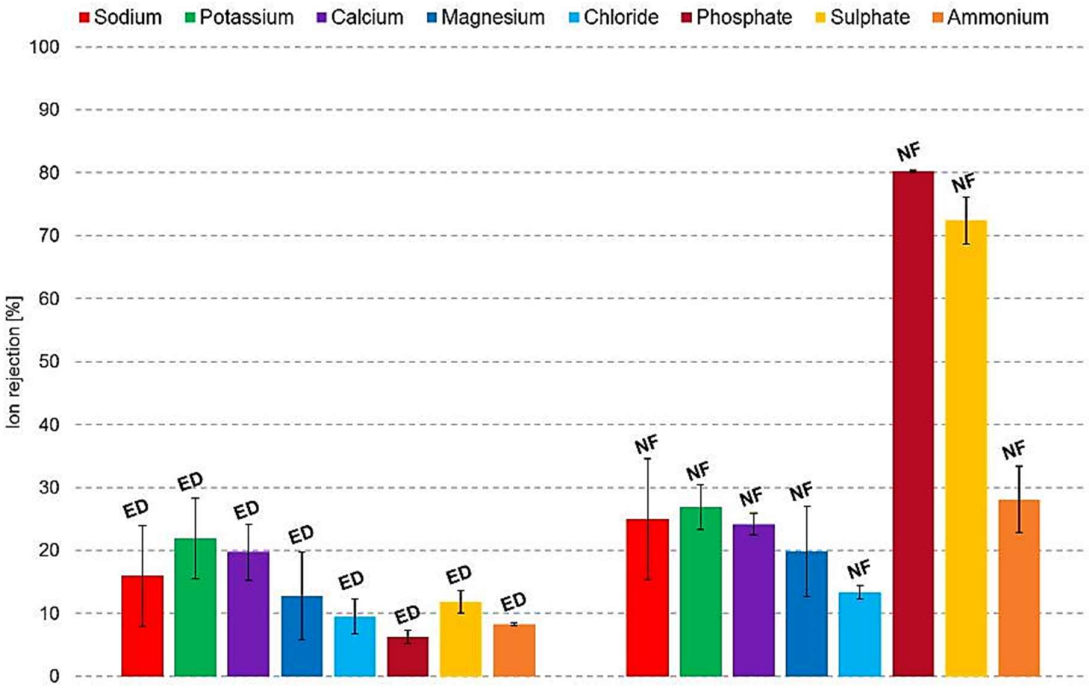

Figure 35: Comparison of the rejection rates for mono and divalent species at ED and NF

The rejection of monovalent ions is higher using NF compared to ED. At NF, the rate for sodium is 9 % higher, for potassium 5 %, for chloride 4 % and for ammonium 20 %. The same accounts for Mg^{2+} where the rate is 7 % higher and for Ca^{2+} where the rate is 4.5 % higher than at ED, whereas the deviation between ED and NF is probably

caused by their low initial concentration in Feed 2 (see Table 10). Remarkable high is the difference of the rejection rates regarding sulphates and phosphates, since they are with 72 % and 80 % 7 times higher at NF. In contrast to latter, the rejection at ED is not based on filtration effects but on the strength of the electrical potential. Since the molecular weight respectively molecular size of multivalent ions is higher than that of monovalent ones, they pass slower through the membrane pores to the attracting electrode. This fact causes the poor rejection rates for multivalent ions at ED shown in Figure 35 [65].

5.6 Suggestion for an overall purification process

Goal of the present work is to decrease the salt concentration of liquid digestate from 23.4 g/l respectively 12.4 g/l in the feed to 10 g/l (= 1 m%) in the permeate (see section 5.2 in Table 10). Based on the performed experiments an overall purification process for an effective and economical purification of the salt containing liquid digestate is suggested. Regarding filtration operations like NF and RO as possible purification techniques, extensive pre-treatment has to be performed because of suspended solids in the liquid digestate, which are able to cause clogging of the membranes and drastically reduce the separation potential. Since RO is a well-known technique for the purification of salt containing liquids and its high rejection effectivity, it is not taken into account for the overall processes further on [28] [29] [37] [38]. The experiments show that ED is less efficient than NF (see 5.5) and due to the lack of knowledge on performance in real scale digestate processing, ED is excluded in the following process proposals. For the overall purification, two different approaches based on NF at 40 bar operation pressure are investigated further on.

First, a purification process consisting of a NF system with 3 respectively 4 stages is evaluated (see Figure 36). The goal for this process suggestion is to decrease the salt concentration in the digestate to 1 m% and reduce the arising concentrate fraction as much as possible. At a second approach, two NF systems are combined together with the goal to gain a fertilizer concentrate, containing phosphates and sulphates, in the first system and afterwards purify the permeate fraction in the second system (see Figure 37). It is assumed that the fertilizer recovery system is equipped with NF membranes with very low NaCl rejection rates (R_{NaCl} < 10 %). As emphasized in section 1, an interesting possibility after the purification is the usage of the permeate

for mashing or cleaning purposes within the biogas facility. Therefore, the two process suggestion are investigated on the effect of the alteration of the total salt concentration in the permeate if a fraction of the permeate is recycled for several iterations (see Figure 36 and Figure 37 red lines).

The two overall processes are evaluated for two different scenarios. For the first scenario, the experimental feed (Feed1) with the high chloride content (see Feed 1 Table 10) is chosen to proof the ability of the processes to handle salt concentrations above two mass percent. At the second scenario, the feed (Feed D) has the same composition as the digestate samples taken from real scale plants (see Digestate Table 10). The two different processes are investigated on their ability to decrease the initial salt concentration to the aimed level of 1 m% and the number of NF stages, which are needed. Figure 36 and Figure 37 give schematics on these two processes.

In the process suggestion, given in Figure 36 (NF1), the number of nanofiltration stages “i” is varied. Input is a feed (F1) with 3.13 m³/h. This value of the feed volume stream bases on data given from the company BDI, which states that a typical biogas facility got a digestate output of 25,000 t/y at 8,000 operating hours. The targeted total salt concentration in the permeate (P_{total}) is 1 m%. The red line indicates the investigated recycle possibility, were 50 %, 25 % or 10 % of the total permeate stream(P_{total}) are used within the biogas facility.

The process suggestion shown in Figure 37 (NF2) targets on the fertilizer production in a first step and in the second step the same boundaries as for the process suggestion one are applied. The red line indicates the permeate recycle stream ($P_{Recycle}$) were 50 %, 25 % or 10 % of the total permeate stream (P_{total}) are used in the biogas facility.

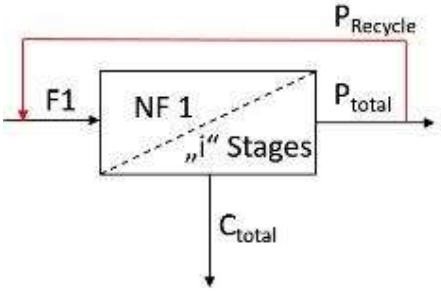

Figure 36: NF1 - Process scheme digestate purification with “i” stages

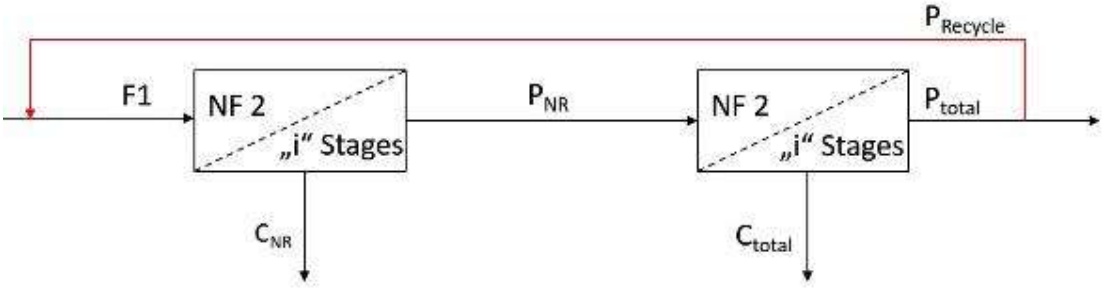

Figure 37: NF2 - Process scheme nutrient recovery and digestate purification

In Table 16, the outcome of the calculation of the different purification approaches without the recycle option is summarized. For the calculations, a digestate mass flow of 3.13 t/h was assumed. At process NF1, the feed should be purified to one mass percent salt concentration. The mass flow ratio of concentrate to permeate is 1/5. If Feed 1 has to be processed the NF system consists of four stages to reach the concentration level of 1 m%. Regarding the purification of Feed D, one stage of NF would be sufficient to reduce the salt concentration below 1 m%. Using three stages, the concentration decreases significantly to 0.57 m%. As a benefit the purified permeate can be used for mashing or other side processes in the biogas plant to reduce the fresh water consumption.

Table 16: Results of the NF purification approaches without recycle option

Process	Feed	$\dot{M}_{Feed}$ [t/h]	Stages [-]	$w_{Feed,0}$ [m%]	$w_{Perm,i}$ [m%]	$w_{Conc,i}$ [m%]	$\dot{M}_{Perm}$ [t/h]	$\dot{M}_{Conc}$ [t/h]	$\dot{M}_{Perm}/\dot{M}_{Conc}$
NF1.1	Feed1	3.13	4	2.34	1.05	8.86	2.61	0.52	1/5
NF1.2	D	3.13	3	1.24	0.57	4.59	2.60	0.53	1/5
NF2.1	Feed1	3.13	1	2.34	2.08	3.14	2.34	0.78	1/3
NF2.2	P2.1	2.34	4	2.08	0.95	7.74	1.96	0.39	1/5
NF2.3	D	3.13	1	1.24	1.11	1.65	2.34	0.78	1/3
NF2.4	P2.1	2.34	3	1.11	0.52	4.03	1.95	0.39	1/5

The second process suggestion (Figure 37) aims on the production of a fertilizer concentrate containing phosphates and sulphates in the first purification step,

afterwards the remaining salts are removed from the permeate in a second NF step. The membrane at the nutrient recovery step was selected in respect to its rejection efficiency of multivalent ions. It is necessary to use a membrane which rejects the ions with high molecular weights and let the small monovalent ions pass through (e.g. Nitto NTR 7410 or Fluid Systems SR 2) [66]. If Feed 1 is inserted, one stage of NF for the recovery purpose and four stages NF are required to meet 1 m% salt concentration in the concentrate. Regarding Feed D, one NF stage in the second step is sufficient to decrease the salt concentration below 1 m%. Using a system with three stages in the second system, the digestate would be purified to 0.52 m%. In both scenarios, the recovered nutrient stream is 0.78 t/h. The recovered quantity of phosphates is between 8 t/y and 15 t/y and the quantity of sulphates ranges around 1.6 t/y depending on the initial concentration in the used feed. According to data published by *Agrar Markt Austria,* the sales quantity of phosphorus based fertilizers was 32,000 t/y in 2015, whereby the price for phosphorus fertilizer is approximately 300 €/t [67], [68]. The price for sulphur based fertilizers ranges between 800-2000 €/t depending on the concentration. The exact amount of sold sulphur fertilizer is not published, but according to literature 60 kg sulphur per hectare are sufficient [69]. Taking the prices and the produced quantity of sulphur and phosphorus fertilizer into account, calculations show that the production of a marketable fertilizer is most likely not economically compared to the cost of the purification system. Another problem is that the fertilizer is a by-product of the digestate processing and thereby may not be marketable as a common agricultural fertilizer. The most important results regarding the different scenarios and processes are emphasized in Table 16. For the calculation of the salt concentration in the permeate and concentrate at NF 1.1 and NF 2.1/2.2, the rejection rates of the NF experiments where used (see Figure 25). The assumed rejection rates for the nutrient recovery system are shown in the Appendix in Table 24.

As mentioned before, the two different process suggestions (NF1, NF2) were calculated in terms of a recycle stream of 50 %, 25 % or 10 % within in the biogas facility. Figure 38 shows the salt concentration in the permeate over 10 recycle iterations for the different used permeate quantities for recycling at the first purification process NF 1 (see Figure 36).

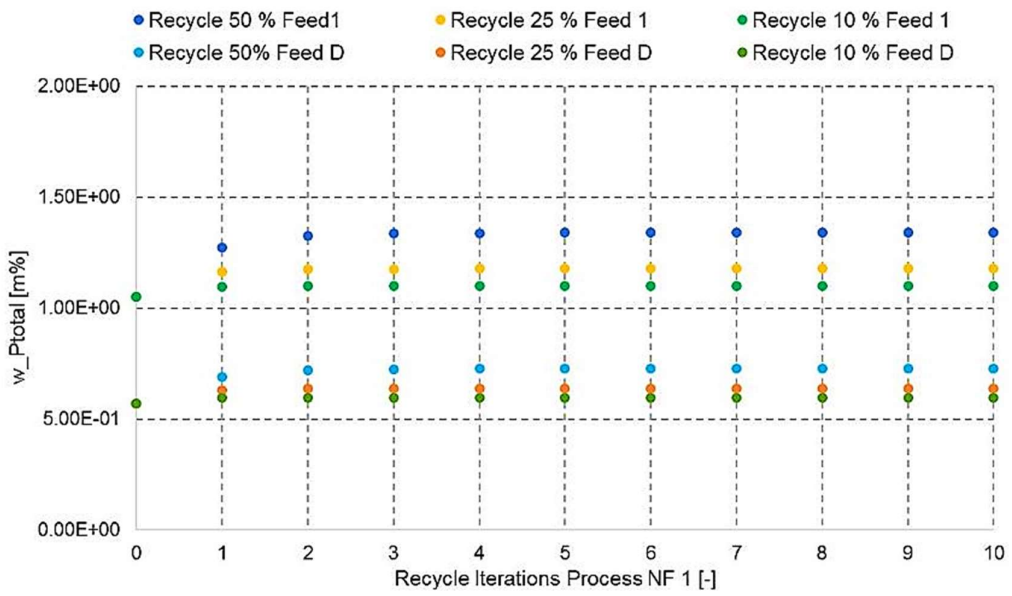

Figure 38: Permeate salt concentration in [m%] over recycle iterations, for one step nanofiltration

If Feed 1 (2.34 m% salts) is purified in the first process NF 1 over 4 stages the initial salt concentration in the permeate which is recycled is 1.05 m% (see Table 16). Figure 38 shows that due to the recycling operation the salt concentration in the permeate increases at first, but gets constant after certain iterations. If 50 % of the permeate stream $\dot{M}_{Perm}$ are recycled, the salt concentration in the permeate (P_{total}) stays constant at 1.34 m% after 6 iterations. 25 % recycled permeate leads to 1.18 m% in the permeate after 4 iterations and if 10 % are recycled the salt concentration stays constant after 2 iterations at 1.10 m%.

At the second scenario Feed D (composition see Table 10) is purified within the first process NF 1 over 3 stages with 0.57 m% initial salt concentration in the permeate (see Table 16). Figure 38 shows that 50 % of $\dot{M}_{Perm}$ lead to 0.73 m% salt concentration after 6 iterations. Using 25 % of the permeate results at 0.64 m% after 4 iterations and for 10 % at 0.60 m% in the arising permeate stream after 2 iterations.

The results of the permeate recycling show that the usage of a permeate fraction as process water initially increases the salt concentration in the permeate of the nanofiltration process. The increase of the permeate salt concentration implicates that the recycling has to be performed in respect to its influence on the salt loads in the purification process. Therefore, it is preferable that 25 % or 10 % of the permeate are

used for recycling purposes when the feed with 2.34 m% is purified in the system NF 1 to remain close to the limit of 1 m% permeate concentration.

In the case of feed D with 1.24 m% initial salt concentration purified over 3 NF stages, 50 %, 25 % or 10 % of the permeate stream could be recycled because the limit of 1 m% is not exceeded.

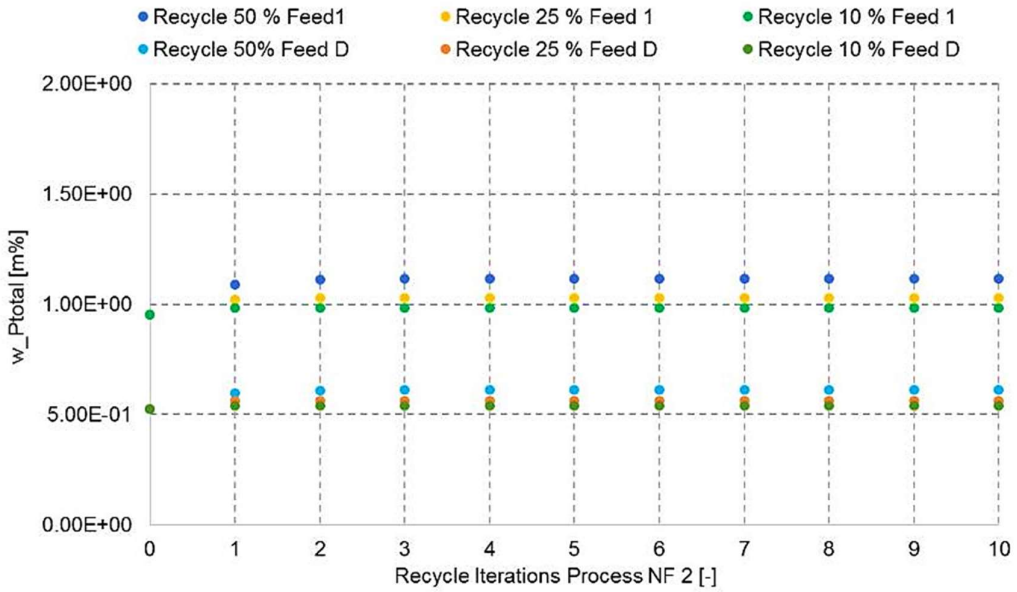

Figure 39: Permeate salt concentration in [m%] over recycle iterations for two step nanofiltration with fertilizer recovery

Figure 39 depicts the resulting salt concentration in the permeate in dependence on the recycle iterations at the second purification system NF 2 with nutrient recovery (see Figure 37). The same boundary conditions as for the recycle process for NF 1 relating to the feed and recycled fraction are applied.

In the case of Feed 1 as process feed, the initial salt concentration in the permeate is at 0.95 m% (see Table 16). If 50 % of the total permeate stream ($\dot{M}_{Perm}$) are recycled the salt concentration in the permeate increased to 1.11 m% after 4 iterations and stays constant afterwards. The recycling of 25 % of $\dot{M}_{Perm}$ leads to 1.03 m% salts after 3 iterations. If 10 % of $\dot{M}_{Perm}$ are recycled, after 2 iterations the salt concentration remains at 0.98 m%.

The curves in Figure 39 show the progress of the salt concentration if Feed D is purified in the NF 2 process and different fractions of the arising permeate are recycled. The

initial salt concentration in the permeate is 0.52 m% (see Table 16). After 4 iterations the concentration increased to 0.61 m% and remains steady when 50 % of the permeate ($\dot{M}_{Perm}$) are recycled. If 25 % are recycled, after 3 recycle iterations the salt concentration stays at 0.56 m% and in the case of 10 % recycled quantity the salt concentration remains at 0.54 m% after 2 iterations.

In general, the outcome of the recycling analysis shows that the usage of permeate within the biogas facility is possible if it is performed in respect to the resulting increase of the salt concentration. Regarding purification process NF 2 with nutrient recovery the analysis shows, that in the case of Feed 1 as process feed a recycling of 25 % respectively 10 % of the total permeate amount is preferable to lower its impact on the resulting permeate salt concentration. If Feed D is purified 50 %, 25 % or 10 % can be recycled because the limit of 1 m% is not exceed after 10 iterations. When nutrient recovery in a first step is applied, the overall salt concentration in the permeate is lower.

Flow sheets and important calculations performed for the different scenarios are shown in the Appendix Figure 40 to Figure 44 respectively Table 25 to Table 31.

6 Conclusions

Within this thesis, the treatment possibilities of salt contaminated liquid digestate from biogas plants were investigated. The present work is subdivided into three parts. In the first part of the thesis a literature research was done. Based on the literature research, in the second part, experiments were performed with a model feed from a biogas facility dealing with food residuals. The third part aims at a process suggestion for the liquid fraction of the digestate. Therefore, two process combinations are suggested including a consideration of using the cleaned water as process water and the combination of the purification with a nutrient recovery stage.

The outcome of the literature research was verified by the development of a decision matrix. The matrix suggests mass transfer unit operations like distillation, membrane distillation and membrane based filtration operations as purification techniques for liquid digestate. Main difference between conventional waste water treatment and digestate treatment is the presence of different ion species. Reverse osmosis, nanofiltration and electro dialysis were investigated in laboratory experiments. Reverse osmosis has rejection rates of dissolved salts of 90 % and higher. In comparison, nanofiltration shows rejection rates of 20% for monovalent ions and for multivalent ions the rates range between 50 % and 80 %. Electro dialysis has rejection rates around 15 ± 5 % and due to the presence of hardly soluble salts, precipitation was observed.

Since nanofiltration has higher permeate fluxes than reverse osmosis, two overall purification processes were conceived. The first process consists of a multi stage nanofiltration system, which purifies the liquid digestate to a salt concentration of 1 m% and below. The second process aims to gain a nutrient concentrate in a single stage nanofiltration system and afterwards purifies the concentrate of the first stage in a multi stage nanofiltration system to the limit of 1 m% and below. The possibility to integrate the nutrient fraction of the digestate in a value chain is an interesting option to run biogas plants more economically. Whereas, the marketing of such a fertilizer seem to be a major challenge.

Additionally, the integration of permeate recycling at the two overall purification processes was investigated too. A fraction of the permeate can be used within the biogas facility to lower the costs for fresh process water used for mashing or cleaning

purposes. The calculations for such a usage of the permeate show that due to the recycling of a permeate fraction the salt concentration of the feed rises at first but remains constant after at least 4 recycle iterations. Since the ion rejection rate of the nanofiltration system stays constant, an increase of the initial salt concentration leads to higher salt loads in the permeate. In general, the permeate recycling is a promising method to lower operating costs of the facility but has to be performed in respect to the resulting salt concentration in order to comply with the limit of 1 m% in the arising permeate after the purification processes. Nevertheless, the integration of post purification steps, such as nanofiltration, in biogas facilities is a promising option to enable the usage or the release of the purified fraction.

Whereby further research on the performance and applicability in real scale plants is necessary in the future. Furthermore, alternative processes such as membrane distillation represents an interesting possibility to selective remove targeted substances like ammonium to gain a nutrient concentrate for fertilizing purposes.

7 Literature

[1] P. P. Capros and A. De Vita, “Development and evaluation of long- term scenarios for a balanced European climate and energy policy until 2030,” pp. 1–8, 2015.

[2] EU, “Eurostat - Statistics Explained,” 2016. [Online]. Available: http://ec.europa.eu/eurostat/statistics-explained/index.php/Energy_from_renewable_sources.

[3] Biomasseverband, “Bioenergie - Basisdaten 2015,” 2015.

[4] *Düngemittelverordnung 2004*. Österreich: Bundeskanzleramt Rechtsinformationssystem, 2016, pp. 1–19.

[5] *Bundesgesetzblatt für die Republik Österreich - Trinkwasserverordnung*, no. 2. Österreich, 2001.

[6] W. Fuchs and B. Drosg, *Technologiebewertung Gärrestbehandlungs Verwertungskonzepte*. Tulln: Universität für Bodenkultur Wien, 2010.

[7] M. Zimmer and J. Lippelt, “Kurz zum Klima : Zu viel Salz verdirbt den Boden,” pp. 51–53, 2012.

[8] L. Montgomery and G. Bochmann, “Pretreatment of feedstock for enhanced biogas production,” *IEA Bioenergy*, no. February, pp. 1–20, 2014.

[9] G. Bochmann and L. F. R. Montgomery, “Storage and pre-treatment of substrates for biogas production,” in *The Biogas Handbook: Science, production and applications*, 2013, pp. 85–103.

[10] K. Mairitsch, W. Wimmer, and S. Aigner, “Über die Erschließung des Potenzials biogener Haushaltsabfälle und Grünschnitt zum Zwecke der Verwertung in einer Biogasanlage zur optimierten energetischen und stofflichen Verwertung.” Arge ECO.in, pp. 1–202, 2011.

[11] T. A. S. Biosantech, D. Rutz, R. Janssen, and B. Drosg, “Biomass resources for biogas production,” in *The Biogas Handbook*, 2013, pp. 19–51.

[12] S. Junne, “Basics of the Biogas Production Process,” Berlin, 2014.

[13] *Leitfaden - Biogas: Von der Gewinnung zur Nutzung*, 6th ed. Fachagentur Nachwachsende Rohstoffe, 2013.

[14] K.-H. Rosenwinkel, H. Kroiss, N. Dichtl, C.-F. Seyfried, and P. Weiland, *Anaerobtechnik*. Berlin, Heidelberg: Springer Berlin Heidelberg, 2015.

[15] A. Petersson, “Biogas cleaning,” in *The Biogas Handbook: Science, production and applications*, Woodhead Publishing Limited, 2013, pp. 329–341.

[16] S. Bernhard, “Arbeitskreis Biogas: Weiterentwicklung durch internationalen Betriebsvergleich,” *Online-Facheitschrift des Bundesministeriums für Land- und Forstwirtschaft, Umwelt und Wasserwirtschaft*, no. 1, pp. 1–8, 2016.

[17] “Energieflussbild Wien 2014,” 2015. [Online]. Available: https://www.wien.gv.at/stadtentwicklung/energieplanung/pdf/energieflussbild-2014.pdf.

[18] C. J. Banks and S. Heaven, “Optimisation of biogas yields from anaerobic digestion by feedstock type,” in *The Biogas Handbook: Science, production and applications*, 2013,

p. 512.

[19] J. D. Murphy and Thanasit Thamsiriroj, “Fundamental science and engineering of the anaerobic digestion process for biogas production,” in *The Biogas Handbook: Science, production and applications*, Elsevier, 2013, pp. 104–130.

[20] R. Pohling, *Chemische Reaktionen in der Wasseranalyse*. Berlin, Heidelberg: Springer Berlin Heidelberg, 2015.

[21] D. Botheju and R. Bakke, “Oxygen Effects in Anaerobic Digestion – A Review,” *Open Waste Manag. J.*, no. 4, pp. 1–19, 2011.

[22] BGR, “Einteilung von Explosionsschutz-Zonen bei Biogasanlagen,” 2014.

[23] ATZ, “Ergebnisbericht zum Forschungsvorhaben: ‘Grundlegende Untersuchungen zur effektiven , kostengünstigen Entfernung von Schwefelwasserstoff aus Biogas,’” 2004.

[24] J. Bärnthaler, H. Bergmann, B. Drosg, D. Hornbachner, R. Kirchmayr, and G. Konrad, “Technologie , Logistik und Wirtschaftlichkeit von Biogas-Großanlagen auf Basis industrieller biogener Abfälle,” *Innovation*, no. September, pp. 1–294, 2008.

[25] B. Drosg, B. Linke, W. Fuchs, and M. Madsen, “Nutrient Recovery by Biogas Digestate Processing,” 2015.

[26] VCM Brugge, “Techniques for nutrient recovery from digestate,” 2013.

[27] M. Mayer, “Herausforderung an die Gärrestbehandlung bei Biogasanlagen durch die Forcierung von erneuerbaren Energien,” Universität für Bodenkultur Wien, 2009.

[28] R. R. Melin T., *Membranverfahren - Grundlagen der Modul- und Anlagenauslegung*, vol. 3. 2006.

[29] R. Bergman, *Reverse Osmosis and Nanofiltration: Manual of Water Supply Practices M46*, 2nd ed. American Water Works Association, 2007.

[30] K. Ohlrogge and K. Ebert, *Membranen - Grundlagen, Verfahren und industrielle Anwendungen*. Weinheim, FRG: Wiley-VCH Verlag GmbH & Co. KGaA, 2006.

[31] H. Döhler, “Düngung von Gülle und Gärrückständen unter den Vorzeichen der neuen Düngeverordnung,” Döhler Agrar, Untermerzbach, 2016.

[32] P. Weiland, “Flaschenhals Gärrestverwertung,” Johann Heinrich von Thünen-Institut, Braunschweig, 2010.

[33] E. Pfundtner, *Der sachgerechte Einsatz von Biogasgülle und Gärrückständen im Acker- und Grünland*, vol. 2. 2007.

[34] *Verordnung des Bundesministers für Land- und Forstwirtschaft , Umwelt und Wasserwirtschaft über das Aktionsprogramm 2012 zum Schutz der Gewässer vor Verunreinigung durch Nitrat aus landwirtschaftlichen Quellen (Aktionsprogramm Nitrat 2012)*, no. 391. 2012.

[35] R. Stratton, D. Mann, and P. Otterson, “The Theory of Inventive Problem Solving (TRIZ) and Systematic Innovation-a Missing Link in Engineering Education,” no. December, 2010.

[36] P. Murray, *Manual of Water Supply Practices–M38: Electrodialysis and Electrodialysis Reversal*, 1st ed. American Water Works Association, 1995.

[37] S. A. Kalogirou, “Seawater desalination using renewable energy sources,” *Prog. Energy Combust. Sci.*, vol. 31, no. 3, pp. 242–281, 2005.

[38] L. F. Greenlee, D. F. Lawler, B. D. Freeman, B. Marrot, and P. Moulin, “Reverse osmosis desalination: Water sources, technology, and today’s challenges,” *Water Res.*, vol. 43, no. 9, pp. 2317–2348, 2009.

[39] M. P. Lopes, C. T. Matos, V. J. Pereira, A. Rodrigues, A. I. Penetra, E. Ferreira, and M. A. M. Reis, “Production of drinking water using a multi-barrier approach integrating nanofiltration: A pilot scale study,” *Sep. Purif. Technol.*, vol. 119, pp. 112–122, 2013.

[40] L. J. Banasiak, T. W. Kruttschnitt, and A. I. Schäfer, “Desalination using electrodialysis as a function of voltage and salt concentration,” *Desalination*, vol. 205, no. 1–3, pp. 38–46, 2007.

[41] K. W. Lawson and D. R. Lloyd, “Membrane distillation,” *J. Memb. Sci.*, vol. 124, no. 1, pp. 1–25, Feb. 1997.

[42] E. Drioli, A. Ali, and F. Macedonio, “Membrane distillation: Recent developments and perspectives,” *Desalination*, vol. 356, pp. 56–84, 2015.

[43] M. S. El-Bourawi, Z. Ding, R. Ma, and M. Khayet, “A framework for better understanding membrane distillation separation process,” *J. Memb. Sci.*, vol. 285, no. 1–2, pp. 4–29, 2006.

[44] P. Wang and T. S. Chung, “Recent advances in membrane distillation processes: Membrane development, configuration design and application exploring,” *J. Memb. Sci.*, vol. 474, pp. 39–56, 2015.

[45] D. Qu, D. Sun, H. Wang, and Y. Yun, “Experimental study of ammonia removal from water by modified direct contact membrane distillation,” *Desalination*, vol. 326, pp. 135–140, 2013.

[46] S. Kim, D. W. Lee, and J. Cho, “Application of direct contact membrane distillation process to treat anaerobic digestate,” *J. Memb. Sci.*, vol. 511, pp. 20–28, 2016.

[47] V. Lebuf, F. Accoe, C. Vaneeckhaute, E. Meers, E. Michels, and G. Ghekiere, “Nutrient recovery from digestates: techniques and end-products,” *Fourth Int. Symp. Energy from Biomass Waste*, vol. 4, no. 1, pp. 1–18, 2012.

[48] T. Y. Cath, A. E. Childress, and M. Elimelech, “Forward osmosis: Principles, applications, and recent developments,” *J. Memb. Sci.*, vol. 281, no. 1–2, pp. 70–87, 2006.

[49] H. P. Latscha and H. A. Klein, *Analytische Chemie*. Berlin, Heidelberg: Springer Berlin Heidelberg, 1990.

[50] M. Kraume and M. Fechter, “Treatment of Digestates from Biogas Production - Status and Trends,” *Treat. Dig. from Biogas Prod. - Status Trends*, p. 38, 2014.

[51] K. Sattler, *Thermische Trennverfahren*. Weinheim, FRG: Wiley-VCH Verlag GmbH & Co. KGaA, 2001.

[52] S. Al-Obaidani, E. Curcio, F. Macedonio, G. Di Profio, H. Al-Hinai, and E. Drioli, “Potential of membrane distillation in seawater desalination: Thermal efficiency, sensitivity study and cost estimation,” *J. Memb. Sci.*, vol. 323, no. 1, pp. 85–98, 2008.

[53] “Osmo Membrane.” [Online]. Available: http://www.osmo-membrane.de/de/produkte/labor-und-pilotanlagen/memcell-classic.html.

[54] C. Hoislbauer, “Spezielle Verfahren in der Abwasserreinigung - photochemische und elektrochemische Methoden,” Technische Universität Graz, 2012.

[55] M. Becke-Goehring and H. Hoffmann, *Komplexchemie*, vol. 72. 1970.

[56] “Bioenergy 2020+.” [Online]. Available: http://www.bioenergy2020.eu/.

[57] “GESTIS - Stoffdatenbank.” [Online]. Available: http://www.dguv.de/ifa/gestis/gestis-stoffdatenbank/index.jsp.

[58] J. V. Nicolini, C. P. Borges, and H. C. Ferraz, “Selective rejection of ions and correlation with surface properties of nanofiltration membranes,” *Sep. Purif. Technol.*, vol. 171, pp. 238–247, 2016.

[59] H. P. Latscha and H. A. Klein, *Anorganische Chemie*, 9th ed. Berlin, Heidelberg: Springer Berlin Heidelberg, 2007.

[60] Y. Kaya, H. Barlas, and S. Arayici, “Nanofiltration of Cleaning-in-Place (CIP) wastewater in a detergent plant: Effects of pH, temperature and transmembrane pressure on flux behavior,” *Sep. Purif. Technol.*, vol. 65, no. 2, pp. 117–129, 2009.

[61] A. L. Carvalho, F. Maugeri, P. Prádanos, V. Silva, and A. Hernández, “Separation of potassium clavulanate and potassium chloride by nanofiltration: Transport and evaluation of membranes,” *Sep. Purif. Technol.*, vol. 83, no. 1, pp. 23–30, 2011.

[62] H. Kurama, “The application of membrane filtration for the removal of ammonium ions from potable water,” *Water Res.*, vol. 36, no. 11, pp. 2905–2909, 2002.

[63] C. G. Zoski, *Handbook of Electrochemistry*, 1st ed., vol. 1. Elsevier B.V., 2015.

[64] D. R. Lide, *CRC Handbook of Chemistry and Physics*, 84th ed. .

[65] B. Van Der Bruggen, A. Koninckx, and C. Vandecasteele, “Separation of monovalent and divalent ions from aqueous solution by electrodialysis and nanofiltration,” *Water Res.*, vol. 38, no. 5, pp. 1347–1353, 2004.

[66] W. M. Samhaber, “Die industrielle Anwendung der Nanofiltration - Potenziale, Erfahrungen und Grenzen,” *Chemie-Ingenieur-Technik*, vol. 77, no. 5, pp. 566–572, 2005.

[67] “Düngemittel - Reinnährstoffabsatz in Österreich,” 2016.

[68] “Düngemittel - Endverbraucherpreise der am häufigsten eingesetzten Düngemittel,” 2016.

[69] “Schwefeldünger im Biolandbau,” 2015.

8 Appendix

Table 17 and Table 18 show the complete decision matrix for mechanical respectively mass transfer unit operations investigated in section 3.

Table 17: Complete decision matrix mechanical unit operations

Properties of target substance		Mechanical unit operations										
Proberty	**Value**	**Sedimentation**	**Flocculation**	**Sieving**	**Chromatography**	**Hydro Cyclone**	**Flotation**	**Electrophoresis**	**Centrifuge**	**Ultrafiltration**	**Nanofiltration**	**Reverse Osmosis**
MW [g/mol]	18.02	n	n	n	y	n	n	y	n	n	y	y
Boiling point [°C]	100	n	n	n	n	n	n	n	n	n	n	n
Density at 20°C [kg/dm³]	0.998	n	n	n	n	n	n	n	n	n	n	n
Viscosity [mPa*s]	1,001	n	n	n	n	n	n	n	n	n	n	n
Dieelectric constant at 20°C	80	n	n	n	n	n	n	y	n	n	n	n
pH value	7	n	n	n	n	n	n	n	n	n	n	n
p_{vapour} at 20°C [mbar]	23.4	n	n	n	n	n	n	n	n	n	n	n
Freezing point [°C]	0	n	n	n	n	n	n	n	n	n	n	n
Enthalpy [J/mol]	2257	n	n	n	n	n	n	n	n	n	n	n
Molecular Size [nm]	0.28	n	n	n	y	n	n	y	n	n	y	y
Acidity (pKa)	15.7	n	n	n	n	n	n	y	n	n	n	n
∑		**0**	**0**	**0**	**2**	**0**	**0**	**4**	**0**	**0**	**2**	**2**

Table 18: Complete decision matrix mass transfer unit operations

Properties of target substance		Thermal unit operations													
Proberty	Value	Absorption	Adsorption	Desorption	Distillation	Flash vaporization	Drying	Electro dialysis	Stripping	Evaporation	Crystallization	Molecular Sieve	Pervaporation	Extraction	Membrandestillation
MW [g/mol]	18.02	n	n	n	y	y	n	n	n	y	n	n	y	n	y
Boiling point [°C]	100	n	n	n	n	n	n	n	n	n	y	n	n	y	n
Density at 20°C [kg/dm³]	0.998	n	n	n	n	n	n	n	y	n	n	n	n	y	n
Viscosity [mPa*s]	1,001	n	y	y	n	n	n	y	n	n	n	n	n	n	n
Dieelectric constant at 20°C	80	n	n	n	n	n	n	n	n	n	y	n	n	n	n
pH value	7	n	y	y	y	y	y	n	n	y	n	n	y	n	y
p_{vapour} at 20°C [mbar]	23.4	n	n	n	n	n	n	n	n	n	n	n	n	n	n
Freezing point [°C]	0	n	n	n	y	y	n	n	n	y	n	n	y	n	y
Enthalpy [J/mol]	2257	n	y	y	n	n	n	y	n	n	n	y	n	n	n
Molecular Size [nm]	0.28	n	n	n	n	n	n	y	y	n	y	n	n	y	n
Acidity (pKa)	15.7	n	n	n	n	n	n	n	n	n	n	n	n	y	n
∑		0	3	3	3	3	1	3	2	3	3	1	3	4	3

Table 19 and Table 20 show the ion concentration and in the permeate, concentrate and feed at 40 bar for nanofiltration in stage 1 respectively stage 2. The values were used for the calculation of the NF rejection rates in section 5.3.1 and section 5.4.1 .

Table 19: NF Stage 1: Ion concentration and SD in the permeate, concentrate and feed at 40 bar

Substance [-]	w_Perm [g/l]	w_Perm [m%]	c_Conc [g/l]	w_Conc [m%]	c_Feed [g/l]	w_Feed [m%]	SD_Perm [g/l]	SD_Perm [m%]	SD_Conc [g/l]	SD_Conc [m%]	SD_Feed [g/l]	SD_Feed [m%]
Na	1.43E+00	1.43E-01	1.67E+00	1.67E-01	1.68E+00	1.68E-01	1.51E-02	1.51E-03	1.01E-02	1.01E-03	5.14E-02	5.14E-03
K	1.23E+00	1.23E-01	1.55E+00	1.55E-01	1.52E+00	1.52E-01	1.01E-02	1.01E-03	1.51E-02	1.51E-03	3.33E-02	3.33E-03
Ca	4.14E-03	4.14E-04	5.68E-03	5.68E-04	5.29E-03	5.29E-04	6.05E-05	6.05E-06	5.79E-04	5.79E-05	3.45E-04	3.45E-05
Mg	4.96E-04	4.96E-05	6.25E-04	6.25E-05	6.19E-04	6.19E-05	6.05E-06	6.05E-07	2.02E-06	2.02E-07	2.18E-05	2.18E-06
NH_4	4.43E+00	4.43E-01	5.29E+00	5.29E-01	5.34E+00	5.34E-01	2.02E-01	2.02E-02	3.53E-01	3.53E-02	1.65E-01	1.65E-02
Cl	1.22E+01	1.22E+00	1.42E+01	1.42E+00	1.43E+01	1.43E+00	5.04E-02	5.04E-03	1.51E-01	1.51E-02	3.80E-01	3.80E-02
PO_4	1.54E-01	1.54E-02	6.66E-01	6.66E-02	6.55E-01	6.55E-02	6.49E-03	6.49E-04	1.55E-03	1.55E-04	1.75E-02	1.75E-03
SO_4	1.94E-02	1.94E-03	7.32E-02	7.32E-03	7.11E-02	7.11E-03	1.06E-03	1.06E-04	4.53E-04	4.53E-05	2.34E-03	2.34E-04

Table 20: NF Stage 2: Ion concentration and SD in the permeate, concentrate and feed at 40 bar

Substance [-]	w_Perm [g/l]	w_Perm [m%]	c_Conc [g/l]	w_Conc [m%]	c_Feed [g/l]	w_Feed [m%]	SD_Perm [g/l]	SD_Perm [m%]	SD_Conc [g/l]	SD_Conc [m%]	SD_Feed [g/l]	SD_Feed [m%]
Na	1.46E+00	1.46E-01	1.59E+00	1.59E-01	1.94E+00	1.94E-01	1.81E-01	1.81E-02	1.66E-01	1.66E-02	5.60E-02	5.60E-03
K	4.21E-01	4.21E-02	5.55E-01	5.55E-02	5.76E-01	5.76E-02	5.80E-02	5.80E-03	3.45E-02	3.45E-03	5.15E-02	5.15E-03
Ca	3.56E-03	3.56E-04	4.24E-03	4.24E-04	4.69E-03	4.69E-04	6.50E-05	6.50E-06	3.70E-04	3.70E-05	9.30E-04	9.30E-05
Mg	5.05E-04	5.05E-05	6.40E-04	6.40E-05	6.30E-04	6.30E-05	4.50E-05	4.50E-06	3.00E-05	3.00E-06	0.00E+00	0.00E+00
NH_4	4.13E+00	4.13E-01	5.39E+00	5.39E-01	5.74E+00	5.74E-01	3.02E-01	3.02E-02	5.04E-02	5.04E-03	0.00E+00	0.00E+00
Cl	1.20E+01	1.20E+00	1.46E+01	1.46E+00	1.39E+01	1.39E+00	1.51E-01	1.51E-02	1.01E-01	1.01E-02	0.00E+00	0.00E+00
PO_4	1.28E-01	1.28E-02	6.57E-01	6.57E-02	6.46E-01	6.46E-02	1.31E-03	1.31E-04	1.08E-02	1.08E-03	0.00E+00	0.00E+00
SO_4	2.03E-02	2.03E-03	7.67E-02	7.67E-03	7.37E-02	7.37E-03	2.72E-03	2.72E-04	4.23E-03	4.23E-04	0.00E+00	0.00E+00

Table 21 shows the values of the ion concentration of the permeate, concentrate and feed at RO at 40 bar. These values were used for the calculation of the RO rejection efficiency shown in section 0 Figure 29.

Table 21: RO Stage 2: Ion concentration and SD in the permeate, concentrate and feed at 40 bar

Substance [-]	w_Perm [g/l]	w_Perm [m%]	c_Conc [g/l]	w_Conc [m%]	c_Feed [g/l]	w_Feed [m%]	SD_Perm [g/l]	SD_Perm [m%]	SD_Conc [g/l]	SD_Conc [m%]	SD_Feed [g/l]	SD_Feed [m%]
Na	7.47E-02	7.47E-03	1.70E+00	1.70E-01	1.80E+00	1.80E-01	3.44E-02	3.44E-03	1.55E-01	1.55E-02	0.00E+00	0.00E+00
K	1.81E-02	1.81E-03	1.30E+00	1.30E-01	1.22E+00	1.22E-01	3.00E-04	3.00E-05	3.00E-02	3.00E-03	2.00E-02	2.00E-03
Ca	5.00E-04	5.00E-05	4.74E-03	4.74E-04	4.88E-03	4.88E-04	0.00E+00	0.00E+00	2.85E-04	2.85E-05	3.70E-04	3.70E-05
Mg	5.00E-05	5.00E-06	5.90E-04	5.90E-05	6.60E-04	6.60E-05	0.00E+00	0.00E+00	1.00E-05	1.00E-06	2.00E-05	2.00E-06
NH_4	3.43E-01	3.43E-02	5.49E+00	5.49E-01	4.94E+00	4.94E-01	1.01E-02	1.01E-03	1.51E-01	1.51E-02	0.00E+00	0.00E+00
Cl	4.22E-01	4.22E-02	1.47E+01	1.47E+00	1.39E+01	1.39E+00	4.54E-03	4.54E-04	3.53E-01	3.53E-02	0.00E+00	0.00E+00
PO_4	9.73E-03	9.73E-04	6.43E-01	6.43E-02	6.18E-01	6.18E-02	3.40E-04	3.40E-05	6.18E-03	6.18E-04	0.00E+00	0.00E+00
SO_4	5.27E-03	5.27E-04	7.59E-02	7.59E-03	7.49E-02	7.49E-03	1.86E-03	1.86E-04	2.26E-03	2.26E-04	0.00E+00	0.00E+00

The data in Table 22 show the concentration of sodium and magnesium in the model feeds for the additional nanofiltration investigations on the influence of chloride ions on the rejection efficiency in section 5.4.2 Figure 26.

Table 22: NF model experiments: Ion concentration in the permeate, concentrate and feed at 40 bar

Substance [-]	c_Perm_MF0 [g/l]	c_Perm_MF1 [g/l]	c_Perm_MF2 [g/l]	c_Conc_MF0 [g/l]	c_Conc_MF1 [g/l]	c_Conc_MF2 [g/l]	c_Feed_MF0 [g/l]	c_Feed_MF1 [g/l]	c_Feed_MF2 [g/l]
Na	0.00E+00	1.27E+00	6.04E+00	0.00E+00	1.56E+00	7.22E+00	0.00E+00	1.59E+00	7.54E+00
Mg	4.64E-01	4.66E-01	6.78E-01	9.05E-01	5.20E-01	7.15E-01	9.05E-01	5.90E-01	7.40E-01

Substance [-]	w_Perm_MF0 [m%]	w_Perm_MF1 [m%]	w_Perm_MF2 [m%]	w_Conc_MF0 [m%]	w_Conc_MF1 [m%]	w_Conc_MF2 [m%]	w_Feed_MF0 [m%]	w_Feed_MF1 [m%]	w_Feed_MF2 [m%]
Na	0.00E+00	1.27E-01	6.04E-01	0.00E+00	1.56E-01	7.22E-01	0.00E+00	1.59E-01	7.54E-01
Mg	4.64E-02	4.66E-02	6.78E-02	9.05E-02	5.20E-02	7.15E-02	9.05E-02	5.90E-02	7.40E-02

The equations (10) and (11) below were used for the determination of the limiting current density shown in Figure 30.

$$y = 0.5814 * x \; ; \; R^2 = 0.88 \qquad (10)$$

$$y = 2.7162 * x - 4.8162 \; ; R^2 = 0.99 \qquad (11)$$

Table 23 below shows the ion concentrations in the membrane chamber before and after the 8 hour ED experiments. The rejection rates calculated are shown in section 5.4.4 Figure 32. The values for the standard deviations are listed below the concentration values.

Table 23: ED Stage 2: Ion concentration and SD in the membrane compartment at the 8 hour experiment

t [h]	c_Na_MC [g/l]	w_Na_MC [m%]	c_K_MC [g/l]	w_K_MC [m%]	c_Ca_MC [g/l]	w_Ca_MC [m%]	c_Mg_MC [g/l]	w_Mg_MC [m%]	c_NH4_MC [g/l]	w_NH4_MC [m%]	c_Cl_MC [g/l]	w_Cl_MC [m%]	c_PO4_MC [g/l]	w_PO4_MC [m%]	c_SO4_MC [g/l]	w_SO4_MC [m%]
0	1.89E+00	1.89E-01	1.44E+00	1.44E-01	3.28E-03	3.28E-04	5.60E-04	5.60E-05	5.49E+00	5.49E-01	1.45E+01	1.45E+00	6.63E-01	6.63E-02	7.68E-02	7.68E-03
8	1.55E+00	1.55E-01	1.11E+00	1.11E-01	2.54E-03	2.54E-04	4.85E-04	4.85E-05	5.29E+00	5.29E-01	1.30E+01	1.30E+00	6.29E-01	6.29E-02	6.63E-02	6.63E-03

t [h]	SD_Na_MC [g/l]	SD_Na_MC [m%]	SD_K_MC [g/l]	SD_K_MC [m%]	SD_Ca_MC [g/l]	SD_Ca_MC [m%]	SD_Mg_MC [g/l]	SD_Mg_MC [m%]	SD_NH4_MC [g/l]	SD_NH4_MC [m%]	SD_Cl_MC [g/l]	SD_Cl_MC [m%]	SD_PO4_MC [g/l]	SD_PO4_MC [m%]	SD_SO4_MC [g/l]	SD_SO4_MC [m%]
0	4.33E-01	4.33E-02	1.50E-01	1.50E-02	5.35E-04	5.35E-05	8.00E-05	8.00E-06	5.04E-02	5.04E-03	2.02E-01	2.02E-02	7.73E-03	7.73E-04	1.66E-03	1.66E-04
8	2.14E-01	2.14E-02	2.60E-02	2.60E-03	1.10E-04	1.10E-05	4.50E-05	4.50E-06	1.51E-01	1.51E-02	1.51E-01	1.51E-02	1.55E-03	1.55E-04	1.36E-03	1.36E-04

The results of the mass flow calculations and the fundamental equations for the purification process suggestion described in section 5.6 are shown in Table 25 respectively equations (12) – (15). Table 24 shows the used rejection rates for the calculations.

Table 25: Mass flows of the different overall purification processes

Stream	m_{Flow} [t/h] NF 1.1	m_{Flow} [t/h] NF 1.2	m_{Flow} [t/h] NF 2.1 - 2.2	m_{Flow} [t/h] NF 2.3 - 2.4
F1	3.125	3.125	3.125	3.125
K1	0.087	0.120	0.065	0.090
P1	3.038	3.005	2.279	2.254
K2	0.117	0.188	0.088	0.141
P2	2.921	2.817	2.191	2.113
K3	0.139	0.217	0.104	0.163
P3	2.782	–	2.087	–
K4	0.174	–	0.130	–
P_total	2.608	2.600	1.956	1.950
K_total	0.517	0.525	0.387	0.394
P_NR	–	–	2.344	2.344
K_NR	–	–	0.781	0.781

Table 24: Rejection rates of the NF systems

	R [%] NF 1	R [%] NF 2.2/ NF 2.4	R [%] NF 2.1 / NF 2.3
Na	25	25	10
K	27	27	10
Mg	20	20	50
Ca	49	49	50
NH4	28	28	5
Cl	13	13	10
PO4	80	80	90
SO4	72	72	90

The equations (12) to (15) below show schematically how the values for the streams respectively concentrations were calculated.

$$F_i = P_i + C_i \tag{12}$$

$$F_i * w_{S,F} = P_i * w_{S,P} + C_i * w_{S,C} \tag{13}$$

$$w_{S,P} = w_{S,F} * (1 - R_S) \tag{14}$$

$$w_{S,C} = \frac{F_i * w_{S,F} - P_i * w_{S,P}}{C_i} \tag{15}$$

Figure 40 below shows the flow sheet of the purification process NF 1 containing 4 stages if Feed 1 is the process feed described in section 5.6. The concentration values of the salts in the different stages are shown in Table 26.

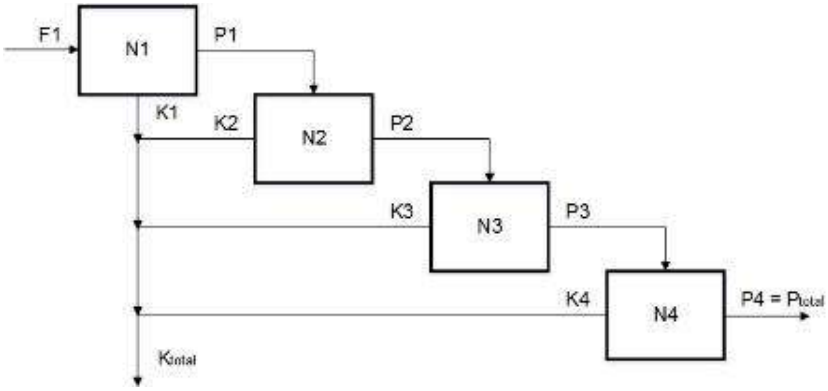

Figure 40: NF1.1 - Process flow sheet of overall purification of Feed 1

Table 26: NF1.1 - Ion concentration in the different streams of the NF system

w [m%]	w_Feed 1	w_K1	w_P1	w_K2	w_P2	w_K3	w_P3	w_K4	w_P_total	w_K_total
w_Na	1.68E-01	1.64E+00	1.26E-01	9.14E-01	9.45E-02	5.67E-01	7.09E-02	3.37E-01	5.32E-02	7.48E-01
w_K	1.52E-01	1.59E+00	1.11E-01	8.60E-01	8.10E-02	5.18E-01	5.91E-02	2.99E-01	4.32E-02	7.01E-01
w_Mg	5.38E-05	4.30E-04	4.30E-05	2.58E-04	3.44E-05	1.72E-04	2.75E-05	1.10E-04	2.20E-05	2.14E-04
w_Ca	6.31E-04	1.15E-02	3.22E-04	4.26E-03	1.64E-04	1.77E-03	8.37E-05	6.99E-04	4.27E-05	3.60E-03
w_NH4	5.29E-01	5.71E+00	3.81E-01	3.05E+00	2.74E-01	1.81E+00	1.97E-01	1.03E+00	1.42E-01	2.48E+00
w_Cl	1.42E+00	7.88E+00	1.24E+00	5.25E+00	1.07E+00	3.87E+00	9.35E-01	2.76E+00	8.14E-01	4.48E+00
w_PO4	6.46E-02	1.87E+00	1.29E-02	2.71E-01	2.58E-03	4.39E-02	5.17E-04	6.72E-03	1.03E-04	3.90E-01
w_SO4	8.17E-03	2.14E-01	2.29E-03	4.35E-02	6.41E-04	9.86E-03	1.79E-04	2.12E-03	5.02E-05	4.92E-02
∑	2.34E+00	1.89E+01	1.87E+00	1.04E+01	1.53E+00	6.82E+00	1.26E+00	4.43E+00	1.05E+00	8.86E+00

The flow sheet in Figure 41 refers to the purification process NF 1 containing 3 stages if Feed D is used as process feed (see section 5.6). The concentration values of the salts in the different streams are shown in Table 27.

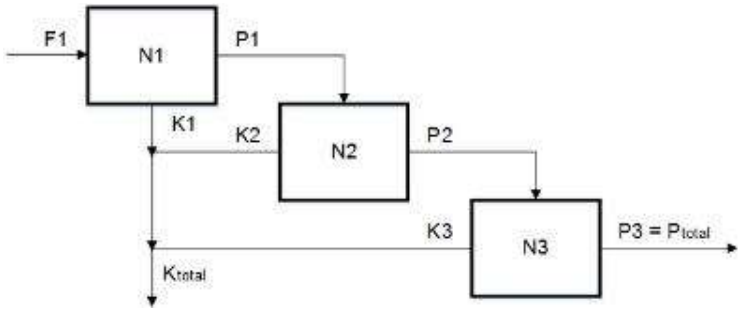

Figure 41: NF1.2 - Process flow sheet of overall purification of digestate D

Table 27: NF1.2 - Ion concentration in the different streams of the NF system

w [m%]	w_Feed 1	w_K1	w_P1	w_K2	w_P2	w_K3	w_P_total	w_K_total
w_Na	1.89E-01	1.37E+00	1.42E-01	6.73E-01	1.06E-01	4.25E-01	7.97E-02	7.31E-01
w_K	1.33E-01	1.03E+00	9.71E-02	4.90E-01	7.09E-02	3.01E-01	5.17E-02	5.36E-01
w_Mg	5.69E-04	3.41E-03	4.55E-04	1.82E-03	3.64E-04	1.24E-03	2.91E-04	1.95E-03
w_Ca	2.75E-03	3.64E-02	1.40E-03	1.17E-02	7.15E-04	4.92E-03	3.65E-04	1.46E-02
w_NH4	4.92E-01	3.94E+00	3.54E-01	1.84E+00	2.55E-01	1.11E+00	1.84E-01	2.02E+00
w_Cl	3.87E-01	1.64E+00	3.37E-01	9.93E-01	2.93E-01	7.50E-01	2.55E-01	1.04E+00
w_PO4	3.41E-02	7.16E-01	6.82E-03	8.87E-02	1.36E-03	1.45E-02	2.73E-04	2.02E-01
w_SO4	6.62E-03	1.26E-01	1.85E-03	2.19E-02	5.19E-04	5.00E-03	1.45E-04	3.87E-02
∑	1.25E+00	8.86E+00	9.40E-01	4.12E+00	7.28E-01	2.61E+00	5.71E-01	4.59E+00

Figure 42 below shows the flow sheet of the nutrient recovery suggestion NF2.1/2.2 described in section 5.6. Process feed is Feed 1 and the values of the ion concentrations in the different streams are given in Table 28.

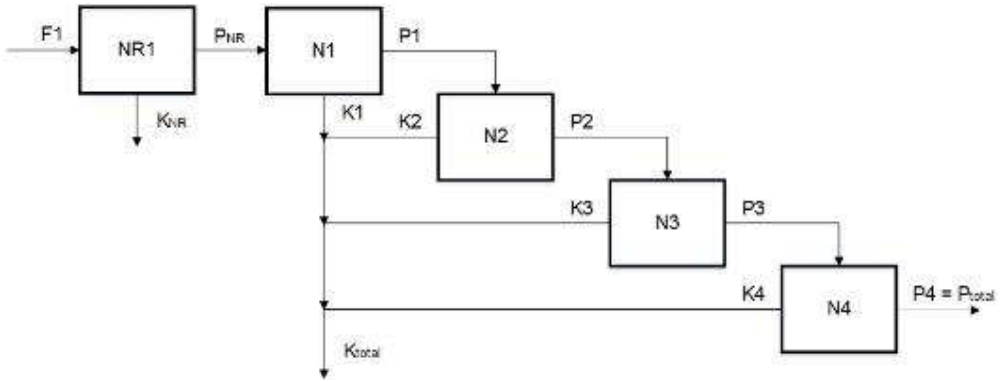

Figure 42: NF 2.1 / NF 2.2 - Process flow sheet of nutrient recovery and purification of Feed 1

Table 28: NF 2.1 / NF 2.2 - Ion concentration in the different streams of the NF system for nutrient recovery

w [m%]	w_Feed 1	w_KNF1	w_PNF1	w_K1	w_P1	w_K2	w_P2	w_K3	w_P3	w_K4	w_P_total	w_K_total
w_Na	1.68E-01	2.18E-01	1.51E-01	1.47E+00	1.13E-01	8.22E-01	8.51E-02	5.10E-01	6.38E-02	3.03E-01	4.78E-02	6.73E-01
w_K	1.52E-01	1.98E-01	1.37E-01	1.43E+00	9.99E-02	7.74E-01	7.29E-02	4.67E-01	5.32E-02	2.69E-01	3.88E-02	6.31E-01
w_Mg	5.38E-05	1.35E-04	2.69E-05	2.15E-04	2.15E-05	1.29E-04	1.72E-05	8.61E-05	1.38E-05	5.51E-05	1.10E-05	1.07E-04
w_Ca	6.31E-04	1.58E-03	3.16E-04	5.73E-03	1.61E-04	2.13E-03	8.21E-05	8.86E-04	4.19E-05	3.49E-04	2.13E-05	1.80E-03
w_NH4	5.29E-01	6.08E-01	5.03E-01	5.43E+00	3.62E-01	2.89E+00	2.61E-01	1.72E+00	1.88E-01	9.75E-01	1.35E-01	2.36E+00
w_Cl	1.42E+00	1.85E+00	1.28E+00	7.09E+00	1.11E+00	4.73E+00	9.67E-01	3.48E+00	8.42E-01	2.48E+00	7.32E-01	4.03E+00
w_PO4	6.46E-02	2.39E-01	6.46E-03	1.87E-01	1.29E-03	2.71E-02	2.58E-04	4.39E-03	5.17E-05	6.72E-04	1.03E-05	3.90E-02
w_SO4	8.17E-03	3.02E-02	8.17E-04	2.14E-02	2.29E-04	4.35E-03	6.41E-05	9.86E-04	1.79E-05	2.12E-04	5.02E-06	4.92E-03
∑	2.34E+00	3.14E+00	2.08E+00	1.56E+01	1.69E+00	9.25E+00	1.39E+00	6.19E+00	1.15E+00	4.03E+00	9.54E-01	7.74E+00

Figure 43 below shows the flow sheet of the nutrient recovery suggestion NF2.3/2.4 described in section 5.6. Process feed is Feed D and the values of the ion concentrations in the different streams are given in Table 29.

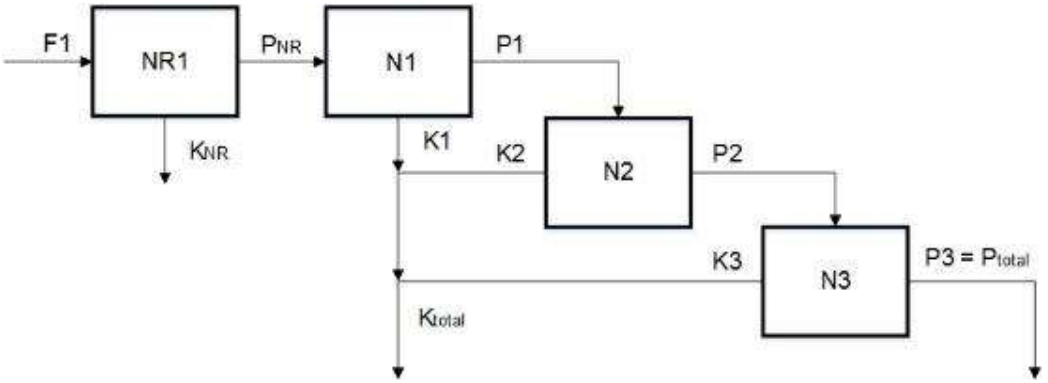

Figure 43: NF 2.3 / NF 2.4 - Process flow sheet of nutrient recovery and purification of the digestate D

Table 29: NF 2.3 / NF2.4 - Ion concentration in the different streams of the NF system

w [m%]	w_Feed 1	w_KNF1	w_PNF1	w_K1	w_P1	w_K2	w_P2	w_K3	w_P_total	w_K_total
w_Na	1.89E-01	2.46E-01	1.70E-01	1.23E+00	1.28E-01	6.06E-01	9.57E-02	3.83E-01	7.18E-02	6.57E-01
w_K	1.33E-01	1.73E-01	1.20E-01	9.28E-01	8.74E-02	4.41E-01	6.38E-02	2.70E-01	4.66E-02	4.82E-01
w_Mg	5.69E-04	1.42E-03	2.85E-04	1.71E-03	2.28E-04	9.10E-04	1.82E-04	6.19E-04	1.46E-04	9.73E-04
w_Ca	2.75E-03	6.88E-03	1.38E-03	1.82E-02	7.01E-04	5.86E-03	3.58E-04	2.46E-03	1.82E-04	7.29E-03
w_NH4	4.92E-01	5.66E-01	4.67E-01	3.74E+00	3.37E-01	1.75E+00	2.42E-01	1.06E+00	1.74E-01	1.92E+00
w_Cl	3.87E-01	5.03E-01	3.48E-01	1.48E+00	3.03E-01	8.94E-01	2.64E-01	6.75E-01	2.29E-01	9.38E-01
w_PO4	3.41E-02	1.26E-01	3.41E-03	7.16E-02	6.82E-04	8.87E-03	1.36E-04	1.45E-03	2.73E-05	2.02E-02
w_SO4	6.62E-03	2.45E-02	6.62E-04	1.26E-02	1.85E-04	2.19E-03	5.19E-05	5.00E-04	1.45E-05	3.87E-03
∑	1.25E+00	1.65E+00	1.11E+00	7.48E+00	8.56E-01	3.71E+00	6.66E-01	2.39E+00	5.23E-01	4.03E+00

Table 26 respectively Table 27 show the initial concentrations that were used for the calculations of the recycling investigations for the purification process NF 1 depicted in section 5.6 Figure 38. The constant mass flows within the nanofiltration stages are shown in Table 25.

For the calculations it was assumed that the recycled permeate stream (P_{Rec}= 50, 25 or 10 % of P_{total}) and the initial process feed stream (F1) are mixed together in a mixing chamber. 3.125 t/h (F1*) of the mixture (F_{mix}) are inserted in the NF system NF 1. Figure 44 shows schematically the mixing chamber and streams.

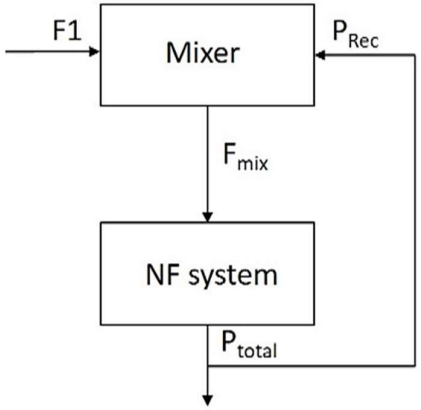

Figure 44: Recycle - Mixing of the recycled permeate and initial process feed before the NF system

The mass streams for the recycle processes with 50, 25 or 10 % of the total permeate stream and the mixer streams, which were used for the calculation of the concentration values in the feed F1* at the process NF 1.1 (Feed 1) respectively NF 1.2 (Feed D) are given in Table 30 below.

Table 30: NF 1 - Process streams for the recycle investigations with the different feeds

Process stream	**NF 1.1** Recycle 50 % [t/h]	**NF 1.1** Recycle 25 % [t/h]	**NF 1.1** Recycle 10 % [t/h]	**NF 1.2** Recycle 50 % [t/h]	**NF 1.2** Recycle 25 % [t/h]	**NF 1.2** Recycle 10 % [t/h]
Ptotal	2.608	2.608	2.608	2.600	2.600	2.600
Prec	1.304	0.652	0.261	1.300	0.650	0.260
F1	3.125	3.125	3.125	3.125	3.125	3.125
Fmix	4.429	3.777	3.386	4.425	3.775	3.385
F1*	3.125	3.125	3.125	3.125	3.125	3.125

The equations (16) to (19) below give an overview how the calculation of the permeate concentration during the recycle iterations was performed (Results see section 5.6 Figure 38). The symbol " * " relates to the resulting concentration due to the recycling iteration.

$$w_{PRec} = w_{Ptotal} \tag{16}$$

$$w_{Fmix} = \frac{w_{Fmix}\left(F1 * w_{S,F1} + P_{Rec} * w_{S,PRec}\right)}{F_{mix}} \tag{17}$$

$$w_{F1^*} = \frac{F_{mix} * w_{Fmix}}{F1^*} \tag{18}$$

$$P^* = (1 - R_S) * w_{F^*} \tag{19}$$

Table 28 respectively Table 29 show the initial concentrations that were used for the calculations of the recycling investigations for the purification process NF 2 depicted in section 5.6 Figure 39. The constant mass flows within the nanofiltration stages are shown in Table 25. The assumption of a mixing chamber is described above.

The mass streams for the recycle processes with 50, 25 or 10 % of the total permeate stream and the mixer streams, which were used for the calculation of the concentration values in the feed F1* at the process NF 2.1/2.2 (Feed 1) respectively NF 2.3/2.4 (Feed D) are given in Table 30 below. The constant mass flows within the nanofiltration stages are shown in Table 25.

Table 31: NF 2 - Process streams for the recycle investigations with the different feeds

Process stream	**NF 2.1/2.2** Recycle 50 % [t/h]	**NF 2.1/2.2** Recycle 25 % [t/h]	**NF 2.1/2.2** Recycle 10 % [t/h]	**NF 2.3/2.4** Recycle 50 % [t/h]	**NF 2.3/2.4** Recycle 25 % [t/h]	**NF 2.3/2.4** Recycle 10 % [t/h]
Ptotal	1.956	1.956	1.956	1.950	1.950	1.950
Prec	0.978	0.978	0.978	0.975	0.975	0.975
F1	3.125	3.125	3.125	3.125	3.125	3.125
Fmix	4.103	4.103	4.103	4.100	4.100	4.100
F1*	3.125	3.125	3.125	3.125	3.125	3.125

The equations (16) to (19) given above are the basis for the calculation of the permeate concentration for the processes in NF 2 during the recycle iterations (Results see section 5.6 Figure 39).